INFORMATION TO USERS

This manuscript has been reproduced from the microfilm master. UMI films the text directly from the original or copy submitted. Thus, some thesis and dissertation copies are in typewriter face, while others may be from any type of computer printer.

The quality of this reproduction is dependent upon the quality of the copy submitted. Broken or indistinct print, colored or poor quality illustrations and photographs, print bleedthrough, substandard margins, and improper alignment can adversely affect reproduction.

In the unlikely event that the author did not send UMI a complete manuscript and there are missing pages, these will be noted. Also, if unauthorized copyright material had to be removed, a note will indicate the deletion.

Oversize materials (e.g., maps, drawings, charts) are reproduced by sectioning the original, beginning at the upper left-hand corner and continuing from left to right in equal sections with small overlaps.

Photographs included in the original manuscript have been reproduced xerographically in this copy. Higher quality 6" x 9" black and white photographic prints are available for any photographs or illustrations appearing in this copy for an additional charge. Contact UMI directly to order.

ProQuest Information and Learning
300 North Zeeb Road, Ann Arbor, MI 48106-1346 USA
800-521-0600

Université d'Ottawa · University of Ottawa

EQUALIZER DESIGN FOR DISCRETE WAVELET MULTITONE TRANSCEIVER

by
Neera Tressler

A thesis submitted to
the School of Graduate Studies and Research
in partial fulfillment of
the requirements for the degree of

Masters of Applied Science
Electrical and Computer Engineering

School of Information Technology and Engineering
University of Ottawa
Ottawa, Ontario, Canada K1N 6N5

September 2001

ABSTRACT

Discrete Wavelet Multi-tone (DWMT) is a multi-carrier technique that uses Wavelet Transform (WT) for modulation. A DWMT communication system is designed and an attempt is made to optimize the equalizer design and the structure of the DWMT receiver. Three plausible receiver designs consisting of a time domain equalizer (TEQ), several frequency domain equalizers (FEQ) and a combination of a simple TEQ and simple FEQs, are examined. The Linear equalizer (LE) is used as the TEQ, whereas the LE and the Decision Feedback Equalizer (DFE) are used as FEQs. These designs are simulated, tested on different twisted pair Very high-speed Digital Subscriber Loop (VDSL) channels and compared with each other in terms of their complexity and performance.

The results indicate that the receiver designs consisting of only TEQ or only FEQs do not give a good signal reconstruction, in spite of using a large number of taps in the equalizers. On the other hand, the receiver structure consisting of a combination of a TEQ and FEQs was found to give a better performance, with lesser complexity in both the TEQ and the FEQs. A few taps in TEQ are found to be sufficient for eliminating most of the ISI in the signal. After demodulation, an FEQ with a few taps for each subchannel is sufficient to equalize the signal further and give a much lower Symbol Error Rate SER, as compared to both the previous structures. The DFE was found to give better performance than the LE. We conclude that the receiver design consisting of a simple TEQ and simple subchannel DFE-based FEQs, is most suitable for the DWMT transceiver among the three different designs tested for a DWMT system.

ACKNOWLEDGEMENTS

I would like to express my sincere gratitude to my supervisor Dr. Tet Hin Yeap for his valuable guidance throughout the period of this project and the duration of my Masters program. I would like to thank him especially for his creative analysis, constructive criticism, excellent suggestions, gentle guidance and constant encouragement. My thanks are also due to Bell Canada for providing me with the financial support during my study.

I would like to thank my colleague and friend Mr. David Fenton for his constant support and valuable suggestions. I am grateful to Mr. Domenic Olivieri for maintaining a smooth working environment for us at all times. I would like to acknowledge the encouragement and support provided by my friends and colleagues Ms. Anita Pathak, Ms. Dai Hong, Ms. Yan Hui Tong and Mr. Jin Wei throughout the duration of this project. I am indebted to my husband, Jacob Pabbathy and the rest of my family members and friends for their contribution and encouragement throughout the period of my Masters' study. It would have been impossible for me to achieve this goal without their support.

TABLE OF CONTENTS

LIST OF FIGURES

LIST OF TABLES

LIST OF ACRONYMS AND ABBREVIATIONS

A/D..... Analog to Digital
ADSL..... Asymmetrical Digital Subscriber Line
AWG..... American Wire Gauge
AWGN..... Additive White Gaussian Noise
BER..... Bit Error Rate
CAP..... Carrier Amplitude Phase
CIR..... Channel Impulse Response
CSA..... Carrier Server Area
D/A..... Digital to Analog
dB..... decibel
DFE..... Decision Feedback Equalizer
DFT..... Discrete Fourier Transform
DMT..... Discrete Multi Tone
DWMT..... Discrete Wavelet Multi Tone
DSL..... Digital Subscriber Loop
DSP..... Digital Signal Processing
FDM..... Frequency Division Multiplexing
FEQ..... Frequency domain Equalizer
FEXT..... Far end cross talk
FFT..... Fast Fourier Transform
FIR..... Finite Impulse Response
FT..... Fourier Transform
FWT..... Fast Wavelet Transform
IBI..... Inter-block Interference
ICI..... Inter-channel Interference
ICBI..... Inter-channel-block Interference
IFFT..... Inverse Fast Fourier Transform
IFWT..... Inverse Fast Wavelet Transform
ISI..... Inter-symbol Interference
kHz..... Kilohertz
km..... Kilometre

LE..... Linear Equalizer
LMS..... Least Mean Square
LOT..... Lapped Orthogonal Transform
MCM..... Multi-carrier Modulation
MHz..... Megahertz
MIMO..... Multiple-input multiple output
ML..... Maximum Likelihood
MLSE..... Maximum Likelihood Sequence Estimation
MMSE..... Minimum Mean-Squared Error
MSE..... Mean-Square Error
NEXT..... Near-end Cross-talk
OFDM..... Orthogonal Frequency Division Multiplexing
P/S..... Parallel to Serial
PAM..... Pulse Amplitude Modulation
PR..... Perfect Reconstruction
PSD..... Power Spectral Density
QAM..... Quadrature Amplitude Modulation
QMF..... Quadrature Mirror Filter
RLS..... Recursive Least Squares
S/P..... Serial to Parallel
SER..... Symbol Error Rate
SIMO..... Single input/Multiple output
SINR..... Signal to Interference Noise Ratio
SNR..... Signal-to-noise ratio
STFT..... Short-time Fourier Transform
TDM..... Time Division Multiplexing
TEQ..... Time domain Equalizer
VDSL..... Very High Speed Digital Subscriber Loop
WT..... .Wavelet Transform
ZF..... Zero forcing

CHAPTER 1

INTRODUCTION

Prior to the period when digital transmission of data was first attempted, twisted pair lines were only used for carrying analog voice signals. These subscriber lines were not engineered to carry digital data. With the advent of digital communications, components such as 'modems' have facilitated the transmission of digital signals over the widely available telephone network of twisted pair channels. As the demand for high-speed transmission over existing subscriber telephone lines is increasing, attention is being focussed on *Asymmetrical Digital Subscriber Lines* (ADSL) [1-3], as it allows for asymmetric or uneven bandwidth allocation for upstream and downstream traffic and enables better utilization of available bandwidth.

Until recently, single-carrier modulation techniques were used for transmitting digital signals over twisted-pair channels. However, the characteristics of the twisted pair channel pose a major problem for transmission of high-speed digital signals. The frequency response of a typical twisted pair channel [1] indicates very high attenuation for higher frequencies (600 kHz – 1 MHz). In addition, there are other limiting factors such as cross-talk noise (between signals carried by other wires in the cable), signal reflections from bridged taps, radio-frequency noise, impulse noise, etc., that generate considerable amount of distortion during transmission. In view of all these channel impairments and increasing speed requirements, it becomes necessary to use a suitable equalizer for retrieving the original signal. However, it may not always be possible to increase the number of taps in the equalizer in order to ensure a good performance for single-carrier modulation. The inability of single-carrier modulation to handle high-speed transmission over long distances on twisted pair channels led to the development of a more sophisticated modulation technique, namely the *multi-carrier modulation* (MCM) [4-9].

One of the most commonly used MCM-based transmission schemes is *Discrete Multitone* (DMT), which has been prescribed as a working standard for ADSL signalling. DMT has already been proven to obtain efficient utilization of transmission band, as it realizes reliable, high-rate data transmission up to 1 MHz over most of the *digital subscriber loops* (DSL) [4,5].

In addition, it incorporates effective techniques for coding and equalization, which enhance the reliability of transportation of such high-bit data rates [4]. However, DMT uses a time-domain equalizer (TEQ) [5,8], whose complexity could become unmanageable if the desired data speed is higher than 1 MHz. Other schemes, similar to DMT, which are being investigated for *Very high bit-rate Digital Subscriber Lines* (VDSL), include filter-bank based modulation [6] and the *Discrete Wavelet Multitone* (DWMT) [7]. DMT uses the *Discrete Fourier transform* (DFT) filter bank for modulation, whereas these schemes use other types of filter banks, which are expected to give a better performance than DMT.

In this thesis, a transmitter-receiver (transceiver) system based on DWMT modulation has been designed and tested for high-speed data transmission. The design of the equalizers has been thoroughly examined for use in the DWMT receiver.

1.1 DWMT MODULATION

DWMT is a transmitter-receiver system operating on the principle of a transmultiplexer [7,10, 11], which is a multi-carrier modulated system mostly used for conversion between *time-division multiplexed* (TDM) and *frequency-division multiplexed* (FDM) signals. DWMT was first introduced by AWARE Inc. in 1995 and is a variation of the well-known and well-developed DMT communication system.

In a DWMT system, the transmission channel is partitioned into several narrow subchannels modulated by different carrier frequencies or 'tones'; hence the collective modulation over all subchannels is labelled as 'multi-carrier' or 'multi-tone modulation'. The carrier frequencies are uniformly spaced and separated by a very small interval that is inversely proportional to the number of subchannels, M. The length of the modulating filters is an integer multiple of M, leading to an increase in the period T over which a symbol is spread after modulation. The finite length of the channel impulse response is expected to be negligible as compared to this symbol period T, making the system robust and less susceptible to channel distortion.

In addition, it is possible to make efficient use of the available bandwidth by using different alphabet sizes on different subchannels. The number of bits per symbol transmitted through each subchannel is obtained through the technique of 'adaptive loading' [9] and is dependent

on the *signal-to-noise ratio* (SNR) of each subchannel. The SNRs are measured during channel estimation, prior to the transmission of actual data. A major advantage of adaptive bit allocation is that a large number of bits can be transmitted on low frequency subchannels, which generally have high values of SNR, thereby increasing the system throughput. In addition, multi-carrier systems can be designed to avoid narrow-band radio-frequency disturbances by transmitting no useful data on the subchannels that indicate unusually low SNR as a result of the disturbances.

The transmission of actual data begins after the procedure of bit allocation. The original serial incoming data bits are interleaved into different subchannels according to the allocated bit-size of each subchannel. DWMT uses Wavelet transform [12,13], realized by M-band filter banks to carry out modulation and demodulation of incoming data symbols. M-band synthesis filters are used to modulate the parallel symbol streams simultaneously. The waveforms from different subchannels are frequency division multiplexed into a single serial sequence. A block of data in this sequence consists of frequency responses of samples from each subchannel. This sequence is transmitted through the analog channel via *analog to digital* (A/D) and *digital to analog* (D/A) converters. Figure 1.2 demonstrates the working of a DWMT system.

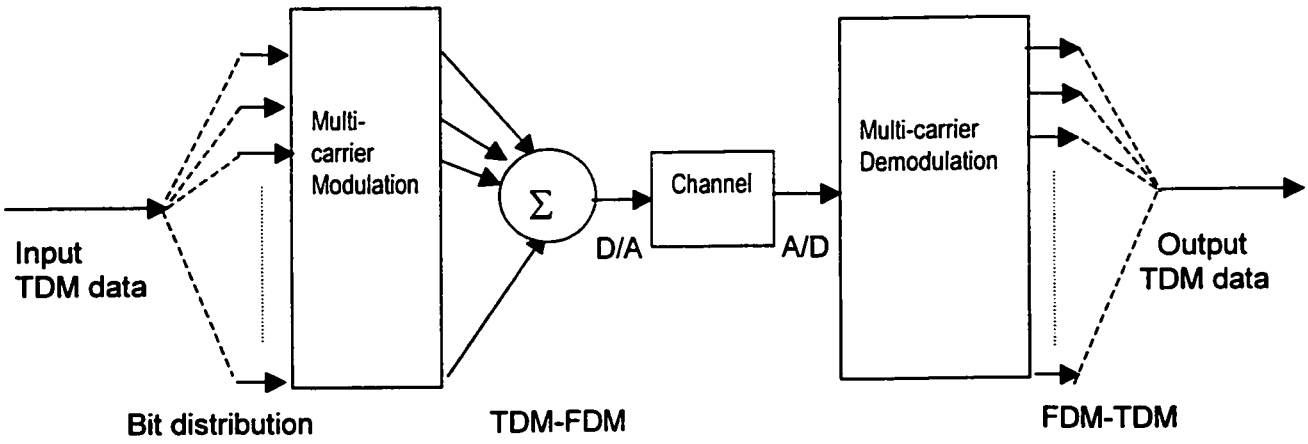

Figure 1.2: Operation of multi-carrier-modulated DWMT communication system

At the receiver end, the received signal is demodulated using the conjugate M-band analysis filters. The received signal could be distorted by the channel, and is therefore equalized to eliminate the channel distortion either prior to, or after demodulation. The equalized signals are

then decoded and de-interleaved to retrieve the original serial TDM data stream.

The need to employ a more sophisticated scheme instead of the existing DMT scheme arises due to poor subchannel isolation in DMT as a result of the nature of the uniform DFT filter bank. The first side-lobe in the frequency response of a DFT filter bank is only 13 dB below the main lobe [14], resulting in considerable amount of *inter-symbol interference* (ISI). For efficient functioning, it becomes necessary to use a guard interval between symbol blocks and a *time-domain equalizer* (TEQ) in a DMT system. On the other hand, the Wavelet transform used in DWMT gives greater subchannel isolation (with the first side-lobe suppressed by at least 40 dB). Extensive research has been done to develop paraunitary M-band filter banks [14-19] that exhibit sharp pass-band to stop-band transition characteristics and can be used to realize the Wavelet transform. As a result, there is less ISI in DWMT than in DMT.

1.2 THESIS OBJECTIVES

The objectives for this thesis can be stated as follows:

(i) Design a multi-carrier-modulated DWMT system using Wavelet transform for modulation, which gives improved frequency domain characteristics as compared to Fourier transform and allows for transmission of symbol blocks without a guard band.

(ii) Incorporate the feature of adaptive loading for bit allocation such that there is maximum utilization of the transmission bandwidth and the system can be used for data transmission at speeds higher than those provided by ADSL.

(iii) Optimize the receiver design and maximize performance for the DWMT system by choosing a suitable combination of time-domain and frequency-domain equalizers, such that the complexity of the equalizers is manageable.

1.3 THESIS CONTRIBUTIONS

The contributions of this thesis are outlined as follows:

(1) The DWMT communication system has been designed with M=32 subchannels, using M-band cosine-modulated filter banks to carry out the wavelet transformation. The length of the filters used for modulation and demodulation is chosen to be five times the number of subchannels.

(2) Procedure of bit allocation based on equal bit error rates for all the subchannels has been used to carry out adaptive loading on different subchannels.

(3) Three different combinations of equalizers are designed. These designs have been simulated and tested as plausible receiver structures for the channel-distorted DWMT system. These structures are compared with each other, in a bid to optimize the structure of the DWMT receiver with respect to their complexity and performance.

(4) Three different twisted pair VDSL channels corresponding to 1 km and 2 km long twisted pair loops operating at 10 MHz sampling frequency have been modelled and used to test the performance of the system, out of which two have a non-linear phase.

1.4 THESIS ORGANIZATION

This thesis is organized into five chapters.

Chapter 1 (the current chapter) gives a brief introduction to a DWMT communication system and discusses the technological requirements that led to the design of such a system.

Chapter 2 provides a background for DWMT modulation. It gives a brief introduction to multicarrier modulation, followed by specific detailed descriptions of DMT and DWMT communication systems. The similarities and differences between the two modulation schemes and the advantages of DWMT over DMT are also discussed in this chapter.

Chapter 3 gives the rationale for the current research and discusses some theoretical aspects of the DWMT system designed in this thesis. The three plausible designs of the DWMT receiver that are proposed in this thesis are presented in this chapter.

Chapter 4 includes the methodology for simulation and the results obtained by simulating a DWMT system using the three different receiver designs described in Chapter 3. Results of simulations using the three different channels for each of the plausible designs are presented. The presentation of each set of results is followed by discussion. Finally, a summary of all the results is also included.

Chapter 5 presents the conclusions derived from the current research and includes some directions for future research.

CHAPTER 2

BACKGROUND FOR CURRENT RESEARCH

This chapter attempts to present an overview of modulation techniques based on *Multicarrier Modulation* (MCM). The first section of the chapter gives a brief discussion on MCM, including the underlying principle and certain features of multicarrier modulated systems. The later sections include descriptions of specific structure of the DMT and the DWMT modulation techniques as well as the differences between them.

2.1 MULTICARRIER MODULATION

MCM employs several carrier frequencies for modulation of digital data. It has gained a considerable amount of interest because of certain advantages it offers over single carrier modulation [20] that include the freedom to use different bit rates over independently modulated subchannels, avoidance of narrow-band interferers, better utilization of transmission bandwidth, greater immunity against channel distortion and less complex equalization techniques, particularly for transmission over twisted pair. MCM optimises the frequency division allocation of energy and bits leading to maximum reliability in transmission over band-limited channels and is also well suited for cable transmission [7,11].

In addition, it is possible to encode data on individual subchannels using existing encoding procedures such as Reed-Solomon and convolutional encoding [4] to improve performance of the system. The throughput of the system can then be increased by using higher bit rates on certain subchannels.

2.1.1 Principle of Multicarrier Modulated systems

As mentioned in the previous chapter, MCM-based systems operate on the principle of a transmultiplexer [21-23]. The structure of a transmultiplexer is opposite to that of a regular *Quadrature Mirror Filter* (QMF) bank (Figure 2.1). Both employ analysis and synthesis M-band filter banks for modulation/demodulation, except for the fact that the roles of these filters are reversed. A transmultiplexer performs FDM<->TDM conversion, while a QMF bank does not.

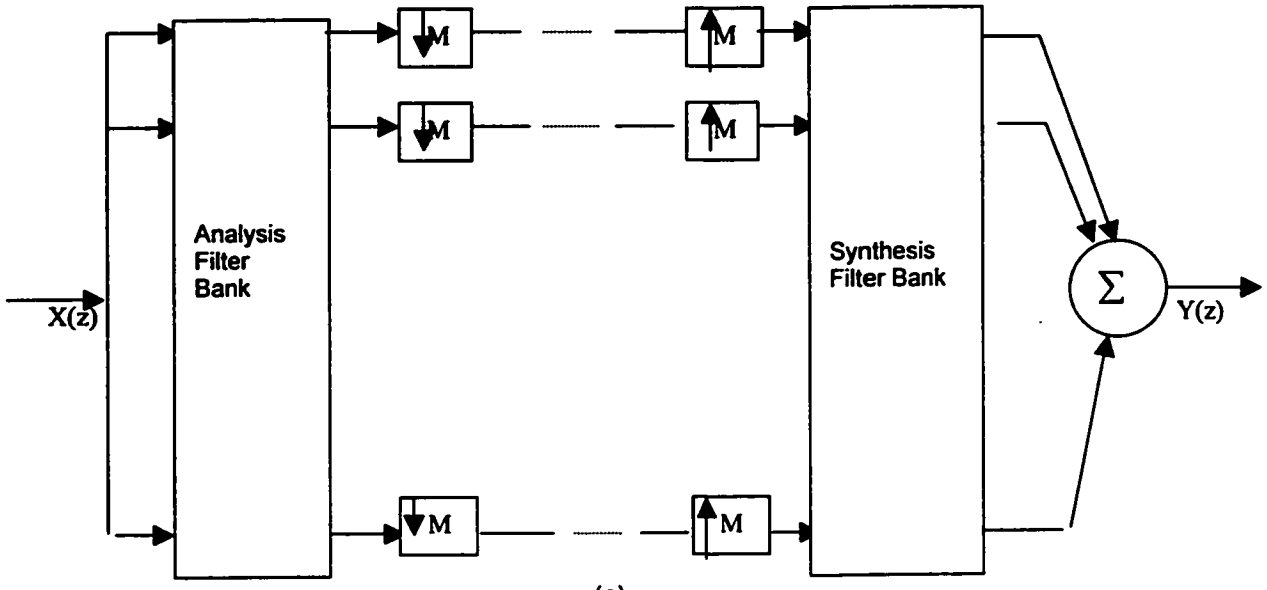

(a)

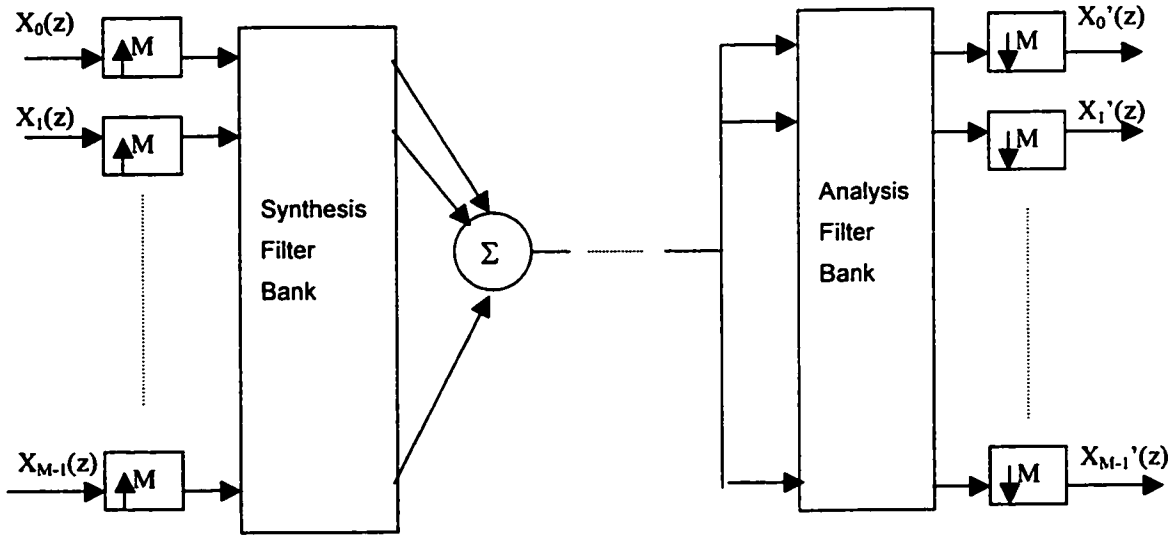

(b)

Figure 2.1: (a) Maximally decimated M-band FIR PR-QMF filter bank structure (analysis/synthesis configuration)

(b) M-band transmultiplexer structure (synthesis/analysis configuration)

As indicated by Figure 2.1, a single data signal in a QMF filter bank is fed into M sub-bands of an analysis filter bank [14] to obtain M different sub-band waveforms. These modulated waveforms are down sampled by M and transmitted. The received signals are upsampled by M, demodulated using the corresponding synthesis filter bank, and then combined to retrieve the original signal. In a transmultiplexer, different signals carried by M different subchannels are first upsampled by M, modulated using the synthesis filter bank and frequency division multiplexed (TDM -> FDM) into a single band having M times higher sampling frequency at the transmitter end. This sequence is transmitted through the channel. At the receiver end, the signal is fed to the analysis filter banks for demodulation and the M data sequences are retrieved. The signal undergoes FDM → TDM conversion at the receiver end.

There could arise a problem of aliasing in QMF filter banks due to the very procedure of signal reconstruction. However, it is possible to cancel aliasing and obtain a perfect reconstruction by imposing certain constraints during the construction of the analysis and synthesis filters [14]. In transmultiplexers, this problem is reflected as cross talk between adjacent subchannels. The condition of alias-free perfect reconstruction QMF filter bank is also responsible for cancellation of cross talk between adjacent subchannels in a transmultiplexer setting. In the absence of any distortion, signals corresponding to different subchannels are exactly reproduced if this condition is met.

2.1.2 Bit Allocation

The ultimate goal behind the use of a system employing MCM is to make efficient use of available bandwidth. The same amount of power and equal number of bits per symbol is not recommended for transmission on all subchannels, due to the varying amount of attenuation experienced at different frequencies. Bit allocation is therefore an important concept in MCM. At lower frequencies, where copper wire attenuation is low and the SNR for the subchannel is good, one can use a high bit rate for data signalling. Modulation for higher frequency subchannels with low SNR can be relaxed by using lower bit rates. It is claimed [9] that a multicarrier system that is developed using appropriate number of bits per symbol and transmit power allocation for each subchannel is capable of giving a better performance with respect to *bit error rates* (BER), as compared to other systems.

The process of bit allocation is demonstrated in Figure 2.2 below [9]. At first, the input serial data bits at $N_{total} f_s$ bits/s are grouped into blocks of N_{total} bits at a block rate of f_s.

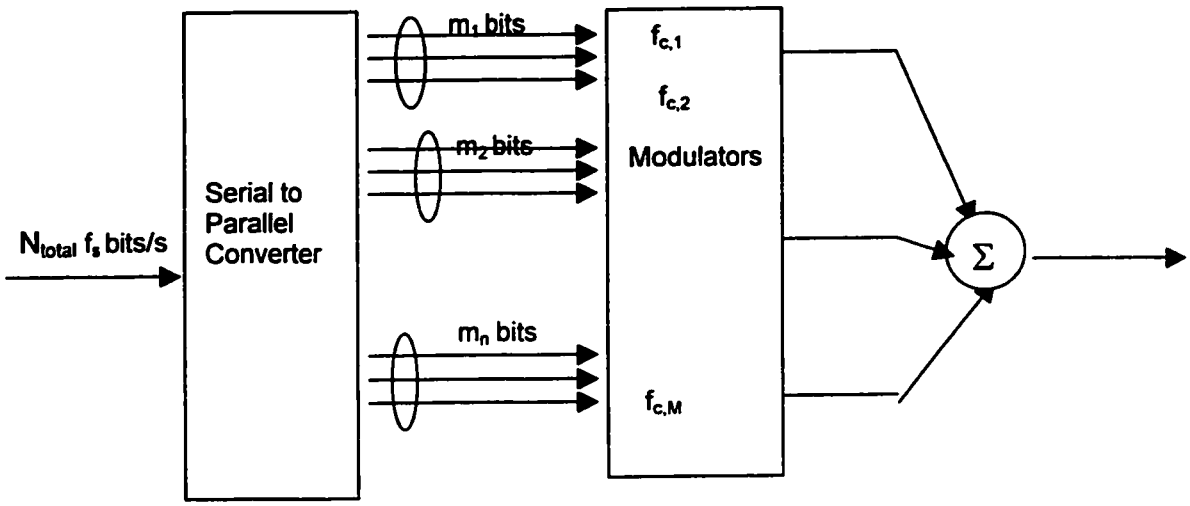

Figure 2.2: Basic multicarrier transmitter

If M bands are to be used, the bits from this block are interleaved into these bands. The mini-group of bits in each band is combined to form a symbol. Let $f_{c,k}$ denote the carrier frequency of a particular sub-band. Suppose m_k bits per symbol are used at frequency $f_{c,k}$, k=1..M, to modulate M bands spaced Δf apart, with

$$\Delta f = f_{c,k+1} - f_{c,k}, \tag{2.1}$$

then the total number of bits is

$$N_{total} = \sum_{k=1}^{M} m_k . \tag{2.2}$$

The modulated signals are summed for transmission, and are separated in the receiver during demodulation. The value of m_k for each subchannel is based on the result of the water-filling algorithm [9,24] obtained by Gallager. Let p_k denote the power level in each subchannel. It is observed that the aggregate bit rate is approximately maximized if m_k and p_k of each subchannel are chosen such that the BER in all the subchannels are equal. Otherwise, the error in one band would increase much more than it would decrease in another band [9].

2.1.3 Inter-symbol interference

A theoretically ideal multicarrier system would use an infinitesimally small frequency spacing (Δf) between carriers, which would be equivalent to using an infinite length symbol-interval. Such a system would be immune to channel distortion because the length of the channel impulse response would be negligible compared to the symbol period. Most systems, however, are far from ideal. If the channel impulse response duration is of the same order as the inverse carrier spacing, the channel distorts the pulses and introduces a considerable amount of overlap between pulses corresponding to adjacent symbols. This results in severe ISI, which poses a serious problem in symbol recovery at the receiver.

The fundamental base band pulse shape x(t) is rectangular, so that

$$x_k(t) = 1/T, \quad 0 \le t \le T, \qquad k=0,2\ldots M-1 \qquad (2.3)$$
$$= 0 \text{ otherwise,}$$

where M is the number of subchannels. These pulses are transmitted through the channel and received at the receiver end. Let $x_k'(t)$ denote the received pulse for k-th subchannel . The demodulating function for this subchannel is given by $\exp(2\pi j f_{c,k} t)$, where $f_{c,k}$ corresponds to the k-th modulating frequency. The output from the demodulator for the k-th subchannel resulting from the input of another (m-th) subchannel is given by

$$y_{k,m}(i) = \int_{iT}^{(i+1)T} x_k'(t)\exp(2\pi j k(\Delta_{k,m} f)t)dt, \qquad (2.4)$$

where $\Delta_{k,m}f$ is the frequency difference between the k-th and the m-th subchannel.
If the channels are non-distorting, the pulse $x_k'(t)$ is zero outside the (0,T) interval, then

$$y_{k,m}(i) = 1, \quad \text{for } i = 0, m=k$$
$$= 0 \text{ otherwise.}$$

However, twisted pair channels could be highly distorting and pulses corresponding to different subchannels tend to lose their orthogonality. If the length of the channel impulse response is comparable to the length of the symbol block, the following situation might arise:

$y_{k,m}(0) \neq 0$ => interference between symbols carried by different carrier frequencies or *inter-channel interference* (ICI), and

$y_{k,k}(\pm 1) \neq 0$ => interference between adjacent symbols for the same carrier, or *inter-block-interference* (IBI).

Both types of interference could also be present simultaneously, giving non-zero values of $y_{k,m}(\pm 1)$, where neither the carrier frequencies nor the desired symbols are the same. This could be classified *as inter-channel-block interference* (ICBI). It becomes important to equalize the output of the channel in order to eliminate the effect of these interferences. Sometimes, a guard band is used between the symbol blocks to reduce the overlap between adjacent blocks. Inclusion of a guard band in combination with effective equalization techniques makes it possible to eliminate ISI and obtain good performance in terms of reliable data recovery in most of the MCM systems.

2.1.4 Systems based on Multi-carrier Modulation

A significant amount of research has been carried out to develop digital communication systems based on multicarrier modulation. Some of these systems, which are already in use, include the *Orthogonal Frequency Division Multiplexing* (OFDM) for wireless transmission and the DMT for ADSL transmission via twisted pair. Other systems that are still being examined for high-speed transmission on twisted pair include DWMT [7] and other filter-bank based modulation systems [6,23,25].

The current study deals with the design of a DWMT system, whose structure is closely related to a DMT system. The design and complexity of the equalizer in the receivers of both systems might differ slightly. We examine the structures of both these systems, in order to understand the similarities and differences between the two.

2.2 THE DMT SYSTEM

The DMT system is probably the most commonly used among the multicarrier modulated systems. The modulation and demodulation in DMT is efficiently carried out by *Inverse Fast Fourier Transform* (IFFT) and *Fast Fourier Transform* (FFT) respectively. To ensure reliable data transmission, the input symbol blocks are separated by a 'cyclic prefix' and a TEQ is used

to shorten the length of the channel impulse response. These concepts, specific to the DMT system, are discussed below.

2.2.1 Cyclic Prefix in DMT

ISI is inherent to most of the multicarrier systems due to the limitation of the minimum frequency separation that can be used between subchannels. One way of minimizing ISI in a DMT system [5] could be to attempt to fully equalize the channel. This approach may not be very practical, as it is computationally extensive for programmable *digital signal processing* (DSP) implementation at data rates required for ADSL and VDSL applications. A practical approach is to use a guard interval of duration T_g, so that the effective symbol length $T'=T+T_g$ is greater that the symbol period T.

Consider a block of M modulated data samples. The length of each block can be increased by prefixing the M samples at the output of the IFFT by a repeat of the last ν samples, as shown in Figure 2.3. The extended time period is $T'= (1+\nu/M)T$, where M = number of samples used in an FFT block. The new length of each block is now $N=M+\nu$.

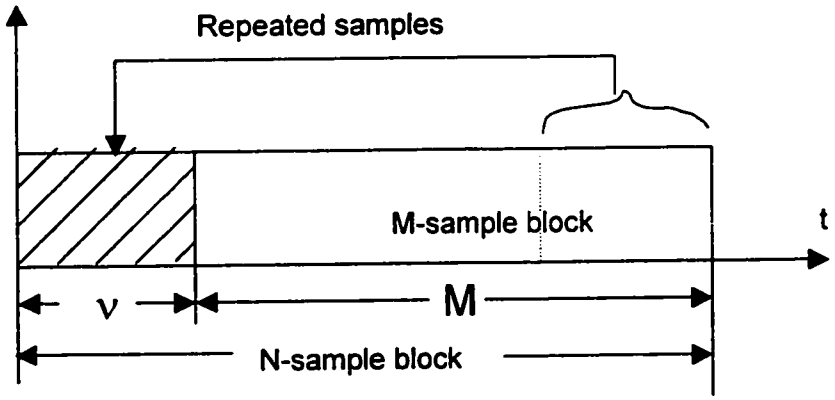

Figure 2.3: Demonstration of cyclic prefix for a symbol block

The repeated 'ν' samples at the beginning of each block are collectively termed as the '*cyclic prefix*', which act as a guard interval between two symbol blocks and also force the data to be periodic as is required by the FFT. During demodulation, the integration is performed over only

the latter T of each symbol, when the transient response of the channel has subsided to a negligible level. The use of a cyclic prefix reduces the overlap between adjacent symbol blocks, but also causes some loss in efficiency due to the excess overhead required. Hence, one has to impose certain constraints on the size of the cyclic prefix to be used, depending upon the length of the filter used for modulation.

2.2.2 *Structure of DMT Transceiver*

Figure 2.4 shows a block level diagram of the DMT system. For a system consisting of M subchannels, the transmitter accepts data in a serial, TDM form and converts it into M parallel lower-rate sequences of information symbols, depending upon the allocated bit size. Each symbol stream in the subchannel is used to modulate a different carrier frequency.

Let s_i^m be the i-th symbol in the m-th subchannel. The modulating waveform of the IFFT matrix F consists of elements given by

$$f_l^m = (1/\sqrt{M}) \exp(2\pi jlm/M), \quad i,m = 0,1...M-1 \tag{2.5}$$

The symbol in the m-th subchannel is modulated by the vector $\mathbf{f}^m$, given by

$$\mathbf{f}^m = [\, f_0^m \quad f_1^m \quad f_2^m \quad \ldots\ldots\ldots\ldots \quad f_{M-1}^m \,].$$

Let $\{s^m\}$ denote the symbol sequence for the m-th subchannel. The output of each subchannel is added to produce an M-dimensional sequence of signal samples $\{x_k\}$, k=0,1..M-1, where

$$x_k = \sum_{m=0}^{M-1} \{s^m * f^m\}_k , \tag{2.6}$$

where the '*' in the above equation denotes convolution. A cyclic prefix of size ν is appended to this output, so that the size of each block increases from M to N=M+ν. The resulting length-N sample sequence $\{x_k\}$ is transmitted through the twisted pair channel via a D/A converter. At the receiver end, the signal is converted back into its digital form through an A/D converter, demodulated using FFT matrix $G=F^T$, detected

The DMT system

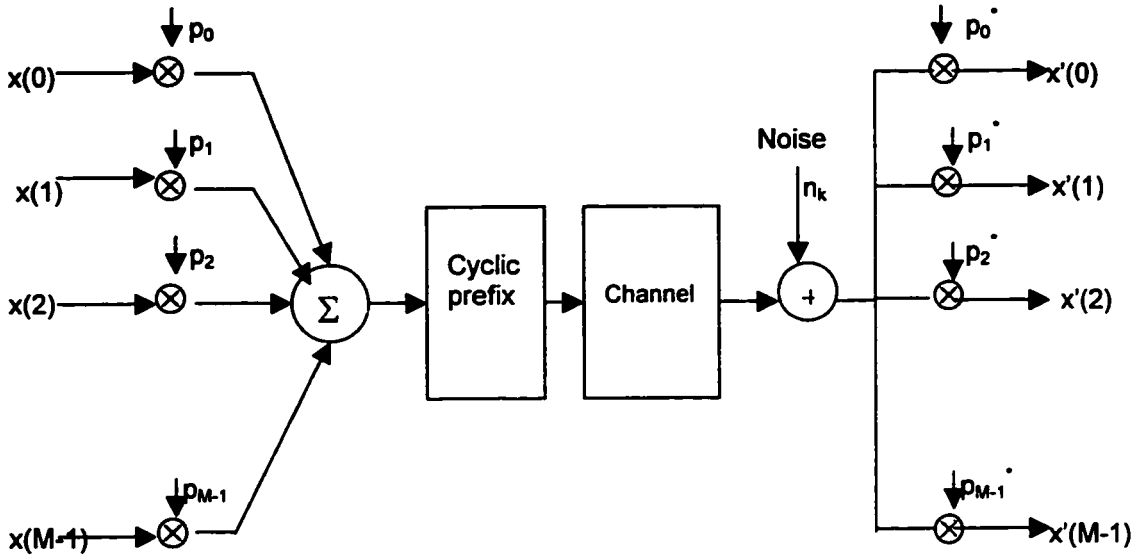

Simplified illustration of DMT transceiver and channel

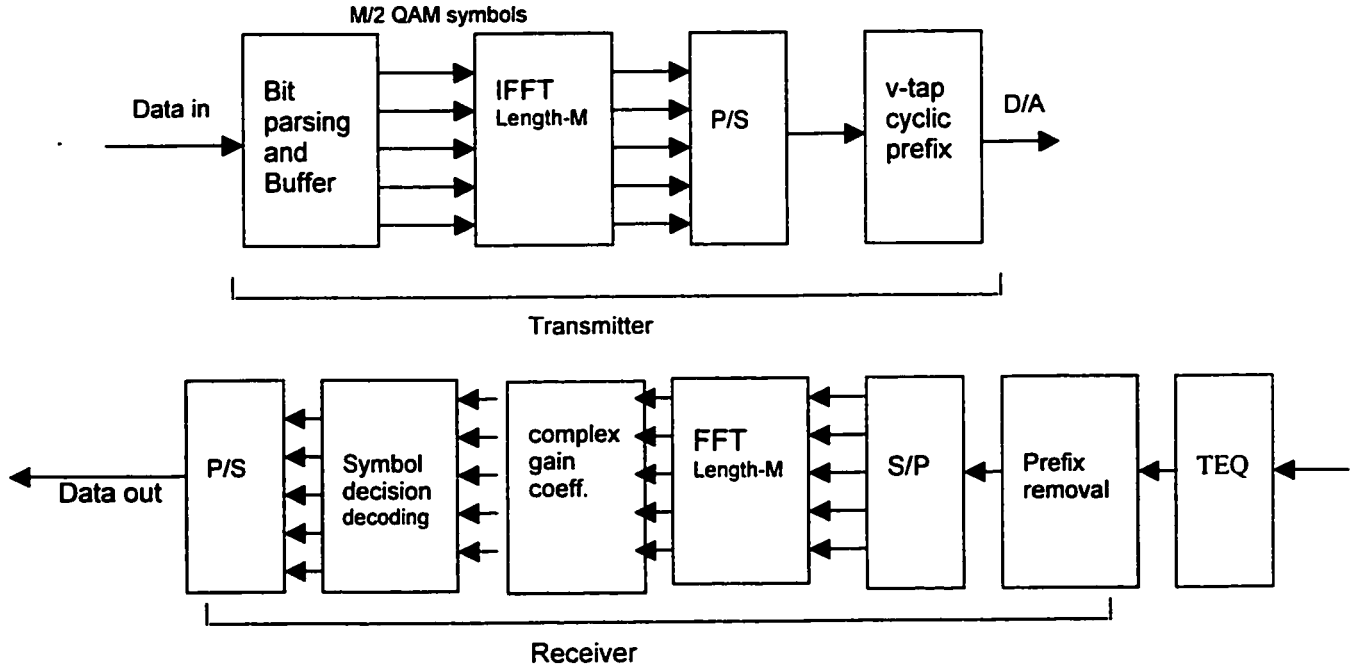

Figure 2.4: Block Diagram for DMT Transceiver

and equalized. The cyclic prefix is removed prior to demodulation. The equalized data on each subchannel is then sent through a decision device, where decisions are made for *Quadrature Amplitude Modulated* (QAM) symbols. The symbols are then decoded and converted back into a serial data output.

2.2.3 Equalization in DMT:

Equalization in a DMT system is performed in two stages, namely, pre-detection equalization and post-detection equalization. The pre-detection equalization takes place on the composite signal at the output of the channel. A TEQ is used for this purpose. The post-detection equalization, as the name suggests, takes place after demodulation or detection of the signal. At this stage, the signal is converted into individual streams of data symbols, and equalization is performed on symbols in each subchannel. Post-detection equalizers are termed as *frequency domain equalizers* (FEQ). Usage of both these types of equalizers is briefly discussed in the following section.

(a) Pre-detection Equalizer:

The impulse response duration of a typical ADSL channel could be quite large. If the duration of the channel impulse response is of the order of the inverse carrier spacing, a large cyclic prefix is required. The fraction of required overhead (with respect to data transmission) for a symbol block of length $N = M+\nu$, (where ν=length of the cyclic prefix) is equal to $\nu/N = \nu/(M+\nu) = (1+\nu/M)^{-1}$, resulting in a loss of the power and bandwidth efficiency by this factor. For high-speed transmission, the length of the cyclic prefix, ν, could be large [4,25].

In order to maintain a low percentage of overhead, it is required to increase the number of actual symbols in a block, M, so that the condition $\nu << M$ is satisfied. Sometimes, the minimum value of M required to satisfy this condition could be in the range of 10,000 samples or more, which could result into a number of problems, such as large memory requirement to store bit allocation tables and intermediate IFFT/FFT results, longer latency in processing, etc. Such a high latency may not be acceptable with some of the higher-level data protocols [4]. In order to avoid these problems and yet maintain a low overhead, it becomes necessary to shorten the length of the channel impulse response. This is achieved by using a TEQ immediately after the

data is sampled at the receiver end. The channel maybe assumed to act like a highly distorting and attenuating filter. The TEQ taps can be trained to overcome the channel distortion effects, thereby removing a certain percentage of ISI before the signal is demodulated. With some (or most) of the channel distortion nullified, the channel impulse response is effectively 'shortened'. Hence, the length of the cyclic prefix, ν, can be reduced and the corresponding value of M could be kept less than a thousand, making it possible to reduce the complexity and latency of the system. It then becomes possible to obtain high performance with the DMT system. It must be kept in mind, however, that the TEQ taps need to be trained at M times higher data rate as compared to the original data rate, which may not be trivial.

Several people in the past [4, 5, 8, 22] have discussed the implementation of a TEQ in a DMT system. The optimum performance for a given computational complexity can be achieved by choosing a TEQ that shortens the length of the channel impulse response such that it is equal to the length of the cyclic prefix [4,7]. The last M samples of the M+ν samples that correspond to the transmitted block are extracted from the output of the demodulator. These M samples are almost free of IBI.

(b) Post detection Equalizer

Using a TEQ in DMT simplifies the post-detection equalization to a great extent. This can be understood in terms of the role played by the cyclic prefix and circular matrices in a Fourier basis [2]. Akansu et. al. [2] have shown that after the use of a TEQ, the post-detection equalization process for a DMT system reduces to the adaptation of a single-tap complex coefficient for each subchannel. Let the coefficient for the k-th subchannel be denoted by w_k. If z_k denotes the corresponding sequence at the output of the demodulator, the resulting output

$$v_k = w_k z_k, \qquad k=0,1,2 \ldots\ldots M-1 \tag{2.7}$$

can then be decoded using a suitable decoder. The tap weight vector w_k is updated using the *Least Mean Square* (LMS) algorithm. The discussion above assumes the use of symbol-by-symbol detector in a DMT system. It may be possible to use a *Maximum Likelihood Sequence Estimation* (MLSE) detection scheme to obtain better results [26, 27].

2.3 THE DWMT SYSTEM

The DWMT is a specialized version of the generic design of a transmultiplexer with overlapping filters. The overall structure for the DWMT system is similar to the DMT system. The implementation complexity between the two is expected to differ, due to the difference between their modulation techniques. The following section briefly discusses the concept of wavelet transformation, followed by the structure of a DWMT transceiver.

2.3.1 Wavelet Transformation in DWMT

The theory of two-band compactly supported discrete wavelet bases was introduced by Ingrid Daubechies [28-30] and developed further by Meyer [31] and Mallat [32], in the context of multiresolution signal analysis. Two-band wavelets are well suited for voice compressing, image processing and analysis of low-frequency signals mixed with sharp transitions [33, 34], where one could isolate the high-frequency disturbances. However, it may not be suited for processing high frequency data signals with relatively narrow bandwidth, or a long RF pulse. , The M-band wavelets were introduced to overcome the inadequacy of two-band wavelets. These wavelets [15, 17] help 'zoom in' onto the narrow-band high frequency components of a signal, while simultaneously having a logarithmic decomposition of frequency channels. They are useful in signal analysis and also give better energy compaction than the two-band wavelets. A brief discussion of the two-band wavelets and their extension to M-band wavelets is given in the appendix –1 (A-1).

Construction of all kinds of wavelet filters is based on the concept of wavelet matrices [35, 36]. In general, a wavelet matrix **A** is an M×Mg matrix of complex numbers, where 'M' is the rank of the matrix and 'g' is called the genus or the overlap factor.

$$\mathbf{A} = \begin{pmatrix} a_0^{\,0} & a_1^{\,0} & a_2^{\,0} & & a_{Mg-1}^{\,0} \\ a_0^{\,1} & a_1^{\,1} & a_2^{\,1} & & a_{Mg-1}^{\,1} \\ & & & & \\ a_0^{\,M-1} & a_1^{\,M-1} & a_2^{\,M-1} & & a_{Mg-1}^{\,M-1} \end{pmatrix} \qquad (2.8)$$

The elements of this matrix are orthogonal, and correspond to complex numbers satisfying two orthogonality conditions, also called the wavelet scaling conditions:

$$\sum_{j=0}^{Mg-1} a_j^k = M\delta_{0,k} \tag{2.9}$$

and $$\sum_{j=0}^{Mg-1} a_{j+Ml}^k a_{j+Ml'}^{k'} = M\delta_{k,k'}\delta_{l,l'} \tag{2.10}$$

where the symbol $\delta_{i,j}$ is the Kronecker delta function which can be defined as follows:

$$\delta_{ij} = \begin{cases} 1, & \text{if } i = j \\ 0 & \text{otherwise.} \end{cases} \tag{2.11}$$

The first condition ensures that the elements of the first row of the wavelet matrix add up to M, while the elements of all the other rows add up to zero. The second condition implies that the rows are orthogonal to each other and to themselves by shifts of M. Hence, they can be shifted by integral multiples of M, overlapped and added.

The M rows of the matrix correspond to the M subchannels. The elements of the matrix could be related to the filter coefficients, in which case Mg =L denotes the length of the filter. The first row represents the low-pass filter and the rest of the rows represent the band/high-pass filters. If the analysis filter bank coefficients for the k-th subchannel are denoted by $h_k(n)$, then

$$a_k^j = (\sqrt{M})\, h_k(j), \tag{2.12}$$

where k=0,1..M-1 and j=0,1...Mg. The above relationship is also valid for the coefficients of a synthesis filter bank, $f_k(n)$. Both M and g take on integer values. A higher value of M results in narrowly spaced frequency subchannels. This is expected to be more robust for transmission over longer distances, if the implementation complexity is manageable. The recommended value of M for DSL transmission is typically from 256-512 subchannels.

Large values of g imply that symbols can be represented by a long signaling vector and yet be overlapped by shifts of M to maintain the same information throughput as the non-overlapping case. The larger the value of g, the longer will the length of the modulated symbol be in the time

domain, making it more immune to channel distortion. In principle, this overlap does not result in any mixing of information between adjacent blocks

The DWMT transmitter needs an M-band wavelet filter bank for performing modulation/ demodulation on M subchannel signals. There exist certain maximally decimated M-band filter banks which obey the orthogonality criteria of wavelet transforms, namely the regular M-band Wavelet Transform [17], *Lapped Overlapped Transform* (LOT), extended LOT [37], cosine modulated M-bank filter banks [14, 16, 38, 39] etc. Koilpillai and Vaidyanathan [16] designed pseudo-QMF filter banks of length N=gM for different values of g, which satisfy the above orthogonality criteria and are suitable for use in a DWMT system.

2.3.3 Structure of DWMT Transceiver

The block level diagram for a DWMT transceiver is presented in Fig. 2.5. The transmitter (starting from the left hand side of the figure) accepts data in the form of a serial, TDM stream of higher rate information bits. This stream is passed through a serial/parallel converter, giving M lower bit rate data streams. These lower bit-rate streams are converted to M sequences of *Pulse Amplitude Modulated* (PAM) symbols, which are up-sampled by M and modulated through an *Inverse Fast Wavelet Transform* (IFWT) matrix realized by an M-band synthesis filter bank.

Let us consider the transmission of data blocks in the time domain. Let time be partitioned into equally spaced 'frames'. Each data block is transmitted over a few time frames, starting at the time index 'i' and ending at the time index 'i+gM-1'. The duration of each time frame = M/F_s, where M is the number of subchannels and F_s is the sampling frequency. Let

s_i^m - symbol transmitted through subchannel 'm' starting at the time index 'i'

f_l^m - impulse response for the subchannel 'm'.

f_l^m is a pass band pulse waveform (elements of the IFWT), given by:

$$f_l^m = p_0(l) \cos(w_m l - \phi_m), \qquad (2.13)$$

where the base band pulse $p_0(l)$ corresponds to the prototype filter and is common to all the subchannels. The band pass pulses are obtained through cosine-modulation of the base-band pulse. Each f_l^m has non-zero values only from l=0,1.. gM-1, where 'l' corresponds to the length

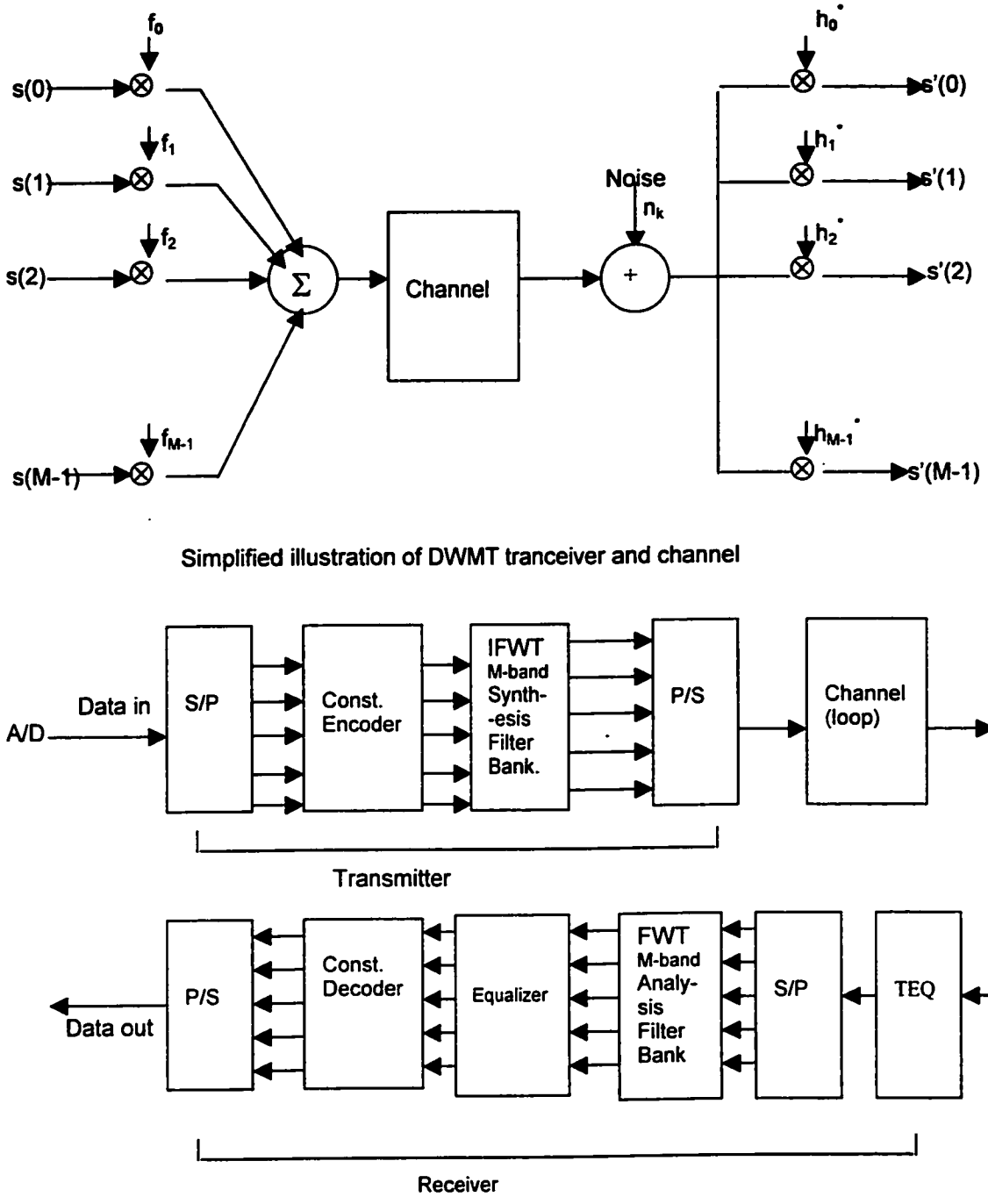

Figure 2.5: Block diagram for a DWMT transceiver

of the prototype filter. Orthogonality between band-pass pulses is achieved by setting a particular constraint that the set of pulses f_l^m, $0 \leq m \leq M$ and their time-shifts by integral multiples of M provide a set of orthonormal waveforms for transmission. This means that the coefficients f_l^m satisfy the wavelet scaling conditions given by the equations (2.9) and (2.10).

Making a change of variables in equation (2.10) and using equation (2.12), we have

$$\sum_{m=0}^{M-1} f_l^m f_{l-iM}^{m'} = \delta_i \delta_{mm'} \tag{2.14}$$

The symbol at the input of each subchannel is modulated by the corresponding subchannel pulse waveform. These M subchannel waveforms are added to give a single sequence x_l for transmission. The sequence at the output of modulator is given by:

$$x_l = \sum_{i=-\infty}^{\infty} \sum_{m=0}^{M-1} s_i^m f_{l-iM}^m \tag{2.15}$$

The sequence x_l is used to excite the composite channel (D/A converter + copper twisted pair + A/D converter) at the rate of F_s samples/sec. Let 'i' denote a particular frame of interest. Every symbol in the g frames starting from i, i-1,.... i-g+1 contribute to the segment of x_l that is transmitted during the i-th time frame. Since the symbols in the M subchannels are transmitted simultaneously, the buffer size for a DWMT transceiver must be equal to gM.

At the receiver end, the signal is down sampled by M and demodulated using elements of the *Fast Wavelet Transform* (FWT) matrix realized by an M-band analysis filter bank. The signal could be equalized either prior to or/and after demodulation. The DWMT receiver decodes the symbol s_i^m in the m-th subchannel by incorporating samples from each of the g time frames (mentioned above), to retrieve the original data stream.

2.4 DMT versus DWMT

Most of the differences between the DMT and the DWMT systems arise due to the difference in the modulation techniques used by them. The resulting impact on the length of the symbol

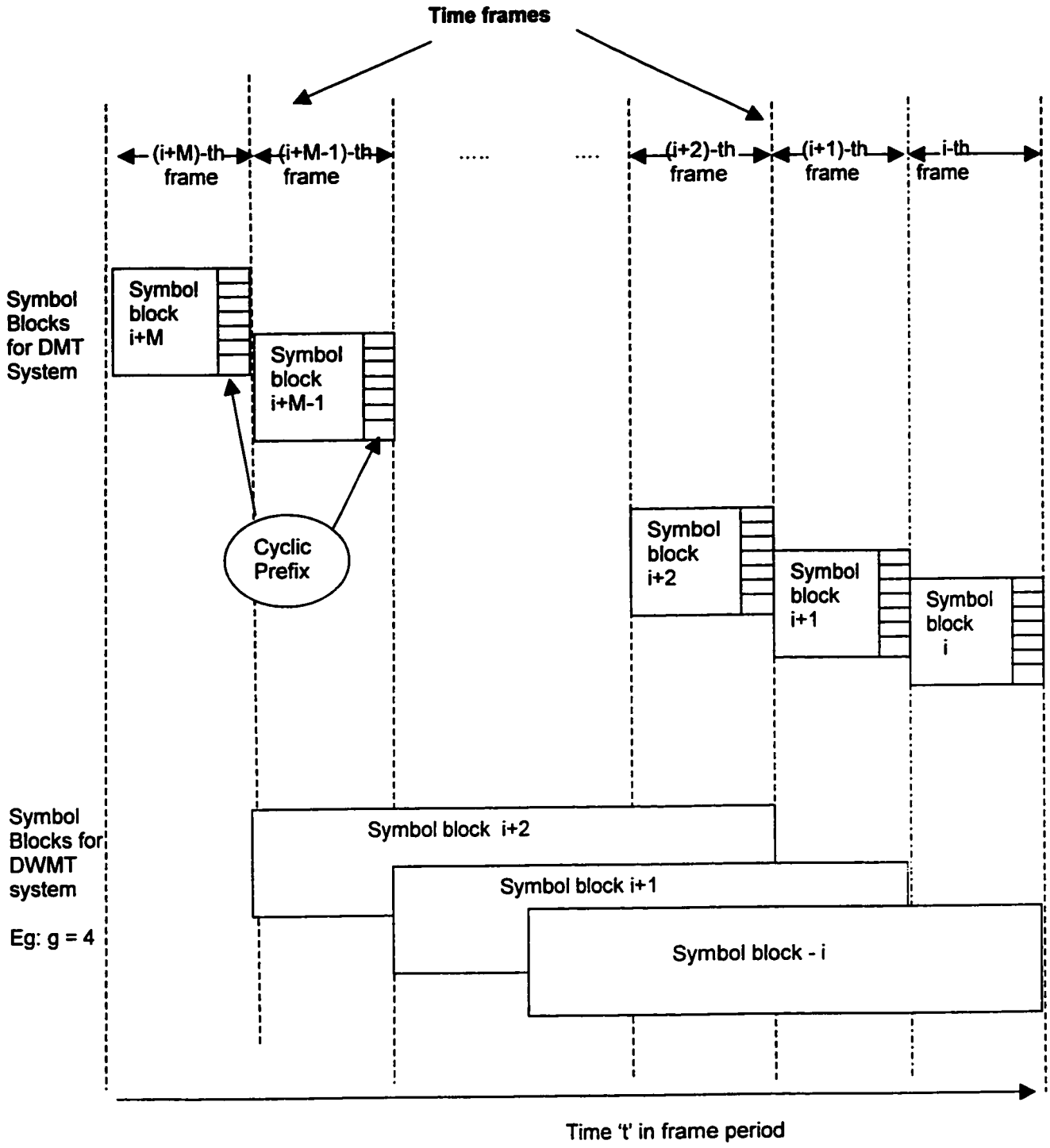

Figure 2.6: Timing diagram for length-M DMT blocks and length-gM DWMT blocks

blocks, including the use of cyclic prefix between DMT blocks is shown in Figure 2.6. In this figure, time is represented in terms of 'frames'. It is assumed that one DMT block covers one time frame. The corresponding DWMT block, for overlap factor g=4 would then cover 4 time frames, and subsequent blocks would be separated by one frame, under the assumption that the adjacent blocks have been shifted by a block of M samples and then overlapped.

Some of the advantages of DWMT over DMT are listed below:

1. In a DWMT system, the freedom to choose the overlap factor g allows a greater flexibility in choosing the length of the modulating filter. The longer the length of a filter, the sharper would the pass-band to stop-band characteristics be, giving more energy in the main lobe and leading to better frequency domain characteristics.
2. Despite the fact that resulting length of DWMT blocks would be longer than DMT blocks, there is no increase in latency in transmission, since DWMT blocks can be overlapped by shifts of M and transmitted. The information throughput rate of an M-band DWMT system would therefore be the same as an M-band DMT system.
3. In a DMT system, due to poor orthogonality characteristics between adjacent subchannels of a DFT filter bank, there arises the need to separate the blocks through cyclic prefix. Orthogonality characteristics for the filter bank used in a DWMT system can be improved by increasing g, for example, thereby forgoing the need to use any guard band between the symbol blocks.
4. Longer symbol duration indicates lesser distortion resulting from the analog channel. For the same number of subchannels (M) in both systems, the DWMT system would be more robust as compared to the DMT system.
5. Due to lesser channel distortion, the time domain equalization becomes simpler.
6. Due to a high level of spectral containment in the frequency domain, lesser ICI is expected in DWMT than DMT.
7. There is some indication [7] that the DWMT system is less susceptible to *Additive White Gaussian Noise* (AWGN) as compared to the DMT system.

In conclusion, the DWMT system can be considered to be a better alternative to DMT when dealing with very high data speeds, which a DMT-based communication system is unable to handle. Although the design of a DWMT system may require more memory for storing the information of longer symbol blocks and could also be more complex as compared to a DMT system, using a DWMT system results in lesser inter-symbol interference, greater noise suppression, and therefore more robustness as compared to a DMT system.

CHAPTER 3

EQUALIZER DESIGN FOR DISCRETE WAVELET MULTITONE

This chapter describes the receiver design for a DWMT system. The first section gives the rationale behind the current research, followed by a discussion of certain theoretical aspects for the current design. The plausible equalizer designs for the receiver structure are also presented and discussed in this chapter.

3.1 RATIONALE FOR CURRENT RESEARCH

The goal behind the current research involving MCM-based DWMT is to develop a transmission technique capable of enhancing the performance of high speed data transmission of existing twisted pair lines, so as to increase the maximum achievable data rate on the *carrier server area* (CSA) loops which carry about 80% of the lines between the central office and the customer premises. MCM is useful from the point of view of higher bandwidth utilization, accessibility and distribution of several multiplexed data streams and making the system more immune to channel distortion as compared to single carrier modulation.

However, the equalizer design for the transceiver systems based on MCM could still be a challenge, due to the large amount of signal degradation at the receiver end caused by the twisted pair channels. As mentioned earlier, the attenuation loss of a typical twisted pair channel varies sharply with the frequency and the phase response is mostly non-linear giving rise to a considerable amount of distortion to signal. The output waveforms corresponding to the modulated data signals transmitted through the channel could be corrupted and transformed. The band-pass pulses of the modulating data symbols in different subchannels could lose their orthogonality, resulting in the non-linearity of the received signal in the form of frequency translation, nonlinear distortion and time dispersion [40]. A symbol transmitted in a certain time period could extend over into the time slots of adjacent symbols, ultimately

resulting in a significant amount of ISI, which is one of the major obstacles for reliable high-speed data transmission over twisted pair.

Higher speed requirements for VDSL transmission make it important to use effective equalization methods in order to combat interference. Existing techniques such as single-carrier modulation based *Carrier Amplitude Phase* (CAP) modulation, QAM or multi-carrier modulation based DMT may not function for VDSL, as equalization requirements for both are stringent and the implementation complexity of the equalizer might become unmanageable at the desired data transmission speeds. Hence, new techniques need to be examined and optimized. One such technique, which is also multi-carrier based but uses a better modulation procedure than DMT is DWMT.

The concept of DWMT modulation was introduced by Sandberg et.al. [7] in 1995. They use cosine-modulated M-band filter bank with an overlap factor of g=8 for modulation. To combat ISI, they use an optimum post-detector combining scheme based on *multiple input/multiple output* (MIMO) design at the receiver end, which is a generalisation of the linear equalization schemes used for single channel serial data transmission systems. The decision statistics for a given symbol is obtained by linearly combining detector outputs from several frames. Settings are derived to maximize the *signal to interference noise ratio* (SINR) and obtain a unit gain for the desired symbol.

A similar contribution towards the structure of a receiver for high-speed data transmission was made recently by Vanderdorpe et.al [25]. They attempted to examine the possibility of using a *single input/multiple output* (SIMO) linear detector, without using the analysis filter bank for demodulation at the receiver end. They have considered a receiver structure optimised for MLSE, by using a symbol-spaced and fractionally spaced *linear equalizer* (LE) and *decision feedback equalizer* (DFE). They claim that the feed-forward part of the equalizer is a modified filter bank that works at a higher rate and provides optimum performance, i.e, it is able to minimize ISI and noise power by reducing the average mean squared error.

Although, both the above groups claim to succeed in obtaining good performance out of their system designs, the receiver structure and the post-detection schemes used in their systems are considerably complex. The first group has focused on using a highly complex post-

detection scheme, claiming that pre-detection equalization doesn't work. The second group has forced the equalizer to function as a demodulator-equalizer combination filter operating at a very high rate on all subchannels, which makes each of the subchannel equalizers very complex. In this thesis, we investigate the possibility using a simpler receiver structure.

The transceiver design used in this thesis is based on the technique introduced by the first group [7]. The modulation scheme used here is similar to their modulation scheme. However, we follow a different approach to tackle the ISI. Instead of using a post-detection combiner, attempt is made to use a combination of TEQ and FEQ to recover the data symbols accurately.

The next section discusses the theoretical concepts related to the current design of the DWMT transceiver. Details of the receiver design incorporating the TEQ and the FEQ are discussed in the third section of this chapter.

3.2 THEORETICAL ASPECTS OF CURRENT DESIGN

As mentioned earlier, bit allocation is an important concept in multi-carrier modulation. The number of bits allocated depends upon the type of modulating scheme (PAM, QPSK or QAM) used for data modulation. The first sub-section gives a derivation of the number of bits allocated per PAM symbol (used in the DWMT system here), starting from the assumption of equal symbol error rates on all subchannels. The next sub-section includes a discussion on symbol recovery statistics. The final result of the symbol decision statistics involving the contribution of the different interfering coefficients is given and discussed. Although a similar result is outlined in [7], a more extensive and explicit derivation of this result is carried out, which is given in the appendix.

3.2.1 Bit allocation for M-ary PAM subchannel

A multi-carrier signal has two variables that are allotted to each subchannel, namely, the number of bits per symbol m_k and the proportion p_k of the total transmitted power, P. The proportion of power p_k allocated to each subchannel is based on Gallager's water-filling algorithm on channel capacity [24]. We follow the approach used by Irving Kalet [41] and Lee

et.al. [4] to derive an expression for power and bit allocation for multitone M-ary PAM signalling that is used in DWMT.

This approach optimises the power distribution between the tones (carrier frequencies) and the number of bits/symbol per tone for a fixed value of the symbol error rate common to all the subchannels. The total transmitted power for M subchannels can be expressed as [42].

$$P = \sum_{k=1}^{M} p_k \,. \tag{3.1}$$

If T denotes the symbol period, then p_k/T denotes the energy per symbol $\varepsilon_{s,k}$. In the presence of AWGN with spectral density N_0, the SNR (γ_k) per symbol is given by

$$\gamma_k = SNR_k = \varepsilon_{s,k}/ N_0 \tag{3.2}$$

The number of bits allocated to any given subchannel can now be expressed in terms of the SNR of that particular subchannel [4], for a desired value of symbol error rate. For M-ary PAM signaling, the probability of symbol error P_M^e can be expressed as [41]

$$P_M^e = \frac{2(M-1)}{M} Q\left(\sqrt{\frac{6\varepsilon_s}{(M^2-1)N_0}}\right), \tag{3.3}$$

where $M = 2^m$ for m bits per symbol and ε_s/ N_0 is the average SNR per symbol.
The probability of symbol error for the k-th subchannel can therefore be written as

$$P_{M_k}^e = \frac{2(M_k-1)}{M_k} Q\left(\sqrt{\frac{6\gamma_k}{M_k^2-1}}\right), \tag{3.4}$$

where M_k corresponds to the alphabet size for k^{th} subchannel. We need to obtain an expression for $m_k = \log_2 M_k$. For large values of M_k, we can approximate M_k-1~ M_k, so that $2(M_k-1)/M_k \sim 2$. In that case, the above equation can be easily inverted, giving

$$\frac{6\gamma_k}{M_k^2-1} = \left[Q^{-1}\left(\frac{P_{M_k}^e}{2}\right)\right]^2. \tag{3.5}$$

Finally, we obtain

$$M_k = \left(1 + \frac{6\gamma_k}{\left[Q^{-1}\left(P^e_{M_k}/2\right)\right]^2}\right)^{1/2}, \tag{3.6}$$

so that the number of bits per subchannel is given by

$$m_k = \log_2(M_k) = \frac{1}{2}\log_2\left(1 + \frac{6\gamma_k}{\left[Q^{-1}\left(P^e_{M_k}/2\right)\right]^2}\right). \tag{3.7}$$

For a constant symbol error rate of 10^{-7},

$$m_k = \frac{1}{2}\log_2\left(1 + 0.206\gamma_k\right) \tag{3.8}$$

Fractional values of m_k are rounded off to the nearest integer. The result is slightly different for M-ary QAM transmission [4]. In the absence of coding, the numbers of bits are usually allocated in the range 1-8. In the presence of coding [4], it may be possible to exceed 8 bits.

A training signal is first transmitted with equal power and bit assignments in all subchannels. The receiver measures the SNR (γ_k) of each subchannel and sends this information back to the transmitter. With this information, the transmitter proceeds to calculate the bit assignments of subchannels.

3.2.2 Symbol Recovery at Receiver End

Isolation of desired symbol at the output of a DWMT receiver is slightly more complex as compared to the DMT system. This could be due to the presence of the overlap factor 'g' in a DWMT system. The length of the modulating vector for each subchannel increases by this factor, leading to increased length of each symbol block, and undesirable ISI components at the demodulator end in the presence of a distorting channel. Decision for a symbol s_{i1}^{m1} in the i1-th block is made based on the contribution from g blocks starting at i1 and ending at i1+g. The detector output θ_{i1+g}^{m1} corresponding to the desired symbol s_{i1}^{m1} unfortunately has

contributions from several other subchannels (m2 ≠ m1) and blocks (i2 ≠ i1), giving rise to different types of ISI. Explicitly, the detector output can be expressed as a combination of all these desirable and undesirable outputs as:

$$\theta_{i1}^{m1} = \sum_i \sum_m s_i^m \sum_j h_{j+d} \sum_l f_l^m f_{l-(i1-i)M+j}^{m1} + \sum_i \sum_j \sum_l n_{l+j+d+iM} f_{l-(i1-i)M+j}^{m1} \quad (3.9)$$

$$= \sum_i \sum_m s_i^m \alpha_i^m + \chi \quad (3.10)$$

where χ (the second term in equation 3.9) is the noise term and α_i^m is the coefficient of the symbol s_i^m given by:

$$\alpha_i^m = \sum_j h_{j+d} \sum_l f_l^m f_{l-(i1-i)N+j}^{m1}. \quad (3.11)$$

A detailed derivation of equation (3.9) is given in the Appendix A-2. The desired symbol in the summation on the right hand side of equation (3.9) is s_{i1}^{m1}, since, in principle, only one of the coefficients corresponding to the pair (m_1, i_1) should have non-zero contribution. Hence except for α_{i1}^{m1}, all other non-zero $\{\alpha_i^m: i \neq i1 \text{ and } m \neq m1\}$ give rise to ISI. Under ideal circumstances, if the equalization is perfect, then $h_j = \delta_{j,0}$, which takes care of summation over j. If the pulses are perfectly orthogonal, the value of α_i^m would indeed be zero for all $i \neq i1$ and $m \neq m1$.

Unfortunately, channel distortion is not negligible and subchannel pulses are not orthogonal. Symbols in same block as i1 give rise to ICI, whereas symbols in same subchannel as m1 give rise to IBI. Symbols that contribute non-zero energy gives rise to ICBI. Equalization of the signal becomes essential to mitigate the effect of interference caused as a result of all of these.

Since any form of ISI results from channel distortion, the extent to which the contribution from the interfering symbols would vary, depending upon the channel. It may not be possible from an implementation point of view to completely invert the effect of the channel distortion. However, it is always possible to compensate for some of the channel distortion immediately after receiving the signal from the channel, by using a TEQ, which essentially 'shortens' the

channel impulse response. The FEQ, which operates on each demodulated signal, is expected to eliminate the residual ISI. If the taps of the equalizers are effectively trained, any further complexity in the receiver consisting of post-detector combiner or MLSE detector may not be required. The next section discusses the receiver structures designed in this thesis, using the TEQ and the FEQ.

3.3 PLAUSIBLE DESIGNS FOR DWMT RECEIVER

In order to determine whether any one of the two types of equalizers, *i.e.*, either the TEQ or the FEQ is sufficient to equalize the signal, we examine three different receiver structures consisting of these equalizers used individually and in combination with each other. These structures are discussed below.

3.3.1 Plausible Design #1

This design includes (Figure 3.1) a TEQ followed by the demodulator.

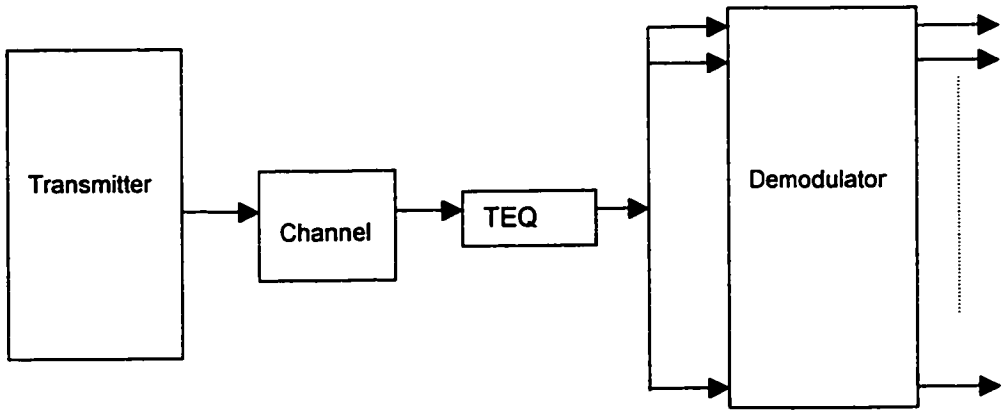

Figure 3.1: Plausible Design #1-only TEQ for DWMT receiver

The above system is based on the design of the DMT receiver, except for the fact that in this design, no single-tap post-detection equalizers are employed. The demodulated outputs of the subchannels are directly passed through the slicer. It is expected that the structure of the TEQ might be at least as complex, or even more complex than the TEQ employed in a DMT system. This complexity could arise due to the fact that the VDSL channel is expected to cause a greater channel distortion than an ADSL channel. The number of taps required to

invert such a channel could be very large. Apart from the complexity, training many taps could cause a convergence problem at the rates at which the TEQ is expected to operate and increase the latency of the system.

3.3.2 Plausible Design #2

In the second plausible design, the TEQ is totally removed, and an altogether new design is attempted, consisting of M post-detection FEQs at the output of each subchannel after demodulation. The received signal is at first demodulated and equalized later. Figure 3.2 gives the block diagram of this system.

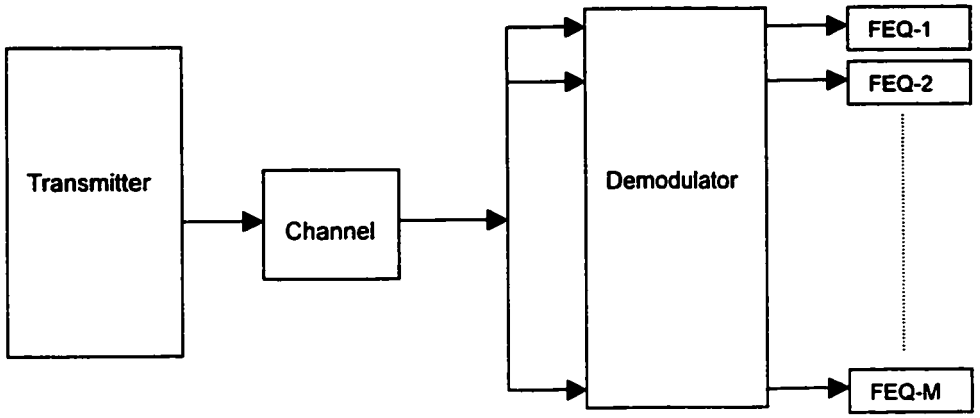

Figure 3.2: Plausible Design #2 for DWMT receiver

For this particular design, since no equalizer is used in the time domain to mitigate the effects of channel distortion prior to demodulation, the entire distortion is transformed in the frequency domain. Therefore, the output of the demodulator is expected to be highly distorted, depending upon the channel. The signals are expected to have considerable amount of ISI. The FEQs would be employed at each subchannel, and are expected to require several taps for equalization of the signal. The situation could get worse for the higher frequency subchannels, which are severely affected by channel distortion. In addition, there could arise problems with the implementation of M different highly complex equalizers.

3.3.3 Plausible Design #3

The third design is a combination of both the designs discussed above. This structure consists of a simple TEQ (labelled as TEQ' to indicate a simple or a fewer-taps TEQ) and simple FEQs (labelled as FEQ'). The TEQ' in this structure is expected to be a simple *finite*

impulse response (FIR) filter, consisting of less than 50 taps. It is expected to play a less demanding role as compared to that of a TEQ in the plausible design #1. The main purpose of using this equalizer is to cancel the phase distortion (which may be extremely difficult to handle after demodulation) and roughly remove some ISI due to channel distortion. Attempt is made to eliminate the rest of the ISI the signal by using a simple FEQ' at the output of each subchannel. Figure 3.3 shows this structure of the receiver incorporating both these equalizers.

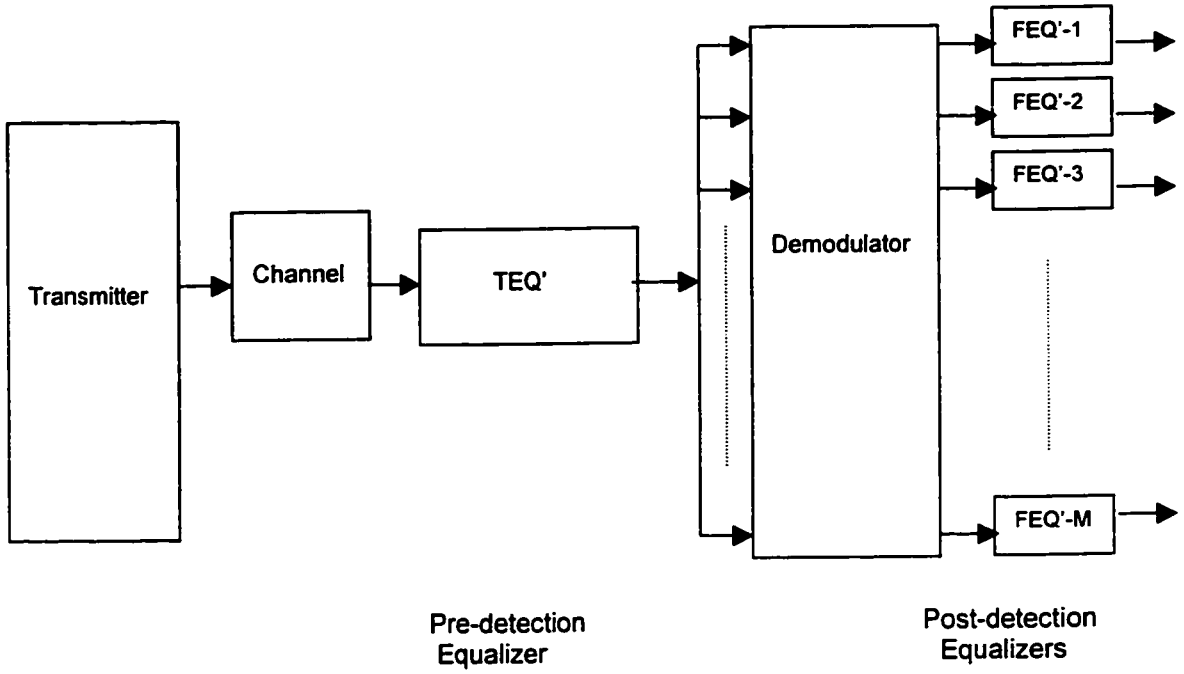

Figure 3.3: Plausible design #3 for the DWMT Receiver

It is expected that the number of taps employed in the FEQ' would also be few (5-15) so that the implementation complexity of both the TEQ' and the FEQ' would be manageable even at higher speeds and longer distances.

The TEQ employs an LE, since it operates on sample sequence that does not correspond to data symbols. The data at the output of the demodulator does correspond to actual data symbols; hence the slicer is used at the post-detection stage for symbol detection. This

makes it possible to perform non-linear equalization in addition to linear equalization at the post-detection stage. Therefore, symbol-spaced LE and DFE are used as FEQs.

The third structure is expected to have the following advantages over the previous structures:

(1) The complexity and the latency of the TEQ would be minimal and manageable, as it has a fewer number of taps as compared to the only-TEQ system.

(2) Once the phase distortion in the signal is removed with the TEQ and the demodulated signals are partially equalized, the expected complexity in the FEQ would also be low, sufficient to remove the residual ISI.

(3) It is easier to optimise the system design by playing with the number of taps in both the TEQ and the FEQ, so that complexity of the equalizers could be balanced, based on the channel requirement.

All the three plausible receiver structures are simulated with different number of taps in the TEQ and the FEQ, and tested out for different ADSL channels. Results of simulation are presented in the next chapter.

CHAPTER 4

RESULTS AND DISCUSSION

This chapter presents a brief review of the different designs under consideration for a DWMT receiver and the criteria used for the performance analysis, followed by a description of the procedure used for carrying out the simulations. The chapter describes the channel models used for testing the system and presents the results of simulating the three receiver designs using these channel models. A discussion of the results of simulations is presented for each case, followed by a summary of all results

4.1 DESIGN REVIEW

A DWMT communication system is designed with M=32 subchannels in order to keep it computationally simple and feasible. Data modulation and demodulation is performed using the M-band cosine modulated filter bank. Three different plausible receiver structures (described in the previous chapter) are simulated and compared with each other. Plausible receiver #1 uses only a TEQ, followed by the demodulator and a slicer for every subchannel at the output of the demodulator. Plausible receiver #2 consists of the demodulator followed by FEQs and slicers for every subchannel. Plausible receiver #3 consists of two-stage equalization process. The first stage (pre-detection equalization) is carried out using a very simple TEQ that has 11-41 taps. The second stage (post-detection equalization) is carried out using simple FEQs having 3-15 taps. The TEQ employs an LE, whereas two different types of equalizers have been tested as FEQ, namely the LE and the DFE.

All the three receiver structures are tested for three different twisted pair channels. Characteristics of these channels are presented and discussed in the next section.

4.2 DESIGN METHODOLOGY

This section discusses different components and requirements that are used for the design and simulation of the DWMT system. The first sub-section discusses the optimisation criterion and the algorithm used for the design of the equalizers, followed by a description of the filter-bank

used for modulation. The last part of this section presents a brief description of the actual simulation technique, along with a flow chart displaying the simulation process.

4.2.1 Criterion and Algorithms

It is very important to choose the right criterion and algorithm for the optimization and convergence of the equalizer taps, depending upon the requirement of the system. Two criteria are extensively used for optimization of the equalizer taps, namely the *peak distortion* (PD) criterion and the *minimization of mean squared error* (MMSE) criterion [43]. An equalizer based on the peak distortion criterion is called the *zero-forcing* (ZF) equalizer, as it maximizes the contribution from the symbol of interest and forces the coefficients of all other symbols to be zero. Such an equalizer is not suitable for noisy channels, as it could enhance the additive noise in the process of eliminating ISI. In the MMSE criterion, the equalizer taps are adjusted to minimize the mean squared difference between the desired symbol and the estimate of the symbol at the output of the equalizer.

Equalizers based on the MMSE criterion give optimum performance without noise enhancement, and are therefore more suitable for noisy channels. The equalizers for this project therefore use the MMSE criterion for tap estimation.

The equalizer is adaptive, and operated in two different modes namely, the training mode and the decision-directed mode. There exist different algorithms to carry out the process of adaptation of tap weights. The most commonly used is the *least mean square* (LMS) algorithm, which has the least complexity in terms of the number of computations required for a given number of tap coefficients. The convergence for LMS however, is slow. Other procedures include the *recursive least square* (RLS) algorithm and the *direct matrix inversion* (DMI), which have greater complexity, but a faster convergence.

Since a longer training signal can increase the latency of the system, it is important to keep the length of the training signal as short as possible, as long as the equalizer converges within the given length. A detailed discussion on adaptive equalization and the convergence of different algorithms can be found in [42,43] and [44]. For this thesis, the RLS algorithm is employed for carrying out the equalization process, owing to its rapid convergence rate.

4.2.2 Design of the Filter Bank

The prototype filter of the cosine modulated filter bank is taken from the pseudo-QMF filter bank designed by Koilpillai and Vaidyanathan [39]. This type of filter bank has the advantage [14] that all the analysis and synthesis filter bank coefficients can be obtained from cosine modulation of a single prototype filter. This drastically reduces the number of parameters that need to be optimized at the design phase of the filter. Cosine-modulated filter banks are therefore easier to implement than some other type of overlapped M-band transforms that could also be used to realize Wavelet Transform. Besides, they offer equally good perfect reconstruction properties.

The impulse response coefficients of the analysis $h_k(n)$ and synthesis $f_k(n)$ filters are obtained by the cosine modulation of a linear-phase, low-pass prototype filter having the impulse response $p_0(n)$, in the following manner:

$$h_k(n) = 2p_0(n)\cos\left(\frac{\pi}{M}(k+0.5)(n-\frac{N}{2})+\theta_k\right) \tag{4.1}$$

and

$$f_k(n) = 2p_0(n)\cos\left(\frac{\pi}{M}(k+0.5)(n-\frac{N}{2})-\theta_k\right), \tag{4.2}$$

where $\theta_k = (-1)^k \pi/4$. The analysis and synthesis filters are related as [15,39]

$$f_k(n) = h_k(N-1-n) \text{ and } F_k(z) = z^{-(N-1)} H_k(z) \qquad 0<k<M-1, \tag{4.3}$$

where $F_k(z)$ and $H_k(z)$ correspond to the transfer functions of $f_k(n)$ and $h_k(n)$ respectively. The prototype filter [45] is of length L=160, which corresponds to an overlap factor of g=5. This causes each of the 32 analysis and synthesis filters also to have 160 impulse response coefficients. The design of the filter bank is such that the overall transfer function of the analysis/ synthesis system has a linear phase, even though the individual synthesis and analysis filter banks do not have a linear phase. Figure 4.1 shows the frequency responses for subchannels 13-20.

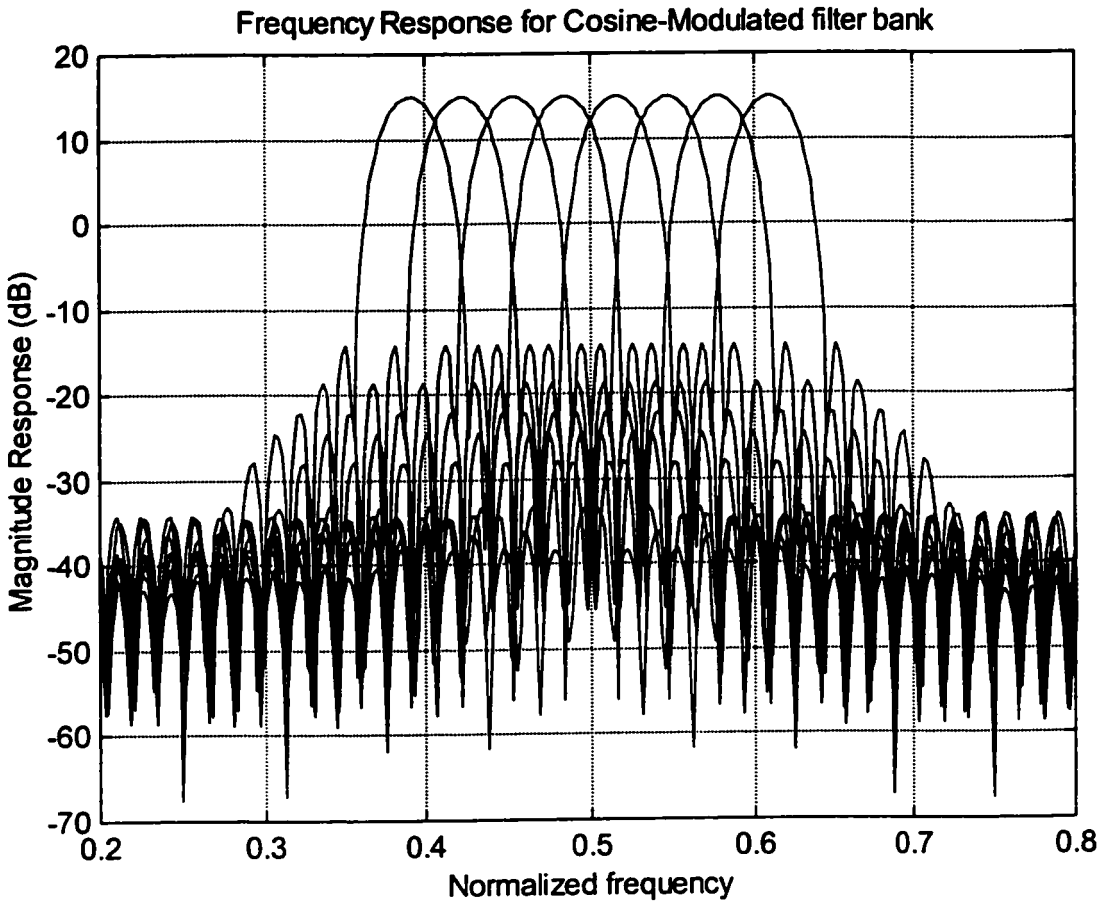

Figure 4.1 : Frequency Response for Cosine-modulated filter bank for Subchannel : 13 - 20

4.2.3 Simulation Technique

The bit-size for each subchannel is obtained using adaptive loading. Once the numbers of bits with reference to a particular channel are allocated, the DWMT system is run with these known bits. The simulation process is explained in Figure 4.2.

The process of bit allocation is carried out in the following manner. At first, all the subchannels are equally loaded with the highest number of bits desired to be transmitted. The input symbol sequences are modulated using coefficients of the synthesis filter bank and transmitted through the channel, by convolution of the signal samples with the impulse response coefficients of the channel. Noise samples are calculated using the noise power at –140 dBm/Hz [46] and added to the signal for certain cases. At this stage, the channel and/or noise-distorted frequency division multiplexed signal is equalized using a TEQ. The TEQ taps are trained using a training sequence of about 3000 samples. The output of the TEQ is demodulated using coefficients of the analysis filter bank. The output of the analysis filter bank is in the form of M=32 subchannel unsliced symbol sequences. In the absence of a TEQ, the distorted signal is directly demodulated. However, since the channel attenuates the signal tremendously, the signal is amplified to match the largest (in magnitude) output symbol with the largest input symbol, for each of the M=32 subchannels. This amplification process is redundant in the presence of a TEQ, since the TEQ taps amplify the signal anyway.

A distinction is made between the noise due to channel distortion (termed here as interference noise) and the AWGN added to the signal after channel. In cases where only the interference or channel noise is considered, the bit allocation is derived from SINR. If AWGN is also included, then the bit allocation is derived from SNR, which includes the total (interference + AWGN) noise power. This terminology is adopted from [7]. Signal power is measured prior to modulation and after demodulation, from which the SINR and SNR values for each subchannel are deduced. The actual signal power (for both transmit and received signals) is measured in watts. The noise power is obtained as a difference between transmitted and received signal power. The output SINR and SNR are then calculated as the ratios between the received signal power and the noise power. The bit-rate for each subchannel is calculated using Equation 3.5.

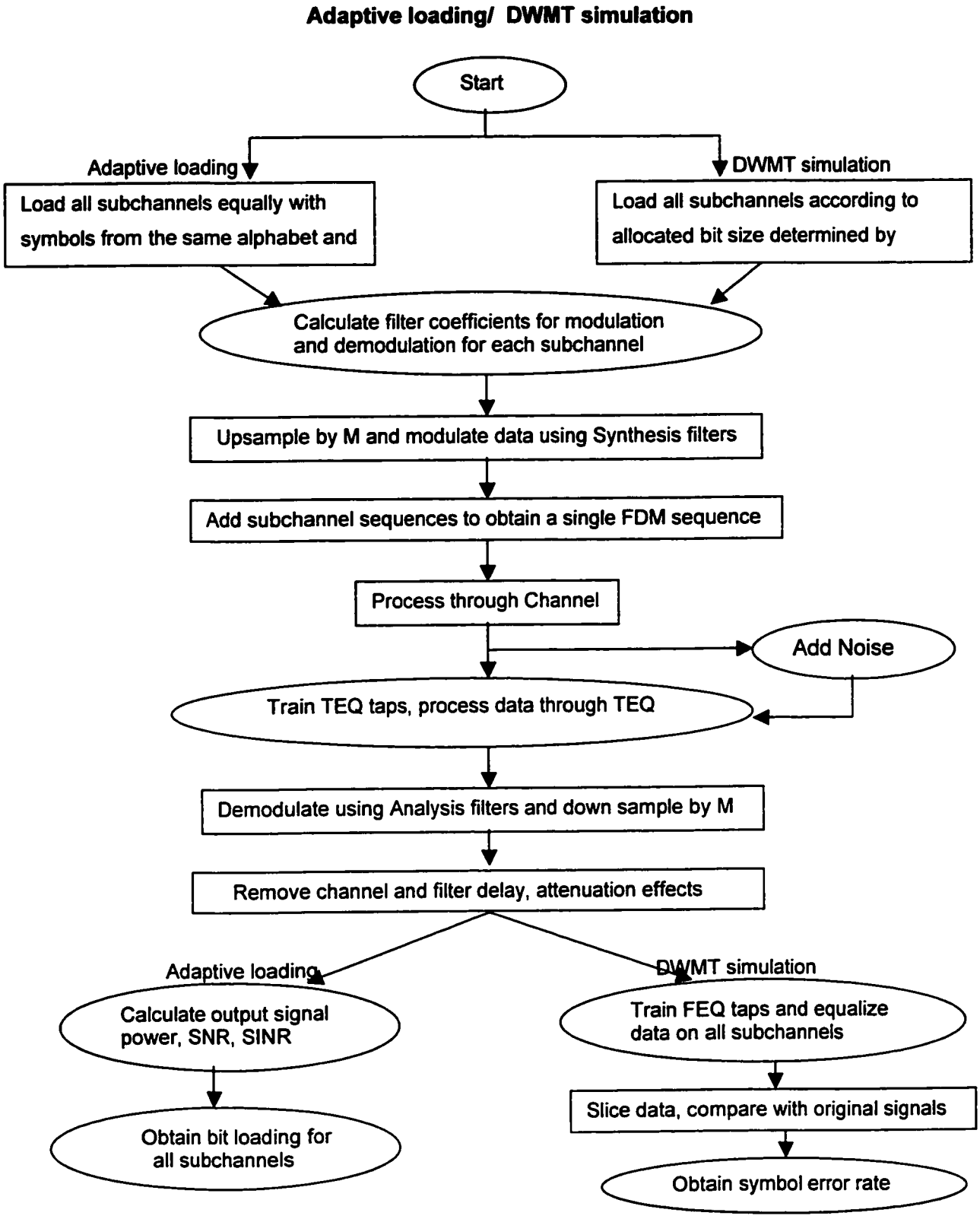

Figure 4.2: Flowchart for Adaptive loading and a regular DWMT simulation

A regular DWMT simulation is similar to the process of adaptive loading, except for the fact the subchannels are now loaded according to the allocated bit size. The entire simulation (starting from adaptive loading) is repeated for different channels, with different number of taps in the TEQ. The output of the demodulator corresponding to a particular number of taps in the TEQ is used with different number of taps in the FEQ. Mostly, the taps of the FEQs are expected to converge within 500 symbols. However, some subchannels might require more time to converge for this value of λ. Hence, the following sets of parameters were used (for all subchannels and channels):

Length of the training signal = 700 symbols

Step size parameter λ = 0.99.

The criterion for a performance evaluation of the receiver is based on the minimization of the *Symbol Error Rate* (SER) at the output of the demodulator A comparison is made between the SERs corresponding to the outputs of the demodulator (with or without TEQ) and the output of the FEQ.

4.3 CHANNEL MODELS

Among the different types of wire gauges used for twisted-pair transmission, the 26-AWG copper loop is commonly used for shorter distances. For longer distances, a heavier gauge wire can be used to avoid excessive loop resistance. A detailed description for transmission on twisted pair is given by Cioffi et.al. [40]. In total, three different channels were modelled for testing the different receiver structures. The sampling frequency for the first two channels is 10 MHz and for the third channel is 16 MHz.

The first channel model corresponds to an FIR filter that heuristically approximates 22-AWG channel's frequency response up to 30 MHz. The channel attenuation (in dB/km) is estimated using the following expression: $5.1+14.3*f^{0.59}$, where the frequency 'f' is measured in MHz. This channel has a perfectly linear phase. The impulse response and the attenuation characteristics in dB/km for this channel are shown in Figures. 4.3.1(a, b) respectively.

The second channel model corresponds to 1-km 26-AWG CSA loop. This channel is simulated with parameters taken from [40] using the two-port network theory. Bridged taps or other kinds of impairments are not taken into consideration. Figures 4.3.2(a-d) display the impulse

(a)

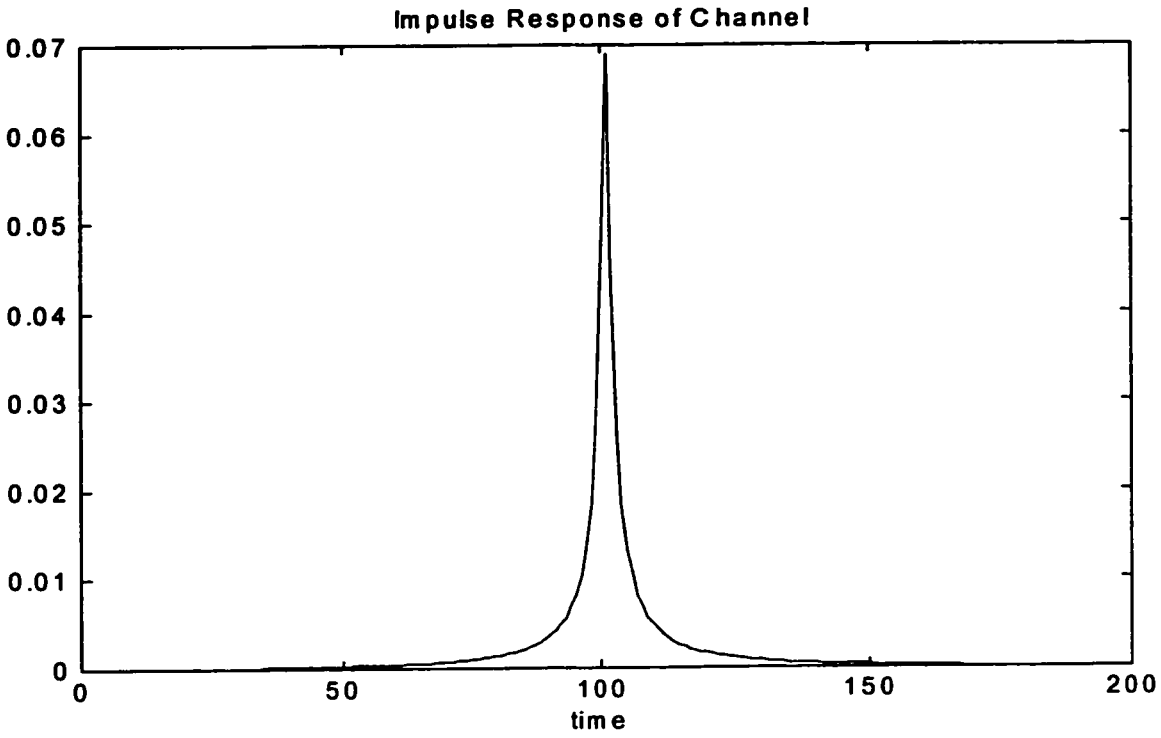

(b)

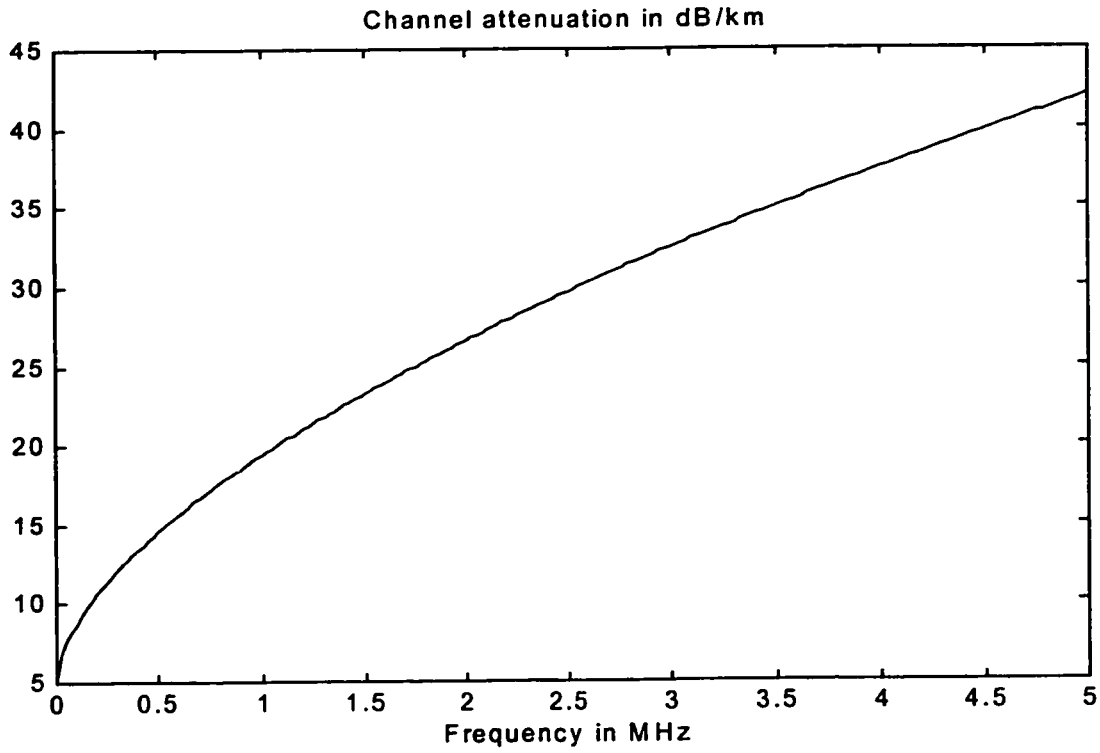

Figure 4.3.1: (a) Impulse Response and (b) Attenuation curve for Channel #1

(a)

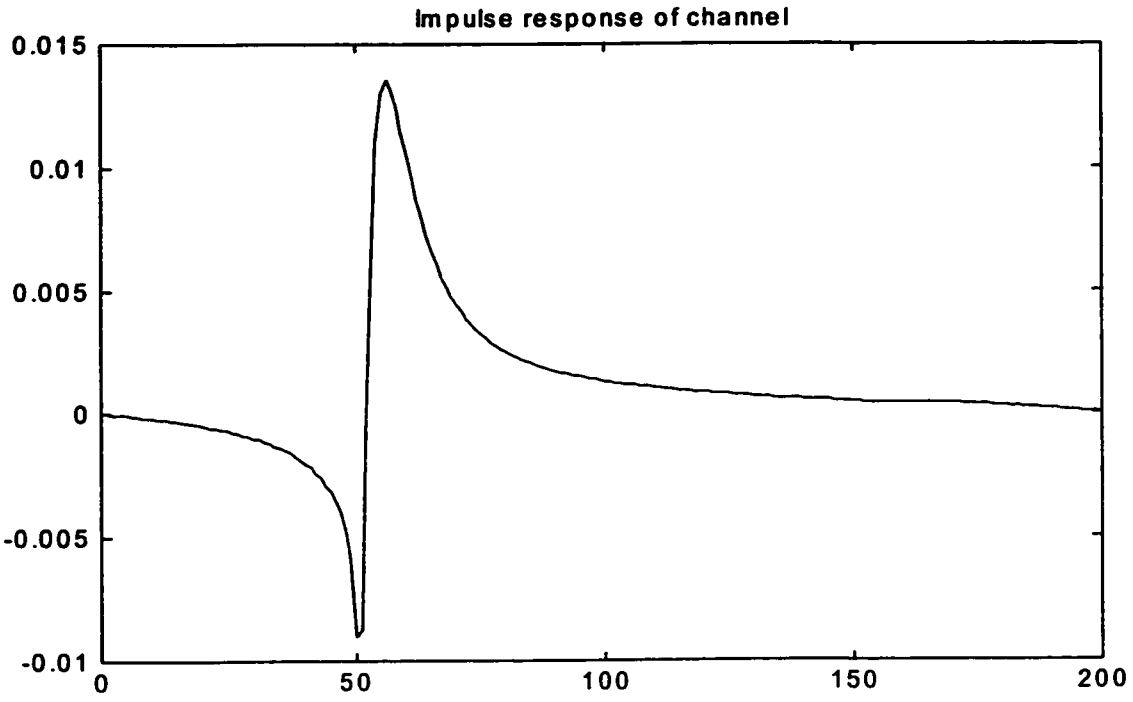

(b)

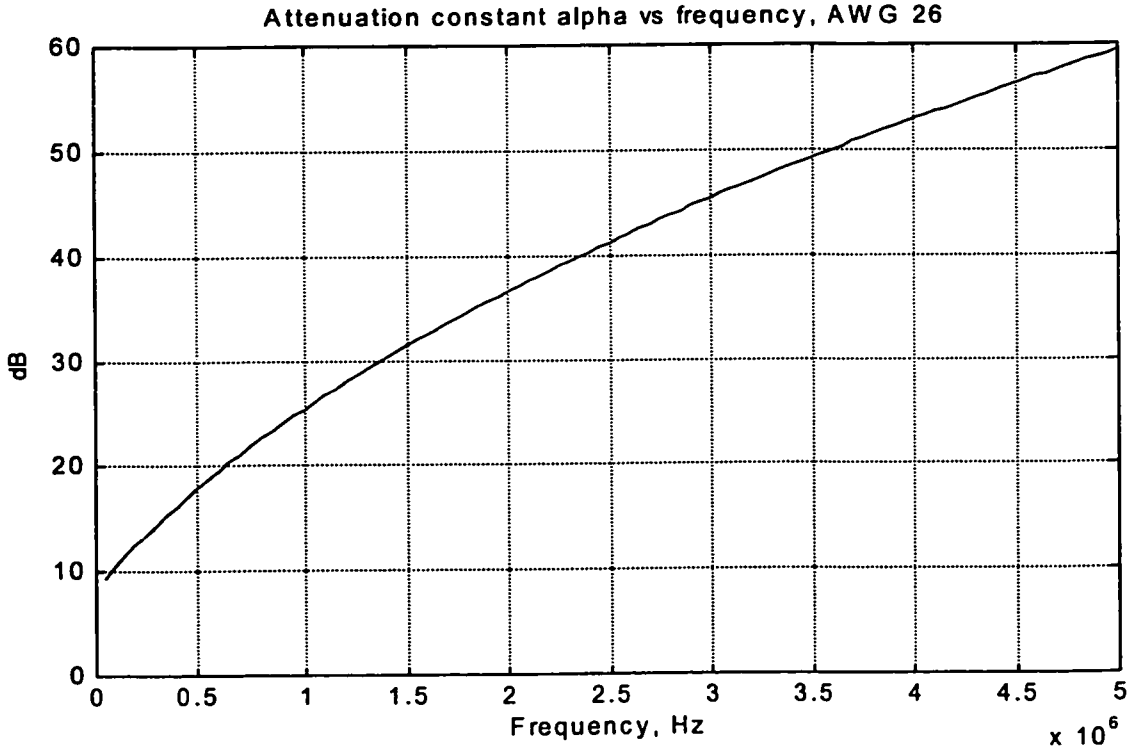

Figure 4.3.2: (a) Impulse Response and (b) Attenuation Constant for Channel #2

(c)

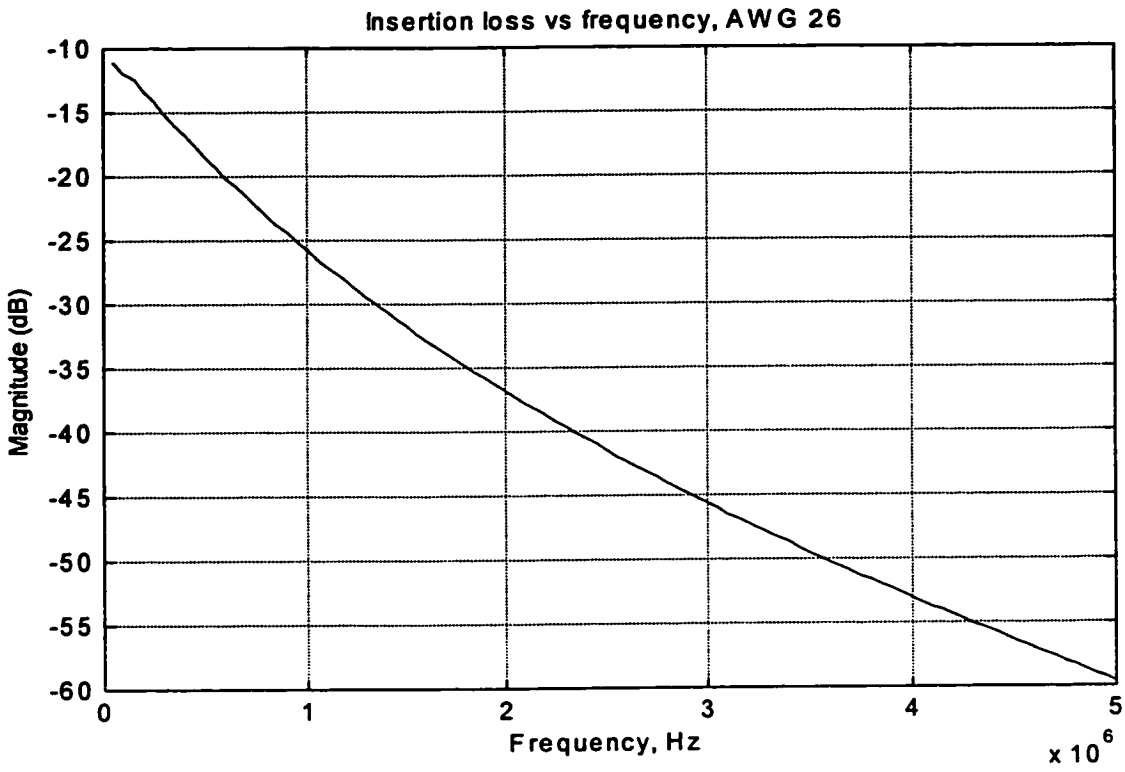

(d)

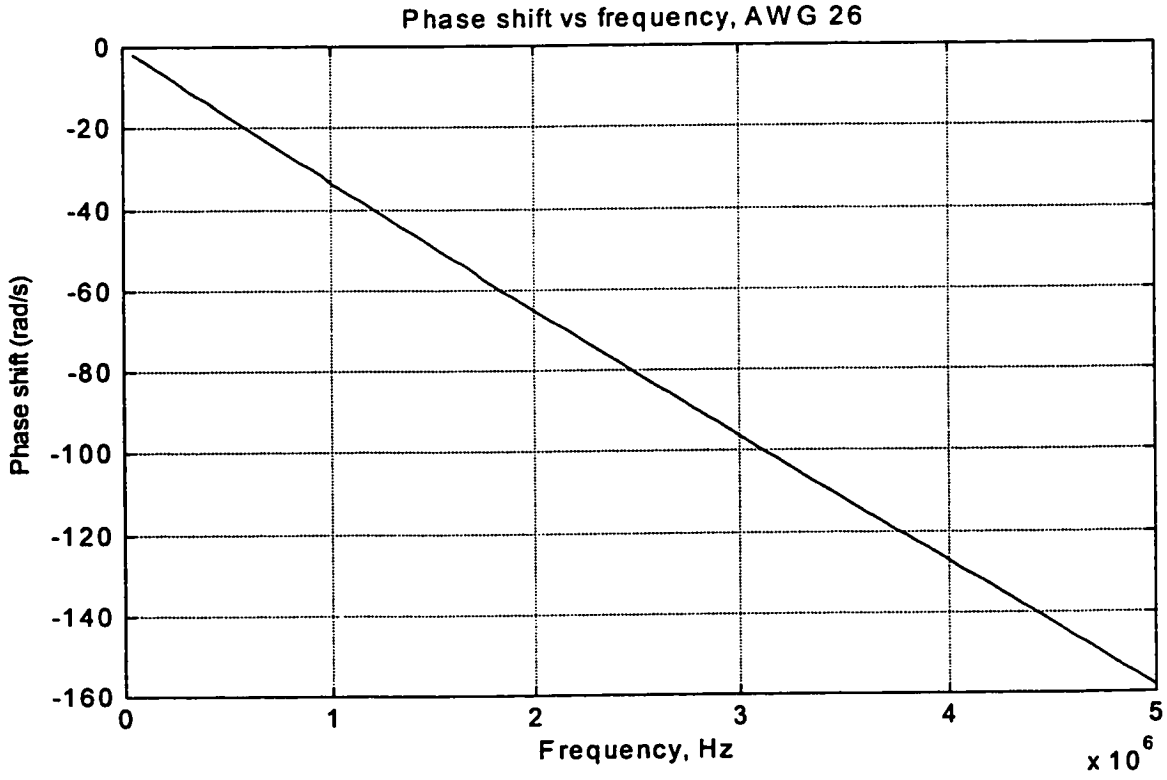

Figure 4.3.2: (c) Insertion Loss and (d) Phase shift for Channel #2

response, attenuation constant, insertion loss and the phase shift for this channel, respectively. It is obvious from Figure 4.3.2a (impulse response) that this particular channel has non-linear phase. The insertion loss drops down by a factor of 50 dB as one reaches 5 MHz, which indicates the expected level of attenuation for this particular channel.

The third channel model corresponds to 1-km 26-AWG loop with bridged taps, also simulated with parameters from [43], however using a sampling frequency of 16 MHz. The impulse response, attenuation constant, insertion loss and the phase shift for this channel are presented in Figures 4.3.3(a-d). The attenuation characteristics for this channel are observed to be sharper than that of the ordinary 1-km channel, as expected. The insertion loss shows a sharper drop and is highly uneven as compared to the previous channel. The impulse response characteristics for this channel are totally different, in addition to the non-linear phase.

Parameters used to simulate the second and the third channel, are given in the appendix (A-3).

4.4 RESULTS

This section gives the results of simulations for the three different receiver structures, as discussed previously. These structures are

(a) Plausible receiver #1 - TEQ only
(b) Plausible receiver #2 - FEQ only
(c) Plausible receiver #3 - simple TEQ' and FEQ'

Results for the first two structures are presented without the inclusion of AWGN in the system, whereas the third structure examined using signals both with and without noise. For (b) and (c), the SER at the output of the FEQ is calculated and presented for different number of taps in FEQ, using both the LE and the DFE.

In the presence of an ideal channel, the conditions for a perfect reconstruction of the synthesis and analysis filter banks are met perfectly. The error between the original and the reconstructed signals at the sliced output for all subchannels is exactly zero. Once the channel is introduced, the signal is highly attenuated and distorted.

Figure 4.4 shows an example of the signal obtained with and without a TEQ, after the signal is

(a)

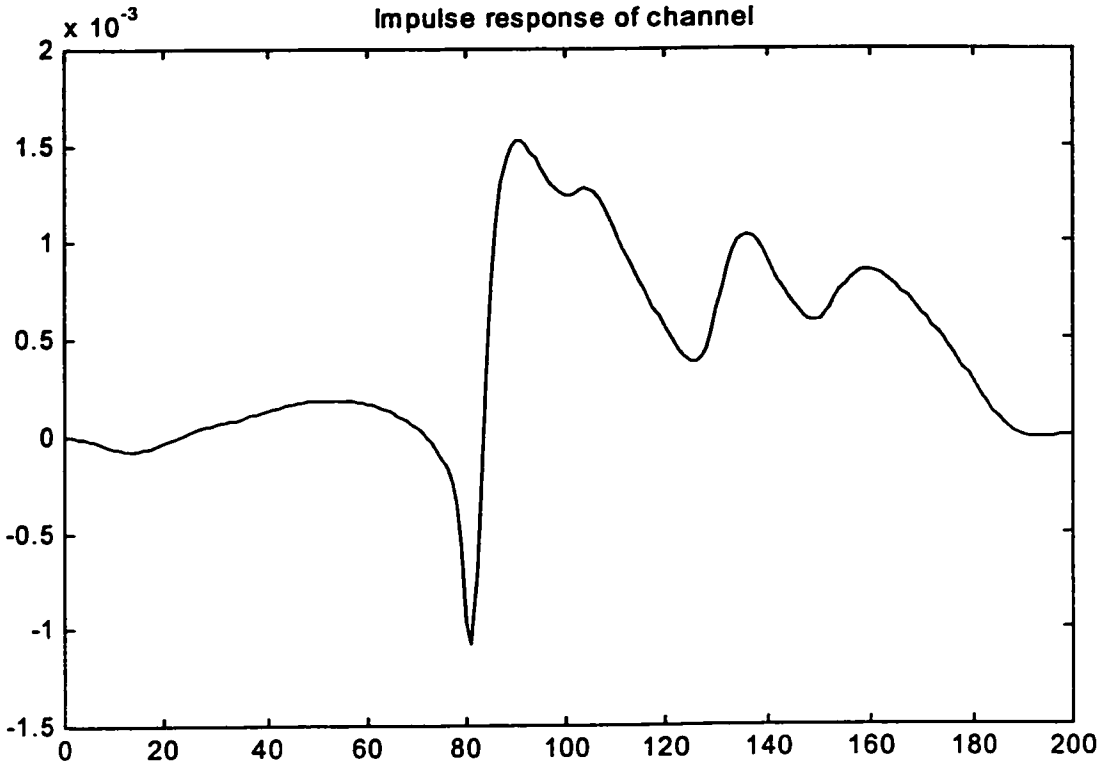

(b)

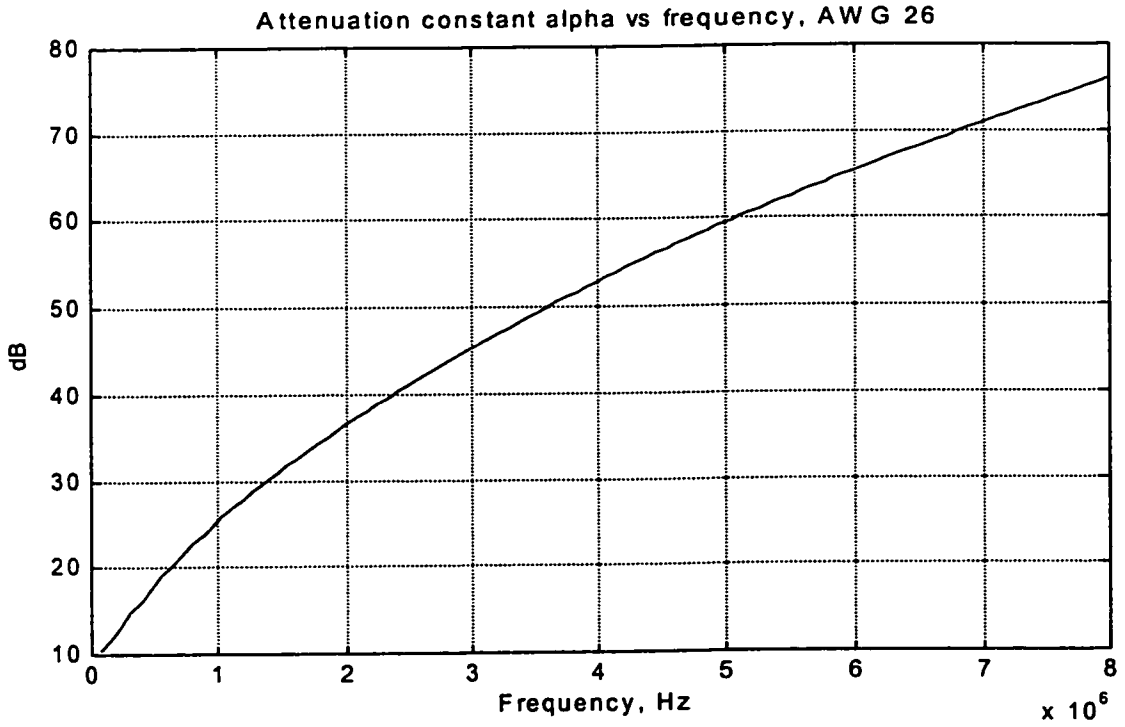

Figure 4.3.3: (a) Impulse response and (b) Attenuation constant for Channel #3

(c)

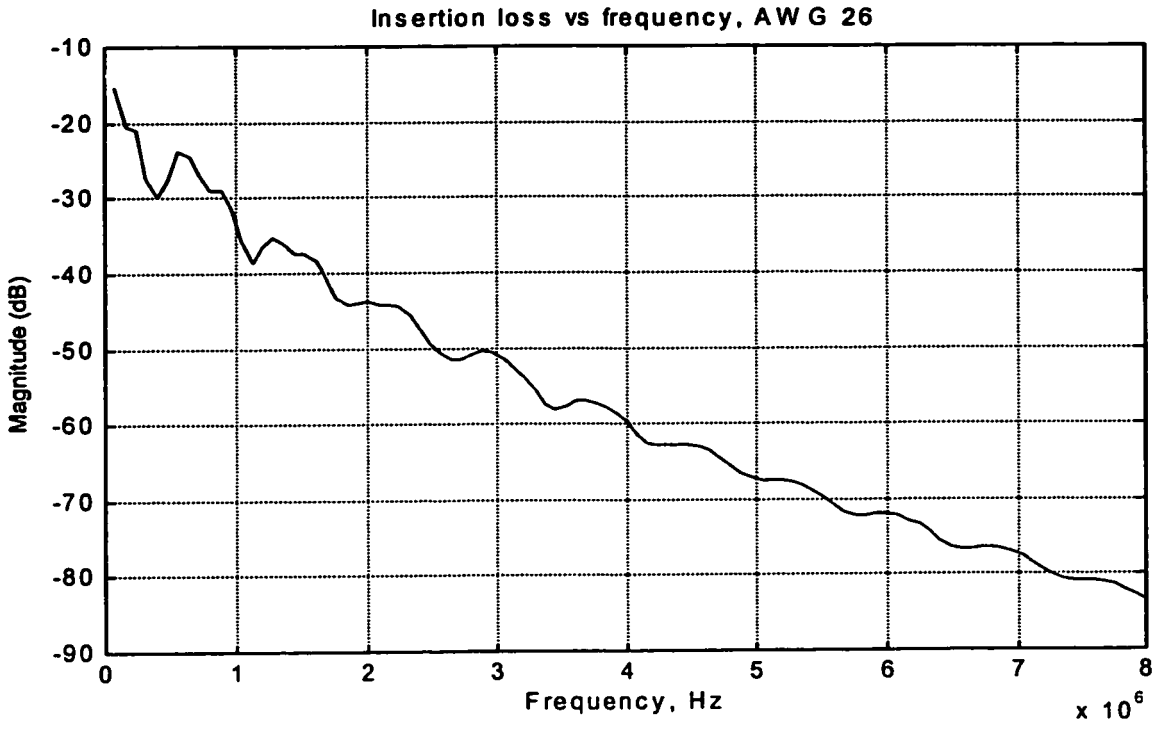

(d)

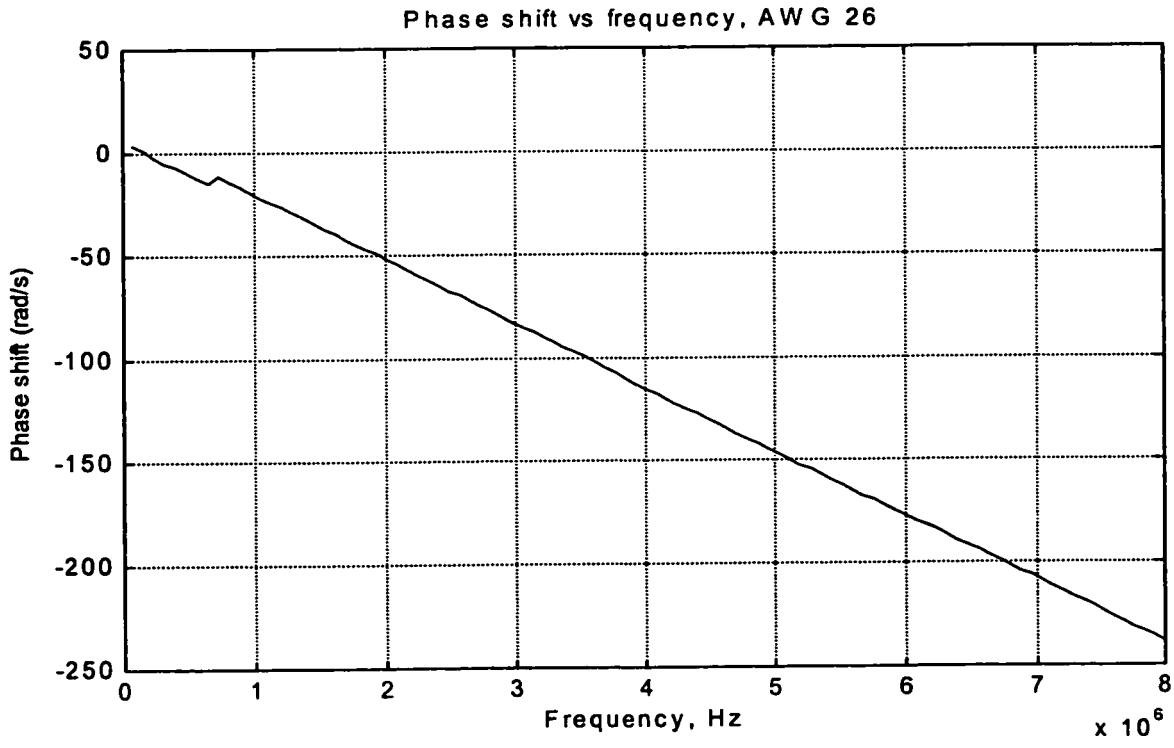

Figure 4.3.3: (c) Insertion Loss and (d) Phase Shift for Channel #3

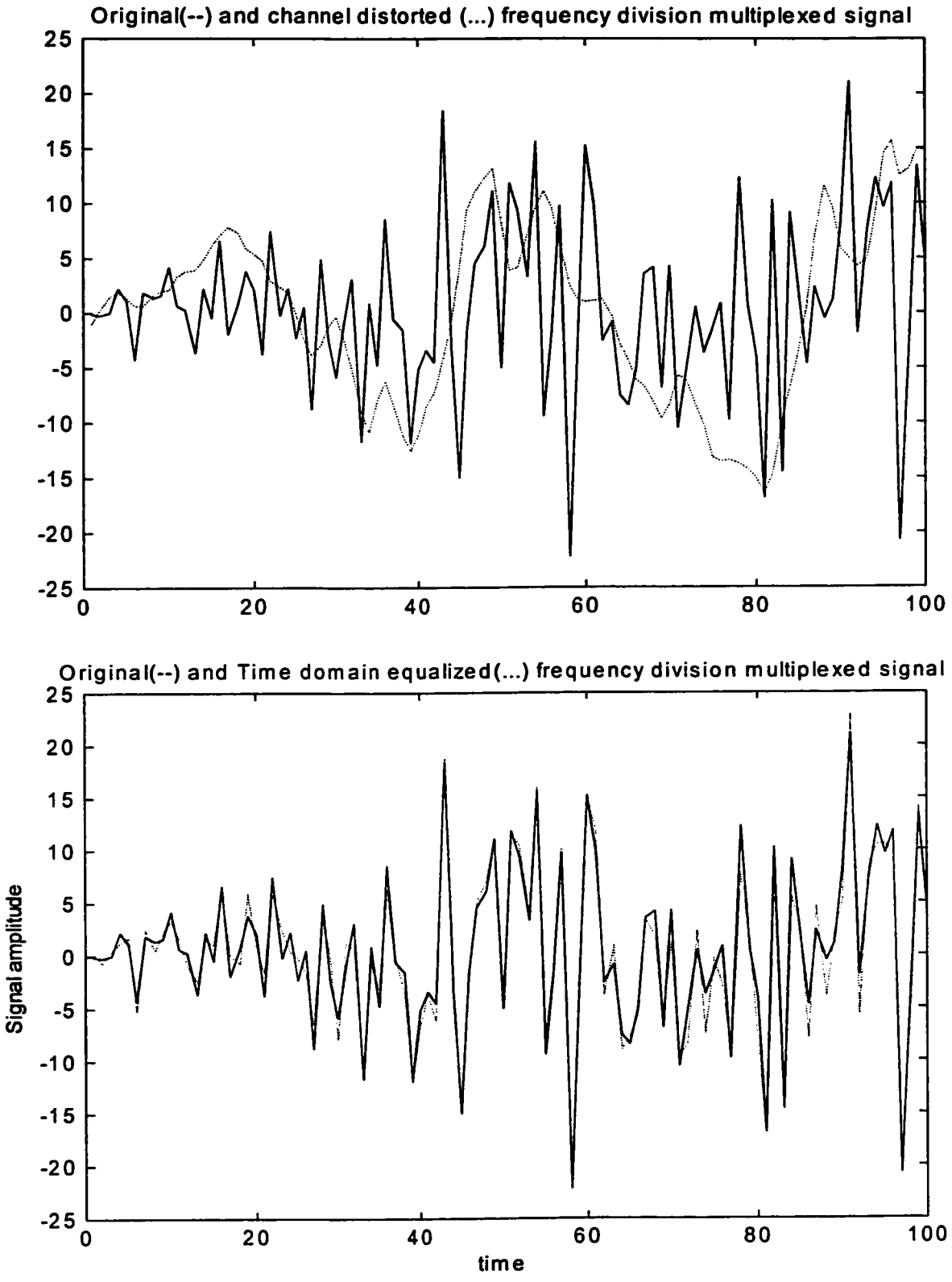

Figure 4.4: Original (--) and output of channel #2 (...) at the input of demodulator
(a) Amplified vs. original signal (b) Time domain equalized vs. original signal

transmitted through the channel. In the absence of a TEQ, the channel output is highly distorted and the sample pulses are totally smeared out and indistinguishable. Once the TEQ is introduced, the reconstructed signal is very close to the original signal, with the pulse shape restored. It is clear from this figure that the TEQ plays a very important role in removing most of the ISI in the frequency domain multiplexed signal.

4.4.1 Case 1: Plausible Receiver #1 - TEQ only

Figure 4.5.1 displays the variation of SINR (in dB) and the SNR (in dB) with subchannel index for Channel #1, obtained using 11-tap TEQ. The AWGN samples are obtained from gaussian random distribution with mean zero and variance of –140 dBm/Hz below the signal variance respectively. Figures 4.5.2 and 4.5.3 display the same result for Channel #2 and #3 respectively, for a system with 21-tap equalizer.

Table 4.1.1 gives the different values of SINR, SNR for all subchannels and the number of estimated and scaled bits for system with 11-tap TEQ. Tables 4.1.2 and 4.1.3 give the same results for Channel #2 and #3 respectively, with a 21-tap TEQ.

The actual numbers of bits used are obtained by scaling the calculated number to reach a maximum of 7 bits for all the three channels. This is done in the following manner: the maximum estimated bit-size among all the subchannels is scaled up to 7. The estimated bits of all the other subchannels are multiplied by this scale factor. This causes the total number of bits, N, to vary for different channels. The SER is expected to rise as a result of scaling up the number of bits. However, the high error rate is useful for testing the performance of the equalizers.

Table 4.2 gives the SER obtained using different number of taps in the TEQ, for all the three channels in the absence of AWGN. Although no FEQ is employed, a slicer is used at the output of the demodulator for each subchannel, and the sliced output signals are compared with the original (input) signals for each subchannel.

Figure 4.6 shows the SER for each subchannel for Channel #3 using different number of taps in the TEQ. The number of taps in the TEQ vary from 21 to 201.

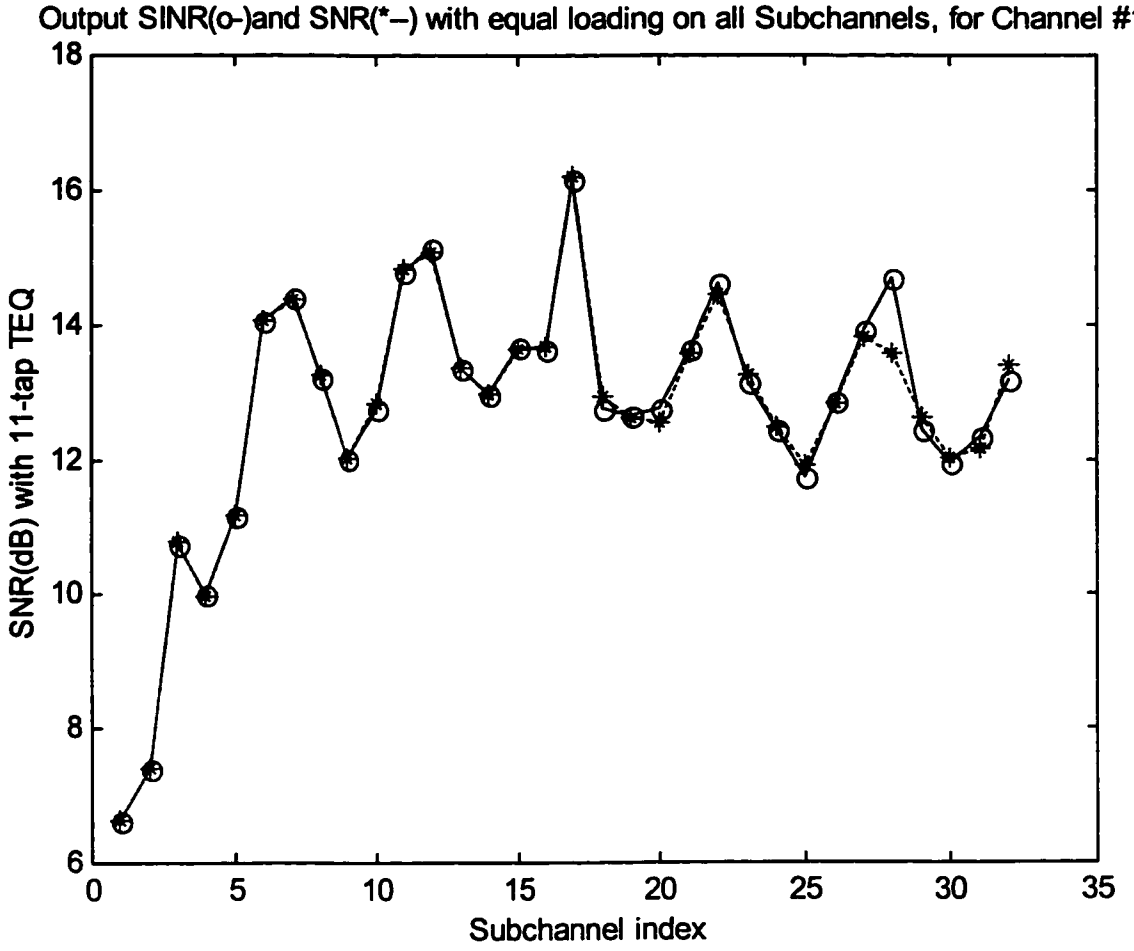

Figure 4.5.1: SINR and SNR for Channel #1 with 11-tap TEQ, for input AWGN variance at –140 dBm/Hz

Table 4.1.1: SINR, SNR and bit distribution for Channel #1 with 11-tap TEQ

Subch index	SINR (dB)	Scaled loading	SNR (dB)	Scaled loading
1	6.6304	2	6.6286	2
2	7.3970	2	7.3925	2
3	10.7670	4	10.7874	4
4	9.9967	3	9.9886	3
5	11.1821	4	11.1816	4
6	14.0747	6	14.0586	6
7	14.4077	6	14.3674	6
8	13.2058	5	13.2611	5
9	12.0100	5	12.0183	5
10	12.7442	5	12.8242	5
11	14.8095	6	14.8218	6
12	15.1550	6	15.0917	6
13	13.3701	5	13.3580	5
14	12.9641	5	12.9626	5
15	13.6729	5	13.6240	5
16	13.6352	5	13.6650	5
17	16.1863	7	16.1956	7
18	12.7642	5	12.9230	5
19	12.6511	5	12.6078	5
20	12.7409	5	12.5626	5
21	13.6241	5	13.5773	5
22	14.6375	6	14.4376	6
23	13.1568	5	13.2367	5
24	12.4245	5	12.4615	5
25	11.7263	4	11.8988	4
26	12.8544	5	12.8256	5
27	13.9135	6	13.8250	6
28	14.7089	6	13.5685	5
29	12.4393	5	12.6117	5
30	11.9398	4	12.0226	5
31	12.3474	5	12.1744	5
32	13.1656	5	13.3866	5

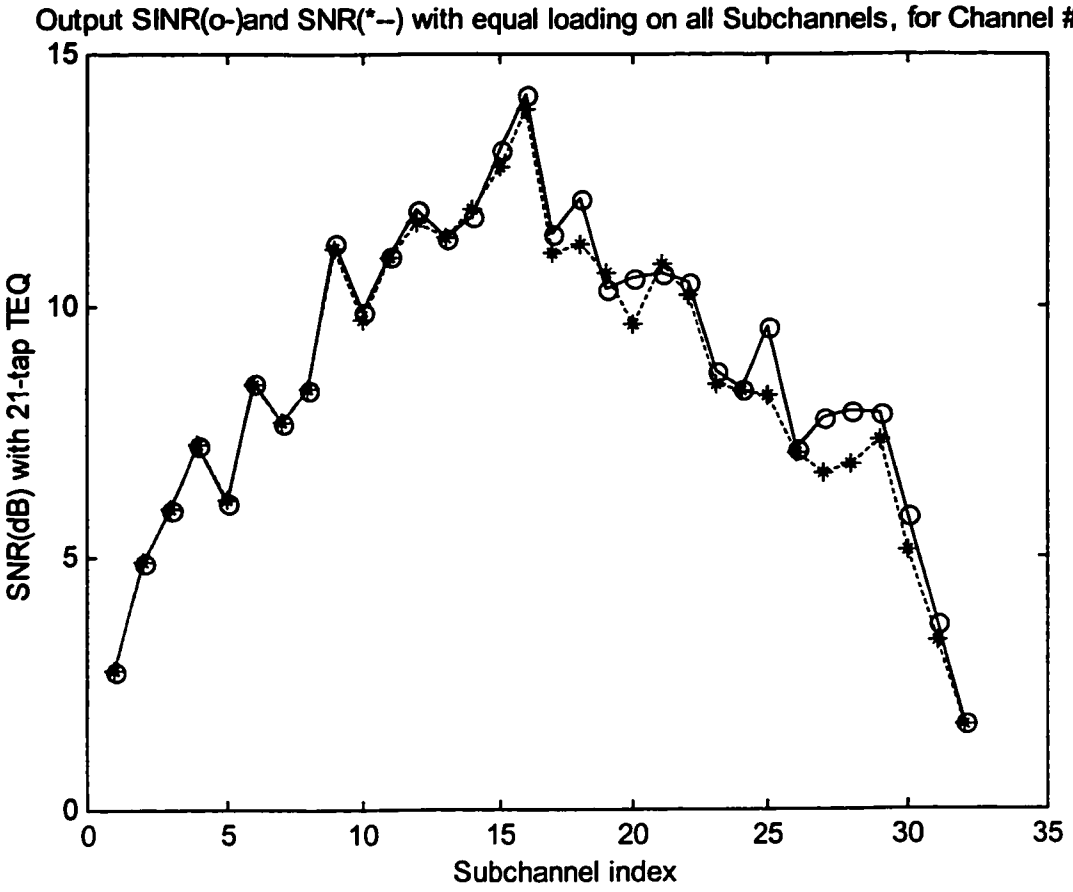

Figure 4.5.2: SINR and SNR for Channel #2 with 21-tap TEQ, for input AWGN variance at –140 dBm/Hz

Table 4.1.2: SINR, SNR and bit distribution for Channel #2 with 21-tap TEQ

Subch index	SINR (dB)	Scaled loading	SNR (dB)	Scaled loading
1	2.7754	1	2.7725	1
2	4.9212	2	4.9100	2
3	6.0034	2	5.9926	2
4	7.2436	3	7.2465	3
5	6.1252	2	6.1493	2
6	8.4813	3	8.4610	3
7	7.6852	3	7.7163	3
8	8.3793	3	8.3456	3
9	11.2548	5	11.1096	5
10	9.8925	4	9.7248	4
11	10.9756	5	10.9696	5
12	11.9285	5	11.6616	5
13	11.3315	5	11.3345	5
14	11.7690	5	11.9325	5
15	13.1048	6	12.7652	6
16	14.1926	7	13.9132	7
17	11.4548	5	11.0484	5
18	12.1584	6	11.2168	5
19	10.3366	4	10.6325	5
20	10.5783	5	9.6428	4
21	10.6558	5	10.8425	5
22	10.4503	4	10.1914	4
23	8.7097	3	8.4480	3
24	8.3408	3	8.3065	3
25	9.6025	4	8.2359	3
26	7.1615	3	7.0854	3
27	7.7950	3	6.6889	3
28	7.9343	3	6.8673	3
29	7.8666	3	7.3668	3
30	5.8404	2	5.1379	2
31	3.6857	1	3.3573	1
32	1.6941	1	1.6828	1

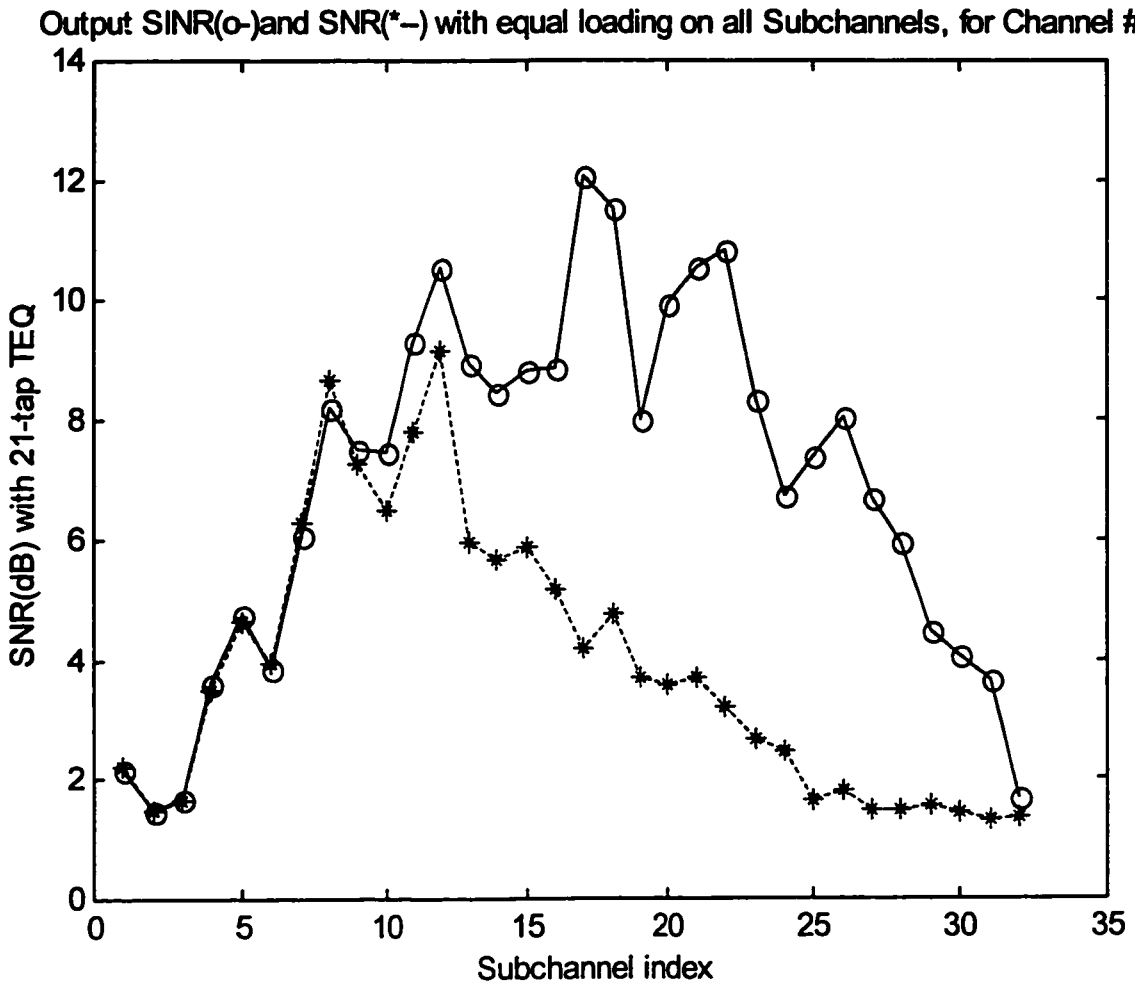

Figure 4.5.3: SINR and SNR for Channel #3 with 41-tap TEQ, for input AWGN variance at –140 dBm/Hz.

Table 4.1.3: SINR, SNR and bit distribution for Channel #3 with 21-tap TEQ

Subch index	SINR (dB)	Scaled loading	SNR (dB)	Scaled loading
1	2.1769	1	2.2237	1
2	1.4638	1	1.4729	1
3	1.6746	1	1.6341	1
4	3.5942	2	3.4863	2
5	4.7792	2	4.6313	2
6	3.8611	2	3.9227	2
7	6.0700	3	6.2901	3
8	8.1941	4	8.6492	4
9	7.5119	4	7.2639	4
10	7.4615	4	6.4923	3
11	9.3103	5	7.8003	4
12	10.5606	6	9.1434	5
13	8.9561	5	5.9465	3
14	8.4617	4	5.6543	3
15	8.8220	5	5.8700	3
16	8.8615	5	5.1574	2
17	12.0870	7	4.1905	2
18	11.5557	7	4.7735	2
19	7.9928	4	3.6824	2
20	9.9552	5	3.5675	2
21	10.5361	6	3.6774	2
22	10.8209	6	3.1879	2
23	8.3213	4	2.6800	2
24	6.7209	3	2.4480	1
25	7.3973	4	1.6404	1
26	8.0361	4	1.7956	1
27	6.6751	3	1.4621	1
28	5.9450	3	1.4606	1
29	4.4570	2	1.5753	1
30	4.0733	2	1.4374	1
31	3.6498	2	1.3142	1
32	1.6850	1	1.3704	1

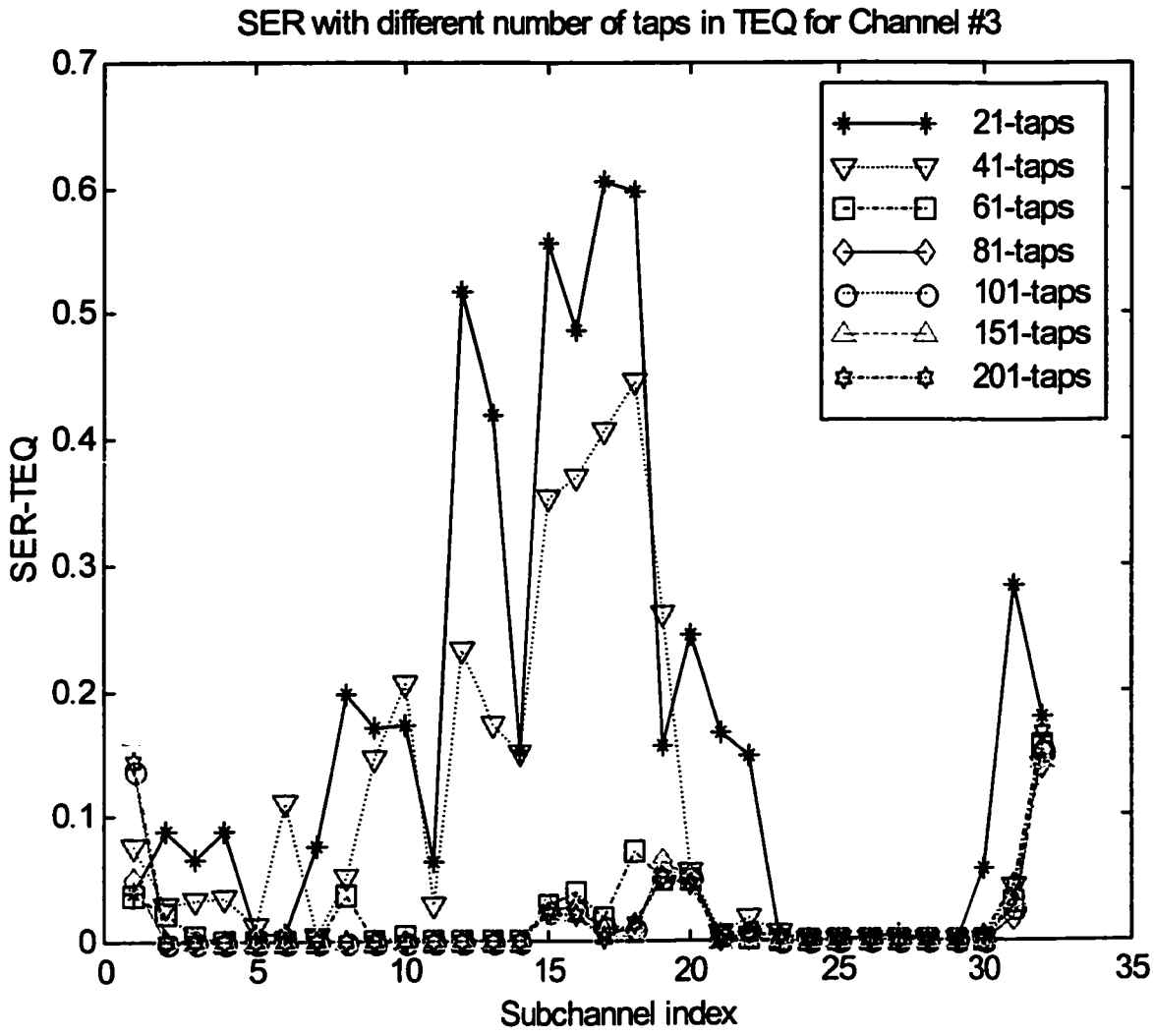

Figure 4.6: SER with different number of taps in TEQ, for Channel #3, with TEQ-only receiver

Table 4.2: SER at the output of the demodulator for different number of taps in TEQ

# TEQ of taps	SER_channel #1	SER_channel #2	SER_channel #3
11	0.000895	0.15263	0.48090
21	0.000645	0.02638	0.17319
41	0.000708	0.01502	0.10585
61	0.000583	0.01385	0.01744
81	0.000625	0.01248	0.01296
101	0.000583	0.01196	0.01581
151	0.000583	0.018956	0.01598
201	0.000583	0.010625	0.01648

The first column indicates the number of taps used in the TEQ. The rest of the columns give the averaged value of the SER over all the 32 subchannels, for the three different channels.

4.4.2 Discussion for Case 1:

Certain observations specific to this case are described and discussed below:

(i) For all the three channels, it can be seen that the SINR for the first subchannel is much lower as compared to the other subchannels. In the case of the first two channels, the SINR and SNR value for the end subchannels is also low. Such a decline in the values of SINR for a few subchannels at the beginning and the end of the spectrum could be a result of band-edges, since no steps are taken to overcome the band-edge effects.

(ii) For Channel #1 (Figure 4.5.1), the values of the SINR and SNR vary roughly between 12 dB and 16 db for rest of the subchannels. This leads to a high bit allocation (between 5-7 bits per symbol) for most of the subchannels. The values of SNR are not very different from those of SINR, leading to the same bit allocation for most of the subchannels. Since the total noise in the SNR calculation is a combination of interference noise and the white noise, this indicates that most of the noise contribution still comes from channel distortion. It can be concluded that for a simple linear phase 1-km channel, white noise doesn't cause much signal impairment.

(iii) For Channel #2 (Figure 4.5.2), the SINR roughly displays an upward trend till the middle of the spectrum, after which the trend reverses. Subchannels in the middle of the spectrum are most likely to carry the highest number of bits. SNR values lie close to the SINR values, indicating a less dominant presence of white noise for this channel as well.

(iv) The situation quite different for Channel #3 (Figure 4.5.3) as compared to the previous channels. The SINR gradually rises towards the middle of the spectrum and then gradually drops along the spectrum. The variation between subchannels is larger as compared to the previous two channels. The effect of the white noise seems to dominate in this case, as the SNR values are rather low. The gap between SINR and SNR increases as one moves towards the end of the spectrum. This could be as a result of higher sampling frequency (16 MHz) for this particular channel, since white noise is expected to increase with bandwidth (which in this case, is 8 MHz).

(v) Tables 4.1.1, 4.1.2 and 4.1.3 reflect the trend of the SINR and SNR values in the number of allocated bits for different subchannels. The total number of bits N for Channel #1, #2 and #3 are different. Although the highest number of bits assigned to each case is the same (7 bits), the bit allocation over the subchannels is quite different, due to the variation in the SINR and SNR values between the subchannels.

(vi) From Figure 4.6 (presented only for Channel #3), it can be seen that for most of the subchannels, the SER reduces to almost zero when more taps are used in the TEQ. The problem arises for a few higher subchannels, for which the SER continues to be rather high despite 201 taps in the TEQ.

(v) From Table 4.2, it is seen that the SER for the first Channel is considerably low. An 11-tap TEQ is sufficient to drop the SER below 0.001. This is not surprising for a simple linear phase channel. However, for Channel #2 and #3, which are more realistic and correspond to actual models of 1-km and 2-km CSA loops, the SER convergence rate is rather slow after 41 taps. For Channel #2, the best possible performance of a TEQ with 101 taps is an SER of 0.011958, which still is greater than 1% error rate. The situation is similar for Channel #3, where even with 201 taps, the SER does not go below 0.01.

Thus, for the system containing of only TEQ, it becomes very difficult to reduce the average SER below 0.01 for a VDSL channel. This could be due to several reasons, which include the limitations of the current design, channel distortion or problems with equalizer convergence when the number of taps is increased to a large value such as 201, insufficient length of the training signal, etc. Using too many taps in the TEQ not recommended for use in real-time data processing. The latency with 201 taps was itself very high, so that it can be assumed that using more taps would cause even further delay and convergence problems.

Although a TEQ is found to be extremely useful for a DWMT receiver, it does not prove to be sufficient or capable of eliminating all the ISI for a VDSL channel. Hence, other receiver structures need to be considered.

4.2.3 Case 2: Plausible Receiver #2 - FEQ only

Table 4.3 gives the SINR values and the scaled bits for the three different channels for system without TEQ. For this system, the maximum number of scaled bits is restricted to 3 bits for Channel #1 and 2 bits for Channel #2 and #3, since the SINR values for are very low. The bit size is obtained using equation 3.6, and the values are scaled up to the maximum for each channel. All the results correspond to only interference noise, as white noise was not included.

Figures 4.7.1, 4.7.2 and 4.7.3 display the SER of the reconstructed signal at the output of the demodulator and at the output of the FEQ for Channels #1, #2 and #3 respectively. The solid line corresponds to the SER at the sliced output of the demodulator. The dashed and the dotted lines correspond to the SER obtained after using certain number of taps in the FEQ, as indicated by the legends.

Table 4.4 gives the values (for the three Channels) of the averaged SER for different number of taps in the FEQ. There is one value of 'SER_DEM' for each channel, obtained by averaging the sliced outputs of the demodulator over all the subchannels. Different values of 'SER_FEQ' are obtained for each channel by averaging the sliced output of the FEQ over all subchannels, for different number of taps in the FEQ, as indicated in the first column. The number of taps used in the FEQ are labeled as (a,b), indicating 'a' feed forward and 'b' feedback taps for DFE. All the b=0 results correspond to the LE.

Table 4.3: SINR and bit distribution for different channels without TEQ

Subch index	Channel #1		Channel #2		Channel #3	
	SINR (dB)	Scaled loading	SINR (dB)	Scaled loading	SINR (dB)	Scaled loading
1	7.1513	2	1.5785	1	1.5499	1
2	6.5022	2	1.3808	1	1.4994	1
3	7.0604	2	1.4091	1	2.0349	2
4	11.1240	3	1.2478	1	2.6475	2
5	7.8769	2	1.3620	1	2.1788	2
6	9.2614	2	1.4594	1	1.8461	2
7	8.9868	2	1.3579	1	1.4876	1
8	8.1941	2	1.6631	1	1.3233	1
9	9.6219	2	2.2498	2	1.2773	1
10	10.0327	3	4.5336	2	1.4365	1
11	9.4806	2	4.1346	2	1.5194	1
12	11.0654	3	1.8472	1	1.2881	1
13	8.6129	2	1.7294	1	1.2145	1
14	9.6431	2	1.2799	1	1.3973	1
15	8.8000	2	1.2849	1	1.3711	1
16	10.0693	3	1.4705	1	1.2287	1
17	9.8469	3	1.2614	1	1.2874	1
18	10.1961	3	1.3949	1	1.1356	1
19	9.8983	3	1.8136	1	1.3923	1
20	9.3907	2	3.1895	2	1.0072	1
21	9.3659	2	3.4776	2	1.1869	1
22	9.7028	2	2.0739	1	1.3475	1
23	9.6464	2	1.3158	1	1.1103	1
24	8.9678	2	0.9909	1	0.9105	1
25	10.0898	3	1.0815	1	1.0718	1
26	9.3104	2	1.2132	1	0.9777	1
27	8.4475	2	1.3529	1	0.9471	1
28	9.1301	2	1.8049	1	1.2748	1
29	8.5944	2	2.7865	2	1.0448	1
30	9.6262	2	2.2218	2	1.0308	1
31	7.5957	2	1.8451	1	1.4521	1
32	10.2183	3	1.3195	1	1.0371	1

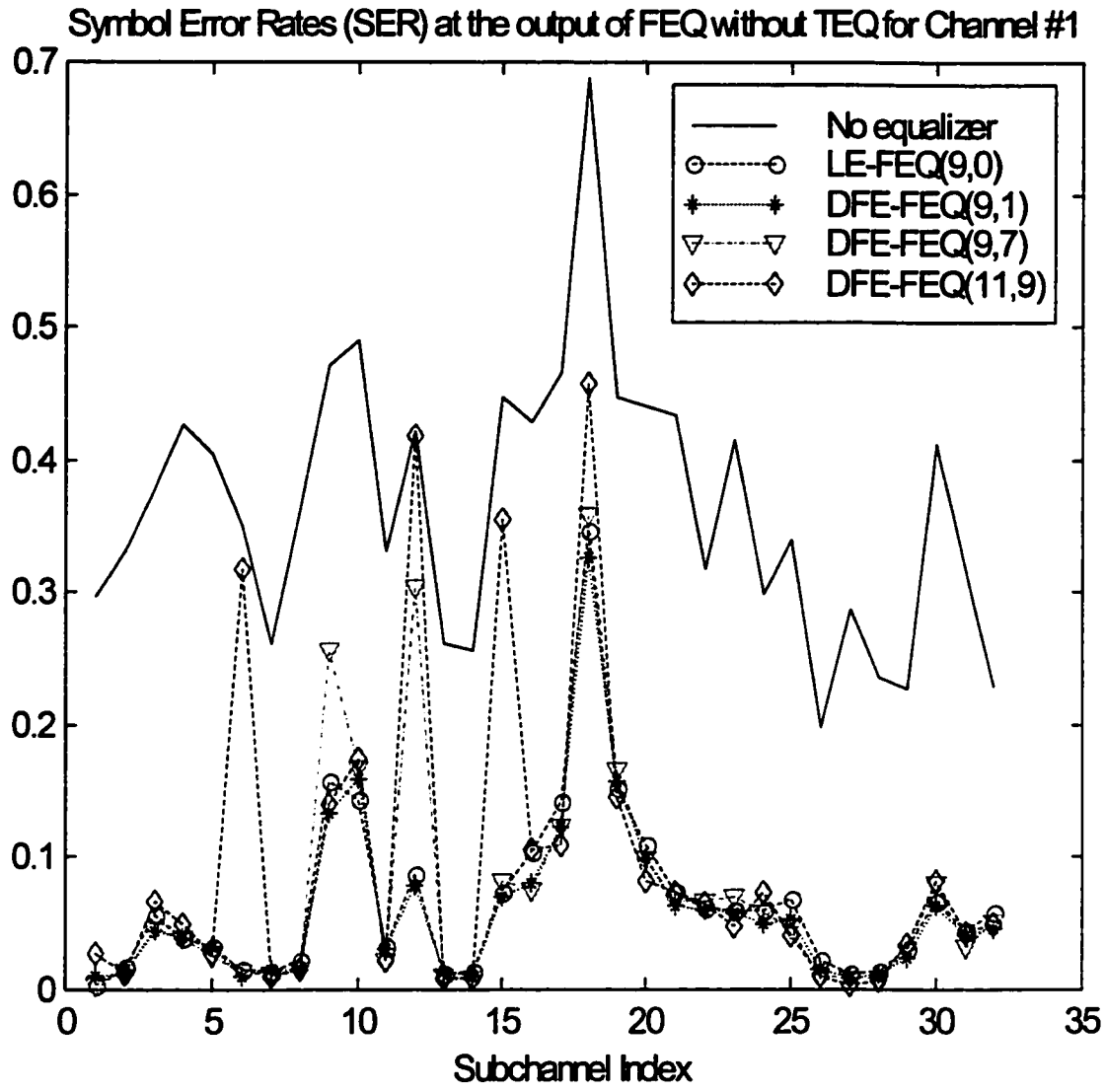

Figure 4.7.1: SER at the output of FEQ without TEQ for Channel #1 without noise, with different number of taps in the FEQ

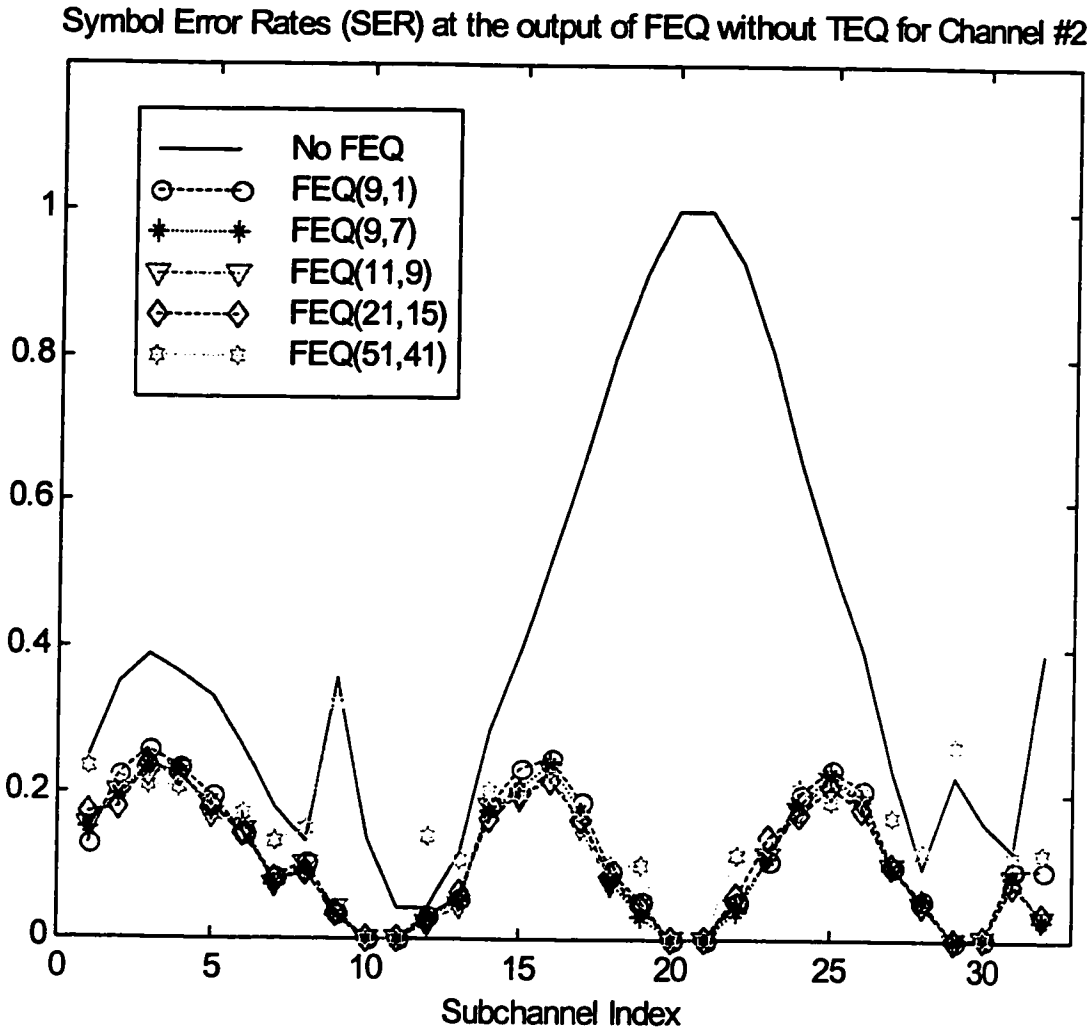

Figure 4.7.2: SER at the output of FEQ without TEQ, for Channel #2 without noise, with different number of taps in the FEQ

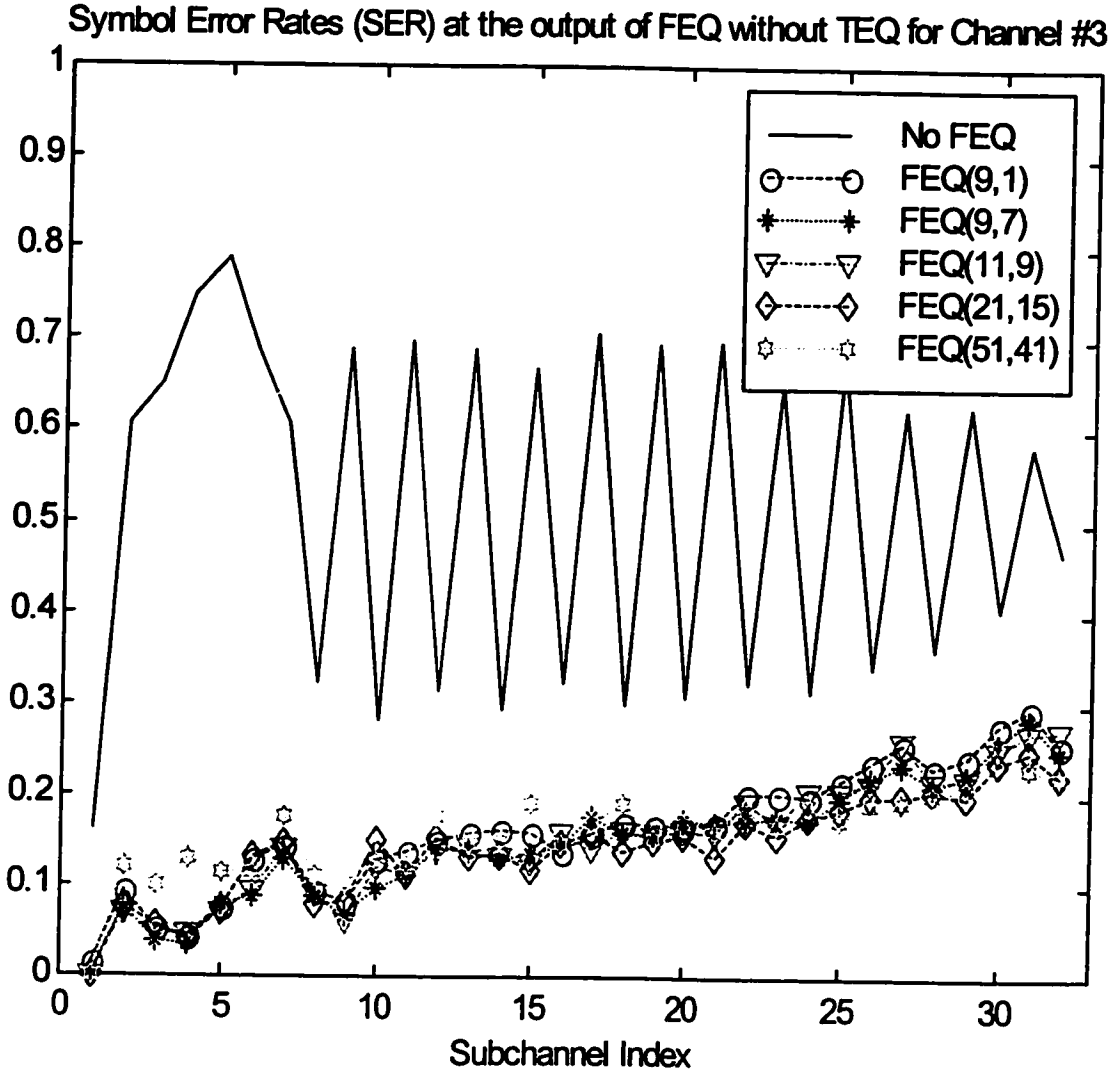

Figure 4.7.3: SER at the output of FEQ without TEQ for Channel #3 without noise, with different number of taps in the FEQ

The table also gives the average percentage improvement obtained by using FEQ, which is calculated using the following expression:

$$\text{Average percentage improvement} = \frac{\text{Average SER\_DEM} - \text{Average SER\_FEQ}}{\text{Average SER\_DEM}} * 100\ \%$$

Table 4.4: Averaged SER at the output of the FEQ and the % averaged improvement of the SER_FEQ over the SER_DEM. All values are averaged over all subchannels.

# Taps		Channel #1 SER_DEM= 0.3647		Channel #2 SER_DEM = 0.40869		Channel #3 SER_DEM=0.5189	
		SER_FEQ	% Impr	SER_FEQ	% Impr	SER_FEQ	% Impr
9	1	0.06108	83.25	0.11502	71.86	0.16315	68.56
9	3	0.07219	80.21	0.10775	73.64	0.15408	70.31
9	5	0.08729	76.07	0.10450	74.43	0.14802	71.47
9	7	0.07402	79.70	0.10567	74.14	0.14771	71.53
11	1	0.05917	83.78	0.11333	72.27	0.16062	69.05
11	3	0.06839	81.25	0.10742	73.72	0.15167	70.77
11	5	0.06800	81.36	0.10390	74.58	0.14940	71.21
11	7	0.07444	74.59	0.10370	74.63	0.14717	71.64
11	9	0.09635	73.52	0.10433	74.47	0.15016	71.00
15	9	0.07785	79.31	0.10398	74.56	0.15112	70.88
15	13	0.12175	66.21	0.10525	74.25	0.14846	71.39
21	15	0.12175	66.21	0.10483	74.35	0.14275	72.49
21	19	0.14502	61.46	0.10360	74.65	0.14512	72.03
31	21	0.19769	47.46	0.10883	73.37	0.14440	72.16
51	41	0.40406	-7.39	0.14796	63.78	0.15927	69.31

4.4.4 Discussion for Case 2

Certain observations and discussion, specific to the results presented for this particular case are given below:

1. From Table 4.3, it is seen that for Channel #1, most of the subchannels carrying either 2 or 3 bits. Since the SINR values for this channel lie between 8-10, this comes to roughly 3 dB SINR per bit. In comparison, the SINR values for Channel #2 and #3 are

lower, with roughly 1 dB per bit. Hence the error rate for these channels is expected to be higher than Channel #1.

2. The SER values are rather high, indicating degradation in performance of the system for all the three channels. For Channel #1 (Figure 4.7.1), the SER at the output of the demodulator is 0.3647, indicating that about an average of 36% symbols are incorrect at the time of detection, without equalization. This is still low as compared to 0.4087 and 0.5189 for Channels #2 and #3 respectively. This may be attributed to the fact that the first channel is simpler and each bit carries a higher value of SINR as compared to the other channels. The FEQs cause the SER for each subchannel to reduce significantly, by about 90% on the average, bringing down the SER to almost 0.05.

3. For Channel #2 and Channel #3 (Figures 4.7.2 and 4.7.3), the situation is different. The SER at the output of the demodulator in the absence of any equalizer is very high, ranging from 0.2 to 0.8 for most of the subchannels. This indicates severe channel distortion, since there is absolutely no equalization done to the signal. Use of an FEQ improves the result significantly, bringing down all the SERs to below 0.2 for most of the subchannels.

4. From Table 4.4, it can be seen that the averaged SER reduces to roughly 0.05, 0.1 and 0.15 for Channels #1, #2 and #3 respectively, indicating about 90% improvement for the first channel and up to 75% improvement for the second and the third channels, over the unequalized results. This is significant, considering the fact that the FEQs are attempting to combat distortion caused by a typical VDSL channel, without the use of any pre-detection equalization technique.

5. It can also be seen from Table 4.4, that there is a gradual improvement (*i.e.*, the value of SER does become smaller) as the number of taps in the FEQ is increased. However, this improvement is very minimal and the result does not get better by using 51 taps in the FEQs!! Attempts to reduce the error rate further by using even greater number of taps in the FEQ did not make sense, as it also caused tremendous amount of latency in the system.

To conclude, this particular design is successful in removing some channel distortion, with the FEQs reducing the SER to less than 15% of the symbol rate. Although this is a significant amount of success for the FEQs to combat channel distortion, it is not enough to obtain an almost 'error-free' output for an operational DWMT transceiver. The error rate as high as 15% is totally unacceptable for reliable data transmission. Hence this receiver design consisting of only FEQs after demodulator cannot be recommended for use in a DWMT system.

4.4.5 Case 3: Plausible Receiver #3 – Simple TEQ' and FEQ'

This receiver design uses a very simple TEQ with 11 or 21 taps to eliminate phase distortion and reduce the ISI to some extent to give a coarsely reconstructed signal. FEQs are then employed to improve the quality of the result.

The numbers of bits allocated for this case are same as Case 1. Since this design simply adds FEQs to the existing system of receiver with TEQ, it can be considered as an extension of Case 1. Adaptive loading is therefore not repeated for this case, and allocated bits are taken from Tables 4.1.1, 4.1.2 and 4.1.3 for Channel #1, #2 and #3 respectively.

Figures 4.8.1, 4.8.2 and 4.8.3 display the SER values at the demodulated and sliced output of the TEQ and the sliced output of the FEQs, with 11-tap TEQ for Channel #1, 21- and 41- tap TEQ for Channel #2 and 41- and 61-tap TEQ for Channel #3 respectively, without the presence of AWGN. The number of taps in the FEQ for the displayed results ranges from (9,0) to (11,7), for each case.

Figures 4.9.1, 4.9.2 and 4.9.3a give similar results with AWGN using 11-tap TEQ for Channel #1, 21-tap TEQ for Channels #2 and 61-tap TEQ for Channel #3 respectively. Figures 4.9.3b and 4.9.3c display the effect of increasing the signal amplitude by a factor of 5 and 10 respectively, prior to transmission through the channel (#3).

Tables 4.5.1, 4.5.2 and 4.5.3 give the SER_FEQ (averaged over all subchannels) and the average percentage improvement obtained by using FEQ over TEQ, for all the three channels. The % improvement of SER_FEQ over SER_TEQ is calculated in a similar manner as in Case 2, except for the fact that the SER_DEM is replaced here by SER_TEQ.

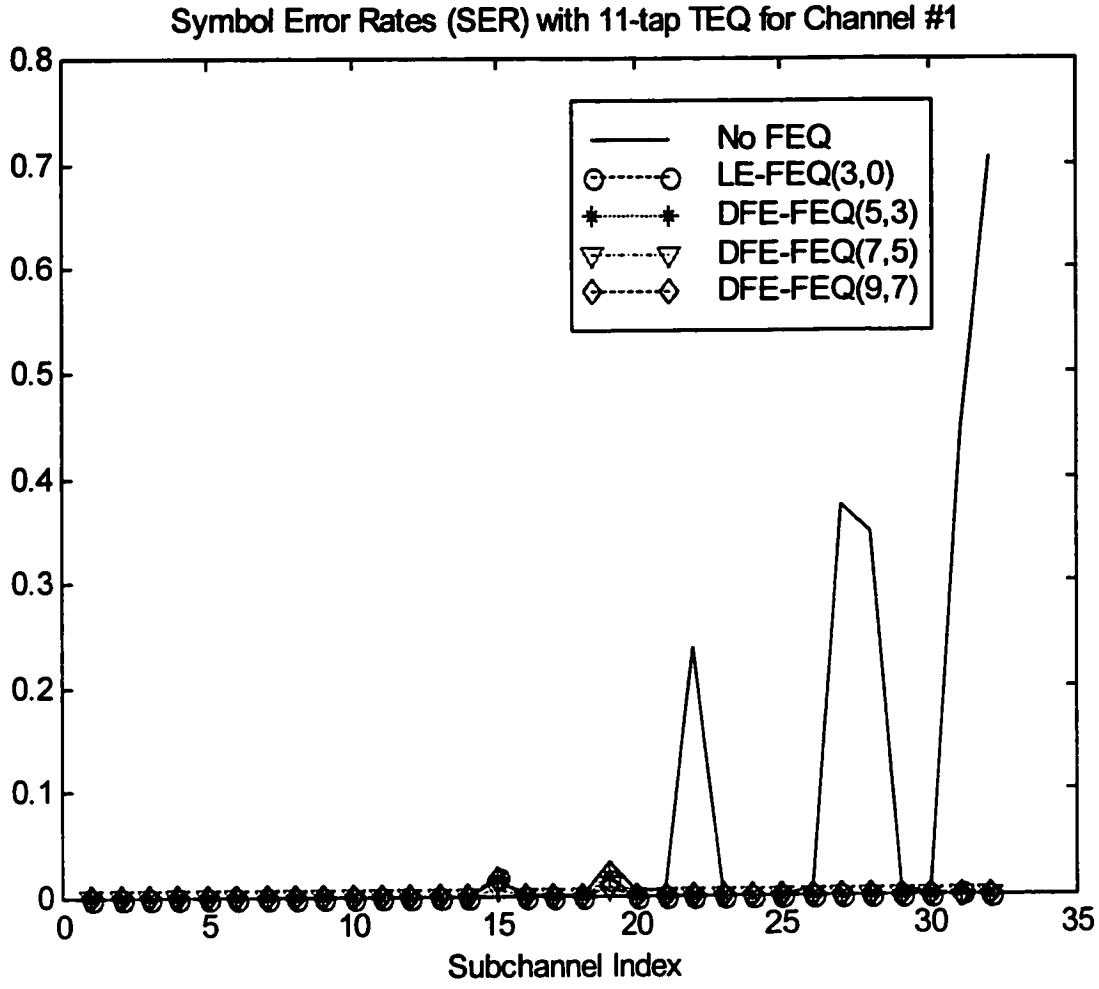

Figure 4.8.1: SER at the output of 11-tap TEQ and FEQ for Channel #1 without noise, with different number of taps in FEQ.

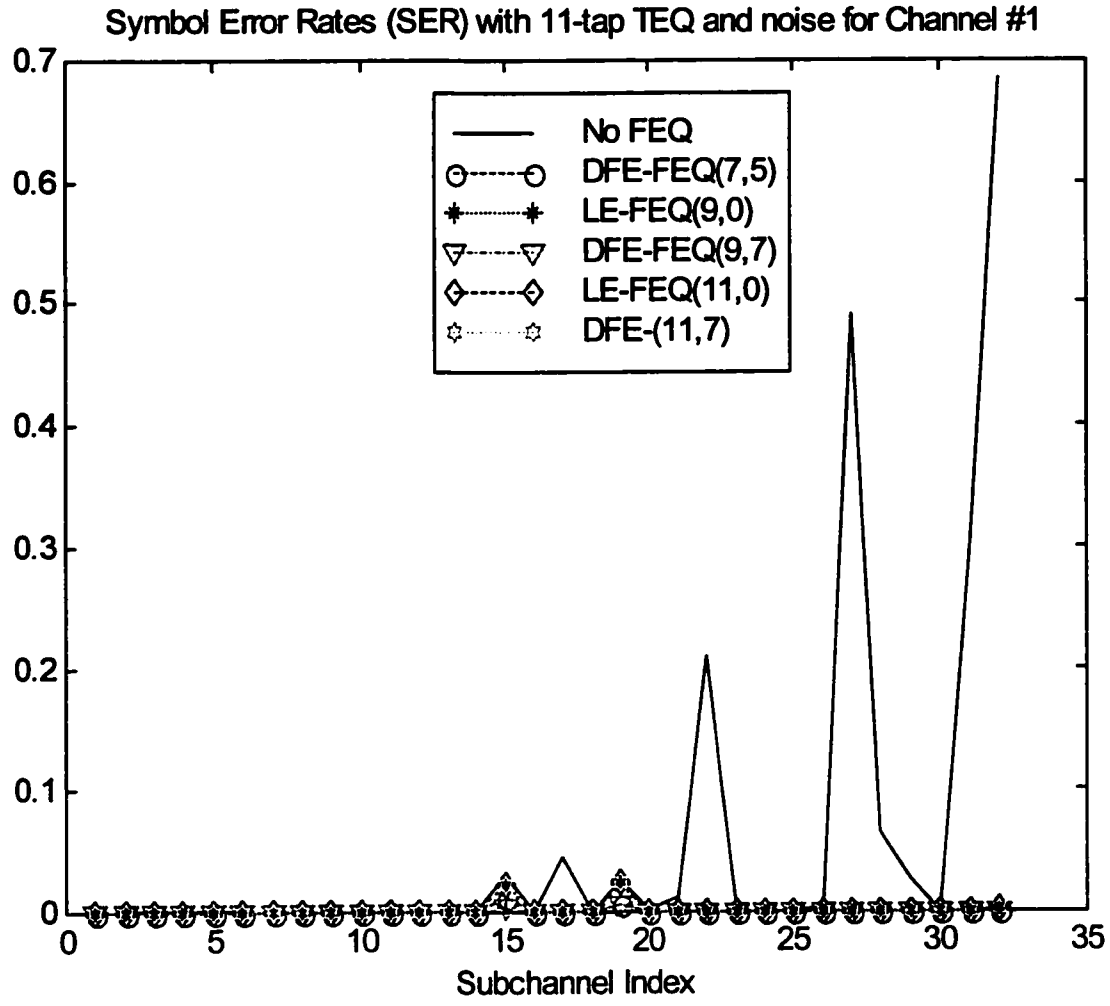

Figure 4.9.1: SER at the output of 11-tap TEQ and FEQ for Channel #1 with noise, for different number of taps in FEQ

Table 4.5.1a: Averaged SER and % improvement of FEQ over TEQ for Channel #1, without Noise

# of FEQ taps		11-tap TEQ Average SER_TEQ = 0.068333		21-tap TEQ Average SER_TEQ = 0.003		41-tap TEQ Average SER_TEQ =0.000979	
FF	FB	SER_FEQ	%Improvement	SER_FEQ	%Improvement	SER_FEQ	%Improvement
1	0	0.001750	97.44	0.001417	52.78	0.001083	-10.64
3	0	0.001250	98.17	0.001271	57.64	0.001042	2.13
3	1	0.001188	98.26	0.001167	61.11	0.000958	-6.38
5	0	0.001333	98.05	0.001292	56.94	0.001187	-21.28
5	1	0.001208	98.23	0.001167	61.11	0.001000	-2.13
5	3	0.001250	98.17	0.001167	63.89	0.000854	12.77
7	0	0.001354	98.02	0.001458	51.39	0.001229	-25.53
7	1	0.001146	98.32	0.001104	63.19	0.000958	2.13
7	3	0.001333	98.05	0.000979	67.36	0.000916	6.38
7	5	0.000563	99.18	0.000458	87.72	0.000432	55.32
9	0	0.001292	98.11	0.001375	54.14	0.001187	-21.28
9	1	0.001229	98.20	0.001188	60.42	0.000979	0
9	3	0.001167	98.29	0.001083	63.89	0.001021	-4.25
9	5	0.000604	99.12	0.000417	86.11	0.000417	57.45
9	7	0.000875	98.72	0.000375	87.50	0.000438	55.32
11	0	0.001354	98.02	0.001375	54.17	0.001125	-14.89
11	1	0.001209	98.23	0.001062	64.58	0.000896	8.51
11	3	0.001108	98.42	0.000875	70.83	0.000896	8.51
11	5	0.000708	98.96	0.000542	81.94	0.000417	57.45
11	7	0.000875	98.72	0.000479	84.03	0.000729	25.53
11	9	0.000271	99.60	0.000229	92.36	0.000063	93.62
13	0	0.001271	98.14	0.001417	52.78	0.001083	-10.64
13	9	0.000292	99.57	0.000250	91.67	0.000021	97.87
13	11	0.000292	99.59	0.000083	97.22	0.000146	85.11
15	0	0.001458	97.87	0.001417	52.78	0.001167	-19.15
15	9	0.000375	99.45	0.000250	91.67	0.000104	89.36
15	11	0.000458	99.33	0.000229	92.36	0.000208	78.72
15	13	0.000625	99.08	0.000042	98.61	0.000354	63.83

Table 4.5.1b: Averaged SER and % improvement of FEQ over TEQ for Channel #1, with Noise

# of FEQ taps		11-tap TEQ Average SER_TEQ = 0.05958		21-tap TEQ Average SER_TEQ = 0.00379		61-tap TEQ Average SER_TEQ = 0.001375	
FF	FB	SER_FEQ	%Improvement	SER_FEQ	%Improvement	SER_FEQ	%Improvement
1	0	0.001750	97.06	0.001229	67.58	0.001187	13.64
3	0	0.001354	97.73	0.001271	66.48	0.001167	15.15
3	1	0.001125	98.11	0.001208	68.13	0.001164	19.69
5	0	0.001563	97.38	0.001479	60.99	0.001292	6.06
5	1	0.001104	98.15	0.001188	68.68	0.001063	22.73
5	3	0.001229	97.14	0.001229	67.58	0.001083	21.21
7	0	0.001521	97.45	0.001479	60.99	0.001271	7.58
7	1	0.001187	98.01	0.001188	68.68	0.001104	19.69
7	3	0.001229	97.94	0.001250	67.03	0.001188	13.64
7	5	0.000604	98.99	0.000588	54.62	0.000688	50.00
9	0	0.001583	97.34	0.001563	58.79	0.001375	0
9	1	0.001125	98.11	0.001229	67.58	0.001021	25.76
9	3	0.001229	97.94	0.001167	69.23	0.001083	21.21
9	5	0.000688	98.85	0.000625	83.52	0.000521	62.12
9	7	0.000396	99.34	0.000750	80.22	0.000521	62.12
11	0	0.001625	97.27	0.001542	59.34	0.001417	-0.03
11	1	0.001000	98.32	0.001279	67.58	0.001021	25.76
11	3	0.001229	97.94	0.001208	68.13	0.001125	18.18
11	5	0.000729	98.78	0.000625	83.52	0.000563	59.09
11	7	0.000417	99.30	0.000729	80.77	0.000563	59.09
11	9	0.000167	99.72	0.000205	94.51	0.000250	81.82
13	0	0.001771	97.03	0.001667	56.04	0.001438	-0.05
13	9	0.000271	99.55	0.000396	89.56	0.000312	77.27
13	11	0.000271	99.55	0.000500	86.81	0.000542	60.61
15	0	0.001583	97.34	0.001521	59.89	0.001354	1.52
15	9	0.000667	98.88	0.001167	69.23	0.000771	43.94
15	11	0.000521	99.13	0.000771	79.67	0.000750	45.45
15	13	0.000563	99.06	0.000542	85.71	0.000479	65.15

4.4.6 Discussion for Case 3

Since this receiver design is a combination of both Case 1 and Case 2, it reflects the advantages of both the cases, without incorporating the factors that lead to or result in the disadvantages of the previous designs, namely the complexity of the equalizers. This design therefore clearly presents a better receiver structure than Case 1 or 2, as is evident from the results. The observations and discussion specific to this case are split into three parts, corresponding to the three different channels.

A. Channel #1

Observations specific to this channel are presented and discussed below:

(i) It can be seen from Figure 4.8.1 that in the absence of noise, the use of a TEQ with only 11 taps ensures almost perfect reconstruction with zero SER at the output of the demodulator for most of the subchannels. The FEQs with 7-9 FF taps and 5-7 FB help in reducing the SER even further, for the subchannels that have a higher value of SER at the output of the demodulator. The higher value of SER for the 15^{th} and the 19^{th} subchannel is odd. This discrepancy seems to channel-related, since it repeats for every signal that is processed through the channel.

(ii) From Figure 4.9.1, which presents the SER for signal *with* white noise, there does not appear to be much difference in performance of the system from the signal without noise, from either the output of the demodulator or the output of the FEQ. The FEQs are successful in reducing the SER below 0.0005, for both types of signal.

(iii) Table 4.5.1, which gives an averaged behaviour of the TEQ and different FEQs, indicates that the use of FEQs results in definite improvement in the average performance over TEQ. This improvement could reach up to almost 100%, if more taps are used in the DFE. This makes the use of FEQs in addition to a TEQ worthwhile, even for a simple channel with a linear phase. There is an improvement in the SER results even when an LE is used, although by a lesser extent as the DFE.

It can be concluded from the above observations that this particular channel does not cause any significant amount of distortion or ISI. For this channel, the system requires very few taps

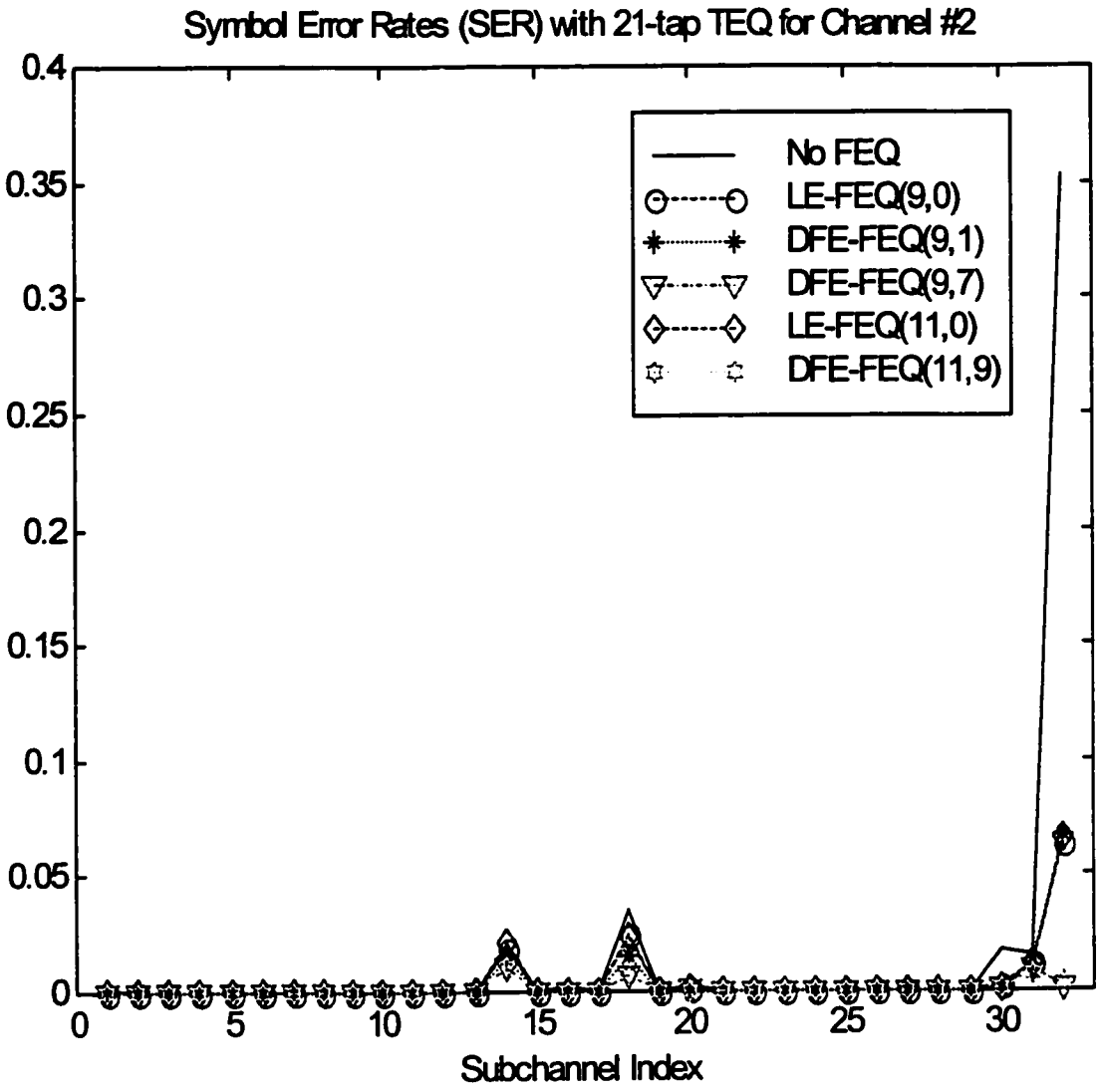

Figure 4.8.2a: SER at the output of FEQs with 21-tap TEQ for Channel #2 without noise for different number of taps in the FEQ

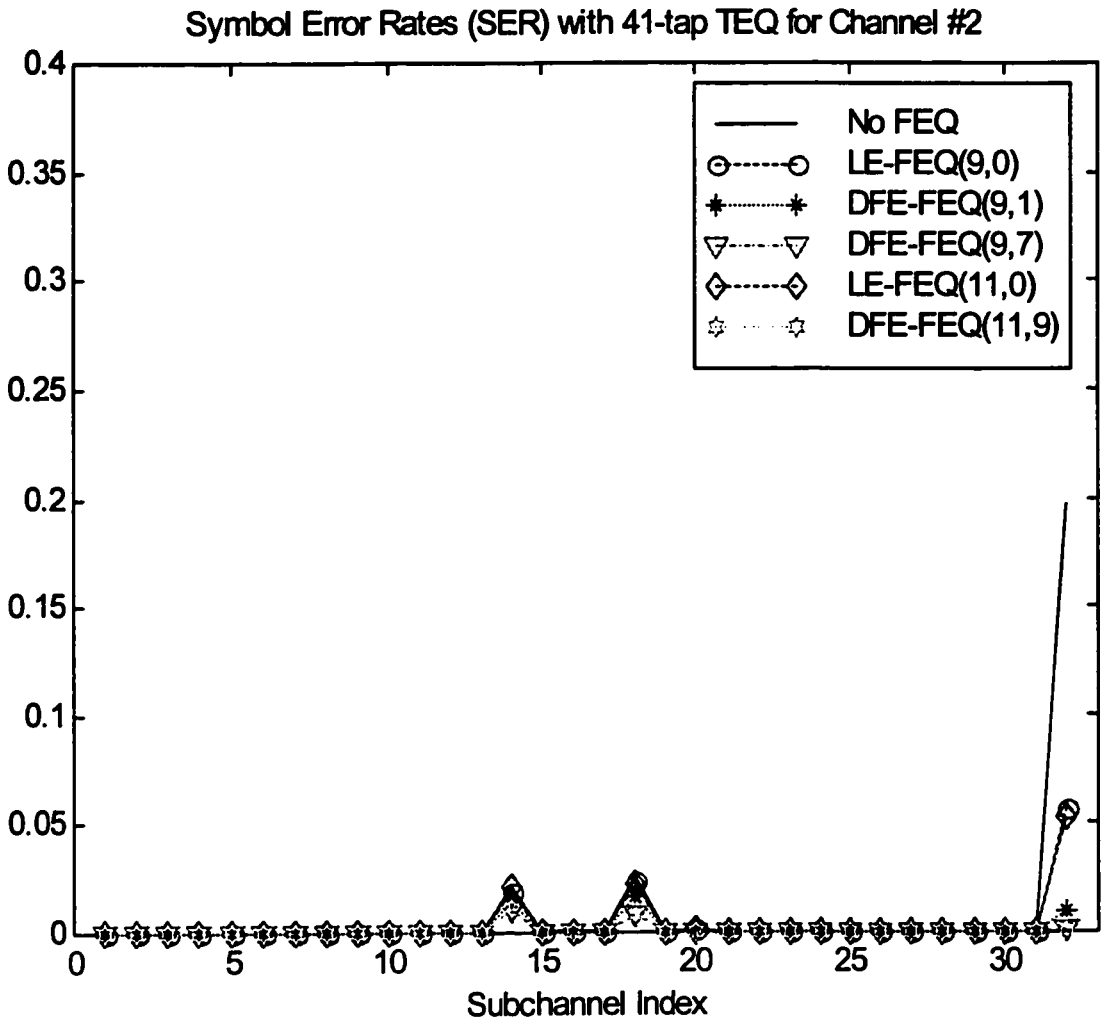

Figure 4.8.2b: SER at the output of 41-tap TEQ and FEQ for Channel #2 without noise, for different number of taps in FEQ

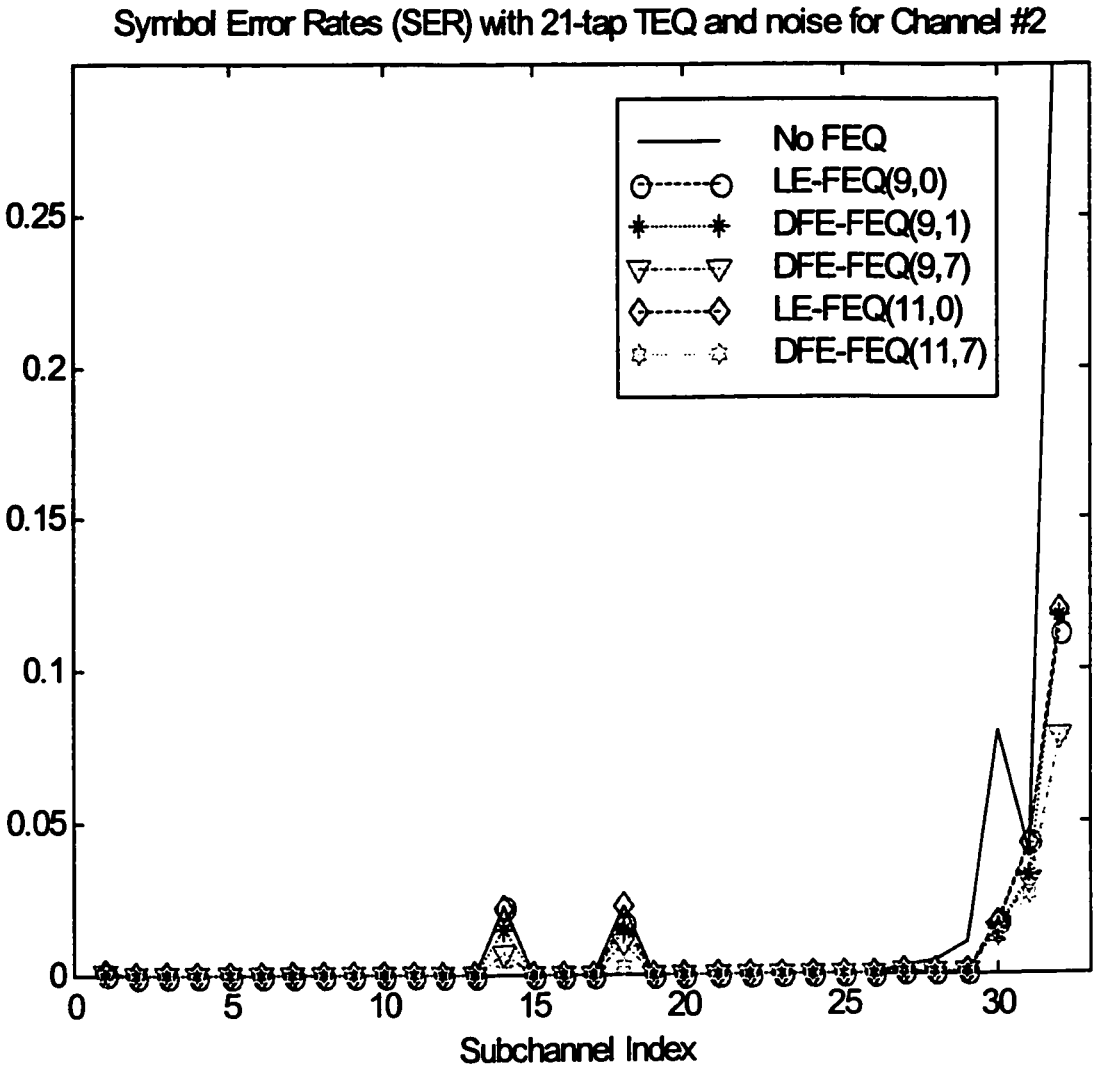

Figure 4.9.2: SER at the output of 21-tap TEQ and FEQ for Channel #2 with noise, with different number of taps in the FEQ

Table 4.5.2a: Averaged SER and % improvement of FEQ over TEQ for Channel #2, without Noise

# of FEQ taps		11-tap TEQ Average SER_TEQ = 0.051125		21-tap TEQ Average SER_TEQ = 0.013958		41-tap TEQ Average SER_TEQ =0.007646	
FF	FB	SER_FEQ	%Improvement	SER_FEQ	%Improvement	SER_FEQ	%Improvement
1	0	0.049271	03.63	0.013.63	06.42	0.007783	-00.82
3	0	0.036271	29.06	0.004750	65.97	0.004146	45.78
3	1	0.033455	34.56	0.0041667	70.15	0.001479	86.65
5	0	0.035771	30.03	0.0045625	67.31	0.003646	52.32
6	1	0.033875	33.74	0.0041456	70.30	0.001542	77.11
6	3	0.031000	39.36	0.0037917	72.84	0.001750	79.84
7	0	0.035188	31.17	0.0039583	71.64	0.003167	58.58
7	1	0.032792	35.56	0.0037500	73.13	0.001521	80.11
7	3	0.030042	41.24	0.0023542	83.13	0.001167	84.74
7	5	0.027708	45.80	0.0011875	91.49	0.000896	88.28
9	0	0.035188	32.23	0.0037705	72.98	0.003146	58.86
9	1	0.031053	39.20	0.0035417	74.63	0.001292	83.11
9	3	0.025512	43.64	0.0024583	82.39	0.001167	84.74
9	5	0.027575	45.48	0.0011250	91.94	0.000750	90.19
9	7	0.027146	46.90	0.0091667	93.43	0.000604	92.09
11	0	0.034646	32.23	0.0035542	72.39	0.003020	60.49
11	1	0.031312	38.75	0.0038125	72.68	0.001479	80.65
11	3	0.029208	42.87	0.0026042	81.34	0.001088	85.83
11	5	0.027146	46.90	0.0011875	91.49	0.000854	88.83
11	7	0.027896	45.44	0.0010625	92.39	0.000708	90.74
11	9	0.025771	49.59	0.0008956	93.56	0.000604	92.09
13	0	0.034021	33.46	0.0039381	71.79	0.003187	58.31
13	9	0.026750	47.68	0.0007917	94.33	0.000542	92.92
13	11	0.027155	46.52	0.0009792	92.98	0.000354	95.37
15	0	0.034657	32.15	0.0041875	70.00	0.003312	56.68
15	9	0.023604	53.83	0.0010417	92.54	0.000500	93.46
15	11	0.026083	48.91	0.0011458	91.79	0.000542	92.92
15	13	0.027583	46.05	0.0013542	91.30	0.000417	94.55

Table 4.5.2b: Averaged SER and % improvement of FEQ over TEQ for Channel #2, with Noise

# of FEQ taps		15-tap TEQ Average SER_TEQ = 0.04546		21-tap TEQ Average SER_TEQ = 0.01731		61-tap TEQ Average SER_TEQ = 0.009229	
FF	FB	SER_FEQ	%Improvement	SER_FEQ	%Improvement	SER_FEQ	%Improvement
1	0	0.043688	3.89	0.014938	13.72	0.009375	-1.58
3	0	0.030438	33.04	0.007063	59.21	0.005625	39.05
3	1	0.029896	34.24	0.007125	58.85	0.004521	51.02
5	0	0.030521	32.86	0.007042	59.33	0.005333	42.21
6	1	0.029000	36.21	0.006896	60.17	0.004208	54.40
6	3	0.028562	37.17	0.006250	63.89	0.003917	57.56
7	0	0.029729	34.60	0.006875	60.29	0.005271	42.89
7	1	0.027708	39.05	0.006220	64.02	0.003938	57.34
7	3	0.026062	42.67	0.006333	63.42	0.003729	59.59
7	5	0.025104	44.75	0.004458	74.25	0.002542	72.46
9	0	0.029227	35.70	0.006833	60.53	0.005125	44.47
9	1	0.027083	40.42	0.006271	63.78	0.003979	56.88
9	3	0.025688	43.49	0.005521	68.11	0.003958	57.11
9	5	0.025625	43.63	0.004583	73.53	0.002542	72.46
9	7	0.025854	43.13	0.004479	74.13	0.002604	71.78
11	0	0.028417	37.49	0.007083	59.08	0.005167	44.02
11	1	0.026646	41.39	0.005792	66.55	0.003833	58.46
11	3	0.026729	41.20	0.005938	65.70	0.003438	62.75
11	5	0.025354	44.25	0.004271	75.33	0.002604	71.78
11	7	0.026542	41.61	0.004000	76.89	0.002375	74.27
12	9	0.025542	43.81	0.003979	77.02	0.002687	70.88
13	0	0.028917	36.39	0.007104	58.97	0.005333	42.21
13	9	0.025417	44.09	0.003771	78.22	0.002896	68.62
13	11	0.025917	42.99	0.003271	81.11	0.002208	76.07
16	0	0.029125	35.93	0.007396	57.28	0.005458	40.86
15	9	0.024896	45.23	0.003771	78.22	0.002661	71.11
16	11	0.026354	42.03	0.003771	78.22	0.001729	81.26
15	13	0.026000	42.81	0.004063	76.53	0.002250	75.61

for a TEQ and a minimum number of taps in the individual FEQs for equalization. In the absence of noise, both the equalizers perform well in terms of reducing the SER to almost zero. Use of FEQ result in definite improvement in the signal, as compared to the system without FEQ. The system continues to show a good performance in terms of a low value of SER in the presence of white noise.

B. Channel #2

(i) From Figure 4.8.2(a, b), it can be seen that about half the subchannels show an SER of zero at the output of the TEQ itself. For other subchannels, there is a marked improvement after the FEQ is employed. The subchannels having a higher value of the SER at the sliced output of the TEQ-demodulator (denoted by SER_TEQ) show more improvement when FEQ is employed, as compared to the subchannels that have a lower initial value of the SER.

(ii) A few observations can be made from the Table 4.5.2, which gives the averaged behaviour over all the subchannels. When a DFE is employed as an FEQ, it is observed that the SER decreases when the number of both the feed forward and the feedback taps in the DFE is increased. Overall, the DFE appears to give a better result as compared to the LE. A DFE with 9 or 11 feed forward taps and any number of feedback taps is better than an LE with 11 taps.

(iii) When a 15-tap TEQ is employed, the value of the SER_TEQ, is higher when compared to the SER_TEQ obtained using 21-tap or 41-tap TEQ. The improvement of FEQ over TEQ reaches a maximum of 55% as the number of taps in FEQ is increased. The SER does not seem to go below 0.01. However, using 21 or 41 taps in the TEQ results in a value of SER_TEQ below 0.015. Using FEQs over this signal results in up to 90% improvement, resulting in the SER at the output of the FEQ (SER_FEQ) to go as low as 0.0006. This indicates that at least a 21-tap TEQ is required in order to obtain low error rates. Not only is the output of the demodulator less distorted, but also the FEQs are more successful in reducing the SER further with a 21- or 41- tap TEQ.

(iv) When noise is introduced (Figure 4.9.2), low frequency subchannels having high SNR continue to show good results, whereas the high frequency subchannels show a slight

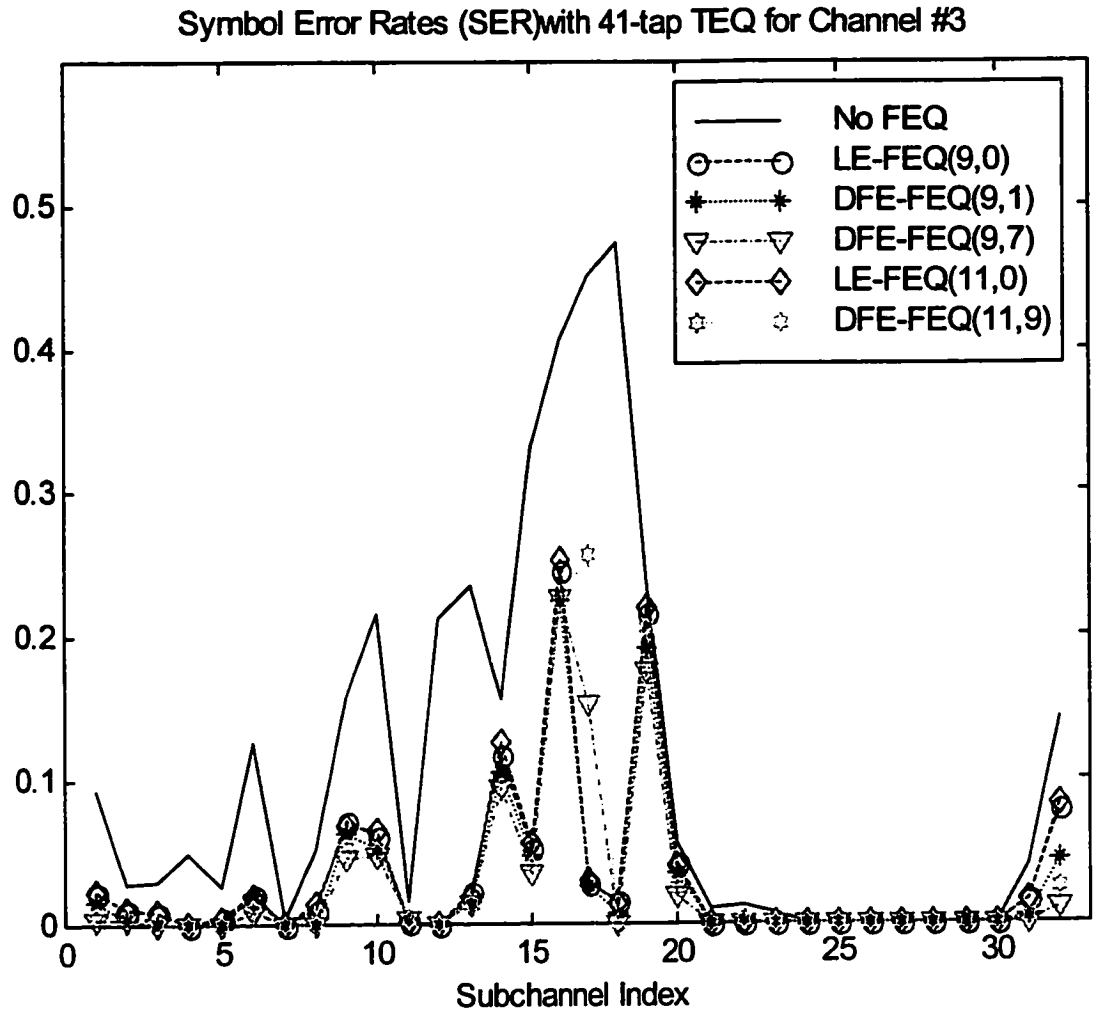

Figure 4.8.3a: SER at the output of 41-tap TEQ and FEQ for Channel #3 without noise, with different number of taps in the FEQ

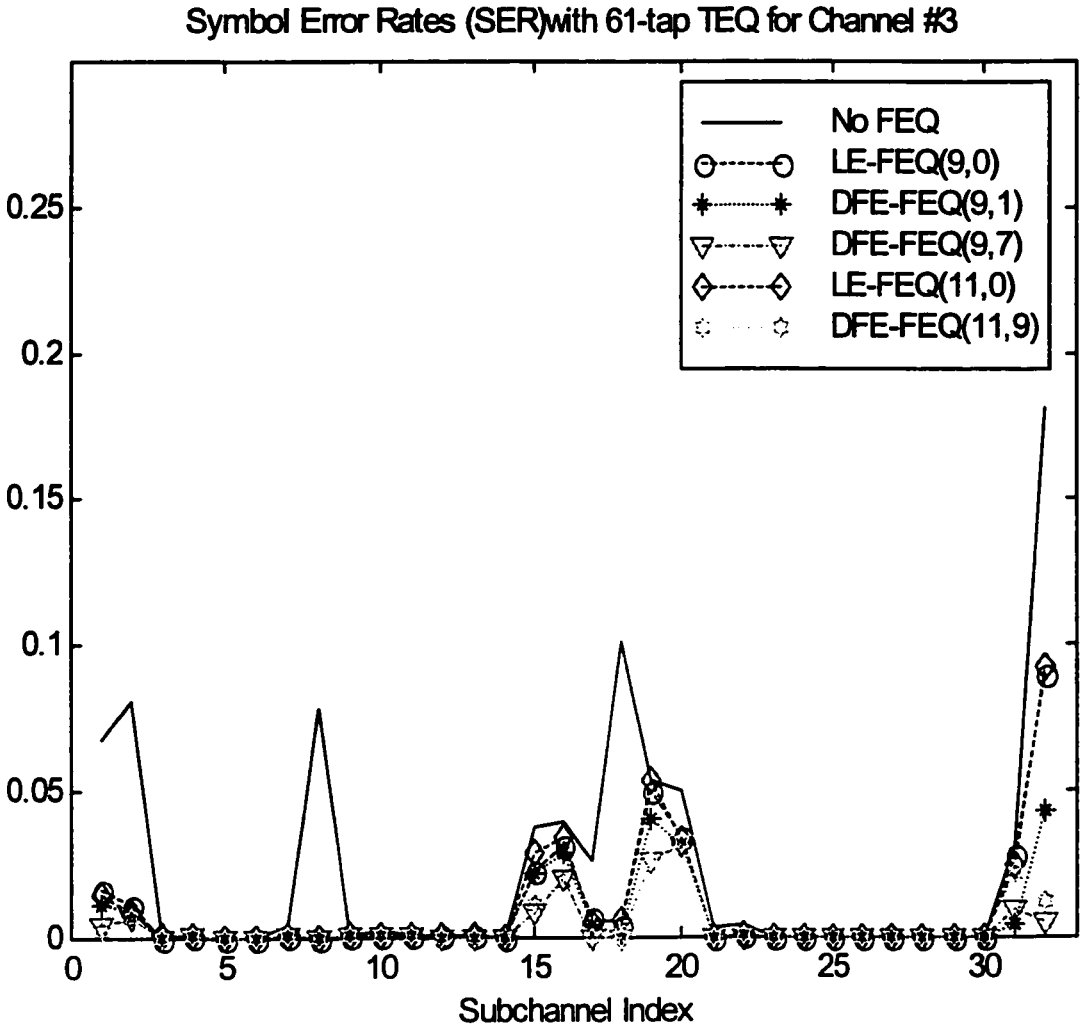

Figure 4.8.3b: SER at the output of 61-tap TEQ and FEQ for Channel #3 without noise, for different number of taps in FEQ

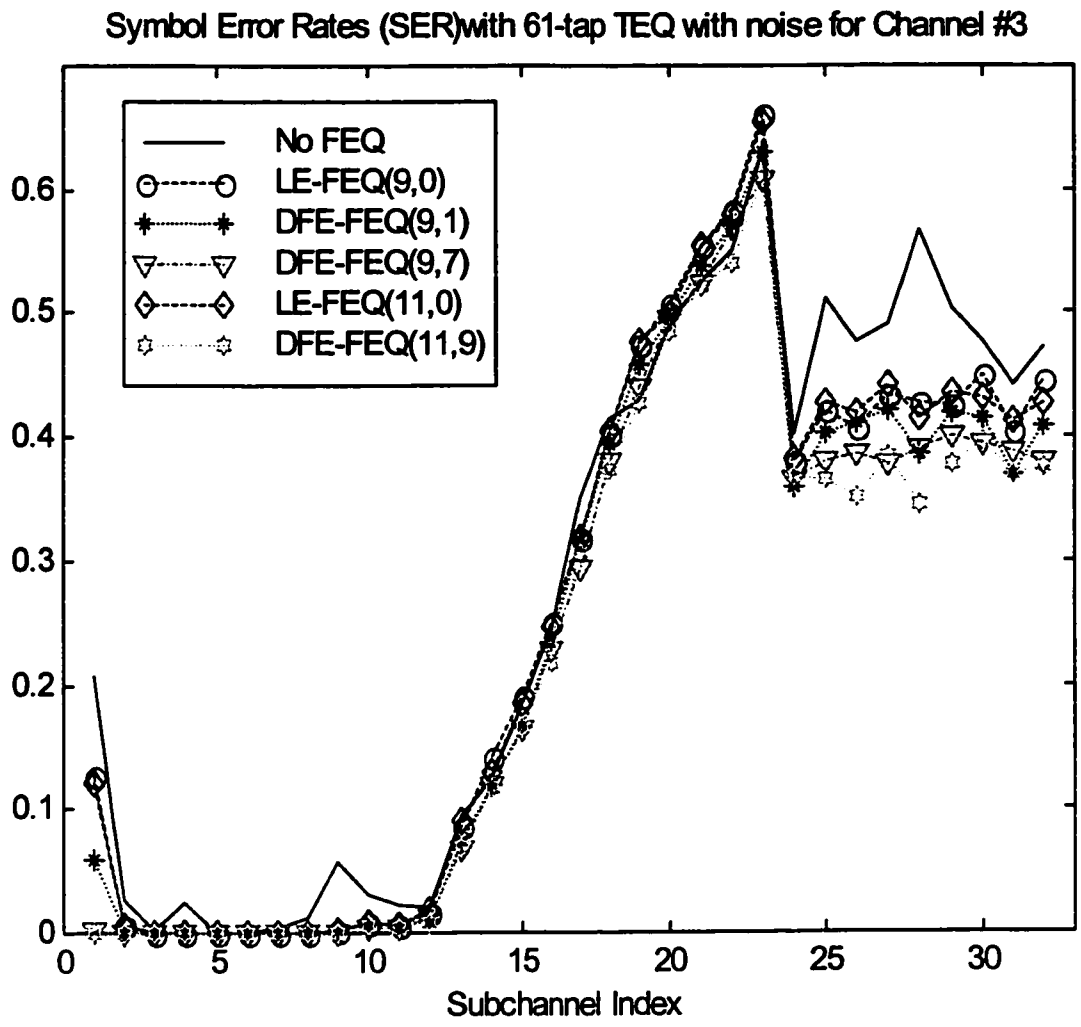

Figure 4.9.3a: SER at the output of 61-tap TEQ and FEQs for Channel #3 with noise, for different number of taps in FEQ

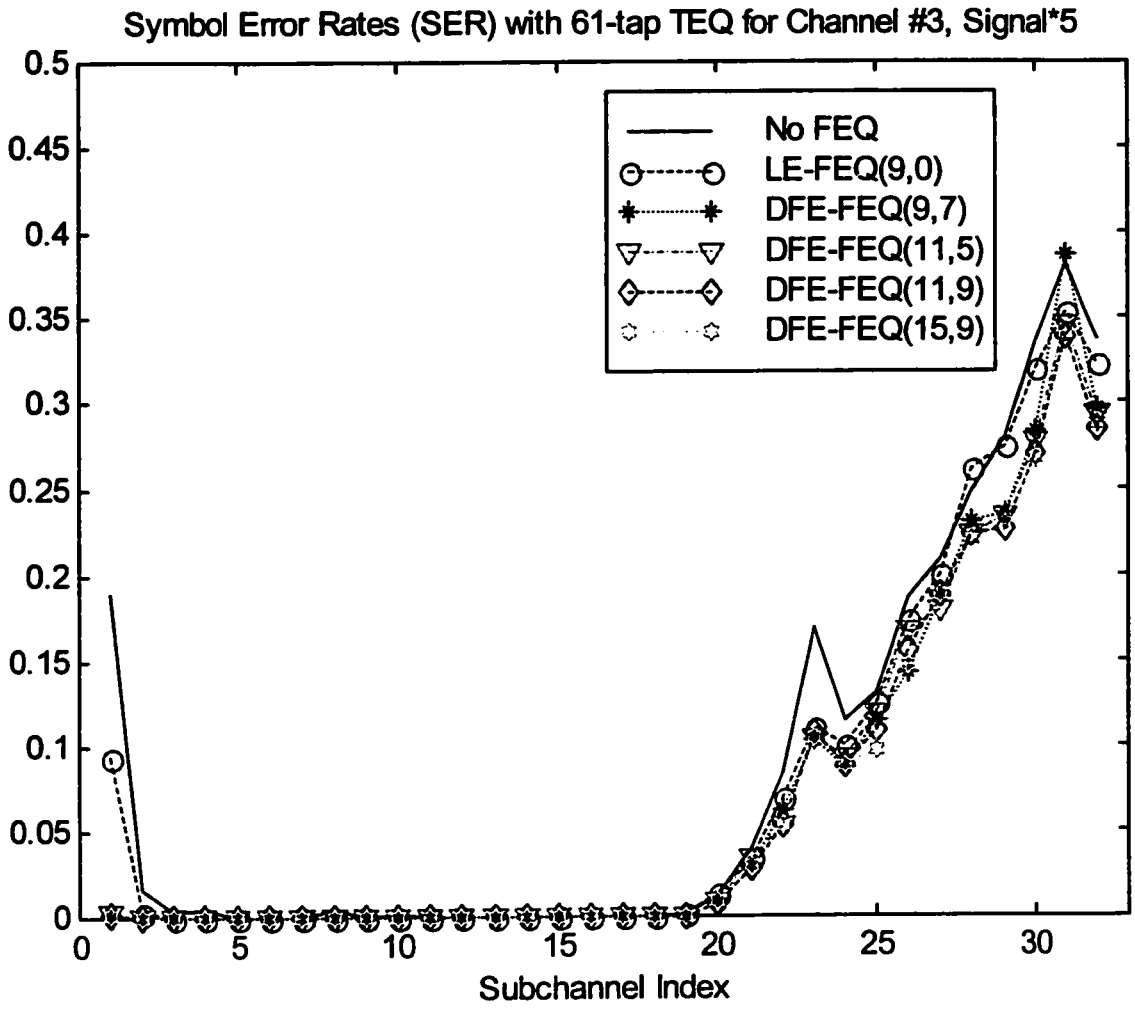

Figure 4.9.3b: SER with 61-tap TEQ for Channel #3 with Noise, Input signal amplification factor = 5

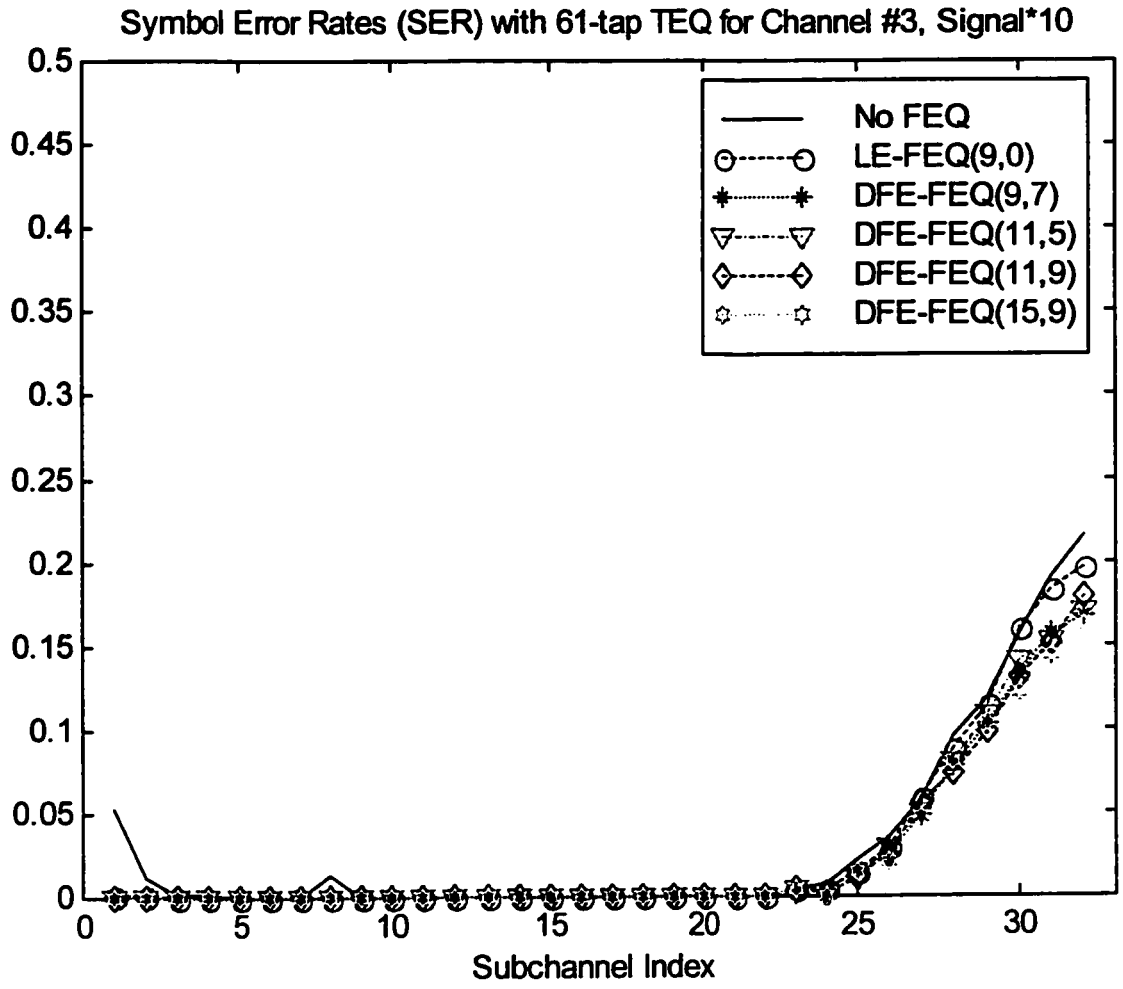

Figure 4.9.3c: SER with 61-tap TEQ for Channel #3 with Noise, Input signal amplification factor = 10

Table 4.5.3a: Averaged SER and % improvement of FEQ over TEQ for Channel #3, without Noise

# of FEQ taps		21-tap TEQ Average SER_TEQ = 0.18225		41-tap TEQ Average SER_TEQ = 0.11175		61-tap TEQ Average SER_TEQ =0.024062	
FF	FB	SER_FEQ	%Improvement	SER_FEQ	%Improvement	SER_FEQ	%Improvement
9	0	0.057396	68.51	0.032875	70.58	0.009396	60.95
9	1	0.047140	74.15	0.027083	75.76	0.006292	73.85
9	3	0.056938	68.76	0.030667	72.56	0.005396	77.58
9	5	0.050208	72.45	0.030083	73.08	0.004479	81.39
9	7	0.040688	77.68	0.026479	76.31	0.003667	84.76
11	0	0.057429	68.46	0.033625	69.91	0.009625	60.00
11	1	0.047190	74.19	0.025646	77.05	0.006205	74.20
11	3	0.048271	73.51	0.032562	70.86	0.004979	79.31
11	5	0.050833	72.11	0.032468	70.96	0.004396	81.73
11	7	0.031813	98.16	0.030208	72.97	0.004354	81.91
12	9	0.055870	69.34	0.031833	71.51	0.004333	81.99
13	0	0.056596	68.78	0.033771	69.78	0.009770	59.39
13	9	0.042479	76.69	0.028021	74.93	0.004542	81.13
13	11	0.042083	76.91	0.031292	71.99	0.004479	81.39
15	0	0.054646	68.37	0.033104	70.38	0.010271	57.32
16	9	0.056646	68.82	0.028938	74.11	0.005083	78.87
16	11	0.051479	91.75	0.034521	69.11	0.006750	71.95
15	13	0.048479	73.40	0.036688	67.17	0.005708	76.28

Table 4.5.3b: Averaged SER and % improvement of FEQ over TEQ for Channel #3, with Noise

# of FEQ taps		21-tap TEQ Average SER_TEQ = 0.2951		41-tap TEQ Average SER_TEQ = 0.25598		61-tap TEQ Average SER_TEQ = 0.27471	
FF	FB	SER_FEQ	%Improvement	SER_FEQ	%Improvement	SER_FEQ	%Improvement
9	0	0.25362	14.06	0.25837	09.65	0.25410	07.50
9	1	0.24319	17.59	0.24310	14.99	0.23965	12.76
9	3	0.23623	19.95	0.23596	17.49	0.23375	14.91
9	5	0.23655	19.74	0.23248	18.71	0.23233	15.43
9	7	0.23029	21.96	0.22915	19.87	0.23040	16.13
11	0	0.25154	14.76	0.25646	10.32	0.25281	07.97
11	1	0.24196	18.01	0.23856	16.55	0.23631	13.98
11	3	0.23604	20.01	0.23115	19.17	0.23200	15.55
11	5	0.23135	21.60	0.22967	19.69	0.23008	16.25
11	7	0.22712	23.04	0.22494	21.35	0.22792	17.03
13	9	0.22540	23.62	0.22650	20.79	0.22452	18.27
13	0	0.25056	15.09	0.25433	11.07	0.25165	08.39
13	9	0.22396	24.10	0.22081	22.79	0.22156	19.35
13	11	0.22035	25.33	0.21933	22.30	0.22015	19.86
17	0	0.25088	14.99	0.25233	11.77	0.25123	08.55
15	9	0.22092	25.14	0.22053	22.89	0.21902	20.27
17	11	0.21946	25.63	0.21790	23.81	0.21704	20.99
15	13	0.21956	25.59	0.21553	23.48	0.21481	21.50

degradation, as expected. The SER is reduced by the use of FEQ to some extent, which is a positive indication. The improvement in the SER values is up to 75% when a DFE-FEQ is employed. The improvement obtained using LE-FEQ is up to 50%. This indicates that in the presence of white noise, the FEQs do not perform as well as they do in the absence of noise. The SER (Table 4.5.2b) values do not go below 0.001.

It can be concluded from the analysis, that for a 26-AWG 1-km channel, the data can be received almost error-free with the use of only a 21-tap TEQ. A 41-tap TEQ gives slightly better result than a 21-tap TEQ. In addition to a 21 or a 41-tap TEQ, a decision feedback FEQ with 9 feed forward and 7 feedback taps suffice for equalizing the channel and reducing the error rate further by almost 90%. There are some subchannels, which give zero error rates without the use of an FEQ. For these subchannels, the FEQ can be bypassed, thereby reducing the latency in the system. A DFE gives better performance than an LE, so that non-linear equalization appears to be a better option than linear equalization.

C. Channel #3

(i) The SER for this channel are worse than those for Channel #2, as can be seen from Figure 4.8.3. Few subchannels still show an SER of almost zero when a 41-tap or a 61-tap TEQ is employed. A significant amount of improvement is observed when the FEQs are employed, especially for the case of 61-tap TEQ.

(ii) In the presence of noise (Table 4.5.3), the situation is even worse. About half of the subchannels indicate a large value of SER, causing the average SER to increase up to 0.2 (i.e, 20% error rate averaged over all subchannels). This implies that the signal power needs to be increased before the signal is transmitted through the channel.

(iii) The result of amplifying the signal by a factor of 5 and 10 prior to transmission through channel is shown in Figures 4.9.3b and 4.9.3c respectively. The resulting SER is drastically reduced at the output of the demodulator, and is further improved when FEQs are employed. This is a positive indication, implying that high-speed data can be transmitted through VDSL channel, if the signal is given more power at the transmitter end. The limit to how much power can be allocated to the signal, however, depends upon the transmitter.

(iii) The averaged SER once again shows a significant amount of improvement as 9-15 taps are employed in the FEQs. The SER at the output of the demodulator with 21- or 41-tap TEQ (SER_TEQ) is rather high, indicating a symbol error of more than 10 %, even in the absence of white noise. This reduces to 2% when 61 taps are used in the TEQ. When a DFE-FEQ is used, this value reduces by about 80% with 9 FF and 5 or 7 FB taps in the DFE, giving an SER of 0.006. The LE gives an improvement of about 60%. This is in agreement with the previous observation that the DFE gives a better performance than the LE.

To conclude, signal degradation due to channel distortion appears to be higher for higher bandwidth channel with bridged taps, which is expected. The signal needs to be given more power to minimize the distortion due to white noise. Most of the channel distortion appears to be cancelled by using a 61-tap TEQ. Although a 41-tap TEQ brings down the SER considerably, a 61-tap TEQ gives better results, and the final values of SER after the FEQs are employed, are reduced below an average of 0.006. The DFE with 9-15 FF and 5-13 FB taps help in removing the residual error up to an average (over all subchannels) of 80%. The success of LE is limited to 60%.

4.4 SUMMARY OF RESULTS

Three different receiver structures were tested to determine their suitability for the receiver structure for a DWMT communication system. Since the best performance of the equalizers can only be measured in the absence of white noise, the simulations were carried out without AWGN for making comparisons between the three systems. Noise was included for testing of the third system.

Certain observations can be made in the case of all the three channels that were investigated. The signal undergoes varying degrees of attenuation and distortion, depending upon the type of channel. The common observation for all the three channels is that that most of the distortion seems to occur for very low and higher subchannels, which carry lower SINR or lower SNR. By and large, subchannels that carry high signal power give a good performance with respect to SER.

For Plausible Receiver #1 consisting of only pre-detection TEQ, it was observed the TEQ is effective in removing most of the distortion that causes ISI. For Channel #1, which was a trivial channel with no phase distortion, an 11-tap TEQ was sufficient to reduce the SER at the output of the demodulator to below 0.001. For the other two channels, the SER at the output of the modulator in the absence of white noise reduces to almost 0.01, but several taps (~201) have to be employed in the TEQ to achieve that result. The length of the training sequence had to be increased to 5000 samples and the step-size parameter λ had to be reduced further in order to obtain convergence of such a large number of taps. Attempts to reduce the SER further were not successful. In addition, the latency in the simulation was very high to limit the number of trials for testing of this system. These results indicate that a TEQ - only receiver may not be suitable for a DWMT system.

For Plausible Receiver #2 consisting of only post-detection FEQs, the signal at the output of the demodulator was found to be highly corrupt. The averaged SER without any type of equalization was found to be ~ 0.38, 0.72 and 0.72 for Channels #1, #2 and #3 respectively. The FEQs help in reducing this by some extent. For the first channel, the reduction in the value of SER was found to be significant (up to 0.07), indicating about 80% improvement over the unequalized total symbol rate. For Channel #2 and #3, the improvement was very little. The SER was reduced to 0.38 (46% of the total symbol rate), even when 51 FF and 41 FB taps were employed in the FEQ. This indicates that this particular structure for the DWMT receiver is also unacceptable.

The third and the final receiver structure consisted of a simple TEQ with 21-61 taps, employed at the channel (or channel and noise) output and a simple FEQ consisting of about 9-15 taps, employed at the demodulated output of each subchannel. In the presence of a 21-tap TEQ, the SER at the output of the demodulator is significantly low to begin with. When these low error rate signals are passed through the FEQs, the SER drops even further, to almost 90% for all the three channels. For the Channel #1, the best possible SER is almost 0.0002 with the FEQs. For the Channels #2 and #3, the SERs could be reduced to below 0.006 with a maximum of 15-FF and 13-FB DFE-FEQ. For all the cases tested, the DFE showed better performance than the LE. It may be possible to further improve the performance of the equalizers by varying the parameters, *i.e.*, by using a 61-tap TEQ if its complexity can be afforded, and 13-15 taps in the FEQ. The length of the training sequence of the FEQ was also

small and manageable, and the total latency for operation of this system was very low, as compared to the latency experienced in running the first system with only TEQ.

Performance of the system was good without input signal amplification up to a sampling frequency of 10 MHz, where the noise power was not so large as compared to the signal power. For higher sampling frequency (nearing 20 MHz), which implies a higher channel bandwidth, white noise caused a significant amount of degradation. To overcome the effect of white noise, it became important to increase the signal power at the transmitter end. The SER reduced significantly when the channel input was amplified by a factor of 5 or 10

It can therefore be concluded that the third receiver with a simple TEQ and FEQ for the DWMT system gives the best results for high-speed data transmission over VDSL technology.

CHAPTER 5

CONCLUSIONS

5.1 CONCLUSIONS

In this thesis, a DWMT communication system based on multicarrier modulation has been designed and tested for transmission of high-speed data on twisted pair channels. Modulation and demodulation was performed by M-band cosine-modulated filter bank. The system was designed for M=32 subchannels. Adaptive loading was used for bit allocation on the subchannels. Three different VDSL channel models are used for testing of the DWMT system.

Three different receiver designs were tested for the purpose of choosing an appropriate equalizer for DWMT transceiver. The first design consisted of using a TEQ prior to the demodulation of the signal. It was found that although the TEQ was able to remove a significant amount of channel distortion, the amount of taps required to totally equalize the entire channel was very high. The increasing complexity of the equalizer also resulted in other problems such as unusually large length of the training sequence and very high latency. Therefore, this design was not found to be suitable for DWMT receiver.

The second design consisted of using an FEQ at the output of the demodulator, for each subchannel. For this design, it was found that the demodulator outputs were highly distorted with a large amount of ISI, resulting in large values of the SER for the most of the subchannels. The FEQs were able to remove some ISI. However, it was difficult to eliminate the ISI completely, even with a large number of taps in the FEQs. This design therefore proved to be unacceptable as a receiver structure for DWMT.

The third design consisted of using a simple 11-61-tap TEQ and about 3-15-tap FEQs. The TEQ employed an LE, whereas the FEQs employed either an LE or a DFE. This design gave a far better performance than the previous two designs, since it

incorporated the features from both the designs, with lesser complexity. The TEQ eliminated most of the channel distortion, reducing the SER of the reconstructed signal significantly. Very simple FEQs with only 9-11 taps were sufficient to reduce the SER further by almost 90%, giving an extremely low value of the average SER. The DFE was found to give a better performance than the LE.

Observing the results obtained from testing of the three receiver designs, the third design, consisting of 11-61 tap LE-TEQ and 9-15 tap DFE-FEQ, is therefore proposed as a receiver structure for the DWMT communication system to be used for VDSL technology.

5.2 DIRECTIONS FOR FUTURE RESEARCH

The current thesis is focused on a DWMT system for M=32 subchannels. Future research based on this design can incorporate a large number of subchannels to further investigate the performance of the system in the presence of larger M.

It might be of interest to investigate other receiver structures, such as those based on MLSE techniques or fractionally spaced equalizers that could perhaps enhance the performance of DWMT even further.

In addition, any coding scheme such as trellis coding, or a pre-coding scheme could be incorporated in the transceiver design to improve the performance.

BIBLIOGRAPHY

1. J. J. Werner, "The HDSL environment", *IEEE Journal in Selected Areas of Communications.*, vol. 9, pp.785-800, August 1991.

2. J. J. Wikner , Y. Gao and N. Tan, "D/A conversion Interface, Design for DMT, ADSL Application", *The Chip: Circuits and Devices*, November 1998.

3. H. Greggains ,"ADSL and High Bandwidth over copper lines", *International Journal of Network Management,* vol. 7, pp. 277-287, 1997.

4. J. S. Chow, J. C. Tu and J. M. Cioffi, "A discrete multitone transceiver system for HDSL Applications", *IEEE Journal in Selected Areas of Communication*, vol.9, no.6, pp. 895-908, August 1991.

5. J. S. Chow, J. M. Cioffi and J. A. C. Bingham, "Equalzier training algorithms for multicarrier modulation systems", *International Conference on Communication, Geneva, Switzerland*, pp. 761-765, May 1993.

6. G. Cherubini, E. Eleftheriou and S. Oelcer, " CAP/QAM, DMT and Filter Bank based modulation Techniques for VDSL ", *ANSI Standard Committee, TIEI.4*, June 1999.

7. S. D. Sandberg, M. A. Tzannes and M. C. Tzannes, "Overlapped Discrete Multitone Modulation for High Speed Copper Wire Communication", *IEEE Journal in Selected Areas of Communication*, vol.13, no.9, December 1995.

8. M. V. Bladel and M. Moeneclaey, "Time domain equalization for multicarrier communication", *IEEE GLOBECOM Mini conference*, pp.167-171, 1995.

9. J. A. C. Bingham, "Multicarrier modulation for data transmission: An idea whose time has come", *IEEE Communication Magazine*, pp. 5 -14, May 1990.

10. M. A. Tzannes, "System Design issues for DWMT transceiver", *ANSI Standard Committee, T1E1.4*, April 1993.

11. M. A. Tzannes M. C. Tzannes, J. Proakis and P. N. Heller, "DMT system, DWMT system and digital filter banks", *Proceedings International Conference on Communication*, 1994.

12. K. R. Rao and A. J. Bopardikar, "*Wavelet Transforms - Introduction to theory and Applications*", Addison Wesley, 1998.

13. N. J. Fliege , " Examples of Wavelet Systems", *Multirate Digital Signal Processing*, Baffin's Lane, Chichester, John Wiley and Sons Ltd., pp. 276 - 283, 1995.

14. P. P. Vaidyanathan , "*Multirate systems and Filter banks*" , Engelwood Cliff, N.J. Prentice Hall, New Jersey, 1993.

15. M. A. Tzannes, M. C. Tzannes and H.L Resnikoff, "The DWMT: A Multicarrier Transceiver of ADSL using M-band Wavelet Transform", Aware Inc., *ANSI Standard committee, T1E1.4*, contribution T3-100, April 1993.

16. R. D. Koilpillai and P. P. Vaidyanathan, "Cosine-modulated FIR filter banks satisfying perfect reconstruction", *IEEE Transactions on Signal Processing*, vol. 40, no. 4, pp. 770 - 783, April 1992.

17. P.Steffen, P.N. Heller, R.A. Gopinath and C.S. Burrus, "Theory of regular M-band wavelet Bases", *IEEE Transaction on Signal Processing*, vol. 41, no.12, pp. 3497, December 1993.

18. T. Nguyen and P. P. Koilpillai, "The design of arbitrary length cosine modulated filter banks and wavelets satisfying perfect reconstruction", *Proc. IEEE Signal Processing, International Symposium on Time-Frequency and Time Scale Analysis*, Victoria, B.C, pp. 299-302, 1992.

19. T. Nguyen, "A class of generalized cosine-modulated filter banks", *Proceedings of IEEE, International Symposium on circuits and Systems*, San Diego, pp. 943 - 946, May 1992.

20. B. R. Saltzberg, "Comparison of Single carrier and Multitone Digital modulation for ADSL applications ", *IEEE Communication Magazine*, pp. 114 - 121, November 1998.

21. H. Sheuermann and H. Goekler, "A comprehensive study of digital transmultiplexing methods", *Proceedings of IEEE*, vol. 69, no. 11, pp. 1419-450, November 1981.

22. A. N. Akansu, P. Duhamel, Y. Lin and M de Courville, "Orthogonal Transmultiplexers in Communications: A review", *IEEE Transaction on Signal Processing*, vol. 146, no. 41, April 1998.

23. M. Vetterli, "Perfect Transmultiplexers", *Proceedings ICASSP*, 1986.

24. R. G. Gallager, "*Information Theory and Reliable Communications*", John Wiley, N.Y. 1968.

25. L. Vanderdorpe, L. Cuvelier, J. Deryek , J. Louveauz and O. van de Wiel, "Fractionally spaced linear and decision feedback detectors for transmultiplexers", *IEEE Transactions on Signal Processing*, vol.46, no. 4, pp.996-1011, April 1998.

26. J. S. Chow and J. M. Cioffi, "A cost-effective M.L Receiver for multicarrier systems", *International Conference on Communication, Chicago*, pp. 948-952, June 1992.

27. F. Daffara and A. Chouley, "Maximum Likelihood Frequency Detectors for Orthogonal Multicarrier Systems", *International Conference on Communication (ICC '93), Geneva*, pp. 766-771, *May 1993.*

28. I. Daubechies , "Orthogonal Basis of Compactly Supported Wavelets, *Communications on Pure and Applied Mathematics*, Vol 41, pp. 909-996, 1988.

29. I. Daubechies , "Ten Lectures on Wavelets", *SIAM,* Philadelphia, P.A., 1992.

30. I. Daubechies , " The wavelet transform, time-frequency localization and signal analysis", *IEEE Trans. Information Theory*, vol. 36, pp. 961-1005, 1990.

31. Y. Meyer, "Wavalets, Algorithms ad Applications", *SIAM,* Philadelphia, P.A., 1993.

32. S. G. Mallat, " A theory for Multiresolution Signal Decomposition: the wavelet representation", *IEEE Transactions On Pattern Recognition and Machine Intelligence*, vol. 11, pp. 674-693, 1989.

33. T. Nguyen and H. Strang, "*Wavelets and Filter Banks*", Wellesley, M.A, Wellesley - Cambridge Press, 1996.

34. O. Rioul and M. Vetterli, "Wavelets and Signal Processing" , *IEEE Signal processing magazine*, pp. 14 - 38, October 1991.

35. H. L. Resnikoff, "Wavelets and Adaptive Signal Processing", *Proceedings SPIE*, Vol. 1565, 1991.

36. H. L. Resnikoff, "Contribution of wavelet matrix windows for harmonic analysis", *Proceedings of the IEEE, SPIE*, 1994.

37. H. S. Malvar, "Extended lapped transforms: Properties, applications and fast algorithms", *IEEE Transactions on Signal Processing*, Vol. 40, No.11, pp.2703-2714, November 1992.

38. S. K. Mitra and P. P. Vaidyanathan, "Low passband sensitivity digital filters: A generalized viewpoint and synthesis procedures", *Proceedings of the IEEE*, 1984.

39. R. D. Koilpillai and P. P. Vaidyanathan, "A spectral factorization approach to pseudo QMF design", *IEEE Transactions on Signal Processing*, pp. 82-92, January 1993.

40. T. Starr, J. M. Cioffi and P. J. Silverman, "*Understanding Digital Subscriber Line Technology*", Prentice Hall PTR, Saddle River, New Jersey, 1999.

41. I. Kalet, "The multitone channel", *IEEE Transactions on Communication, Vol. 37, No.2*, pp. 119, *September 1991.*

42. J. G. Proakis, "*Digital Communications*", 3-rd edition, McGraw Hill Inc, 1995.

43. P. Qureshi , "Adaptive Equalization", *Proceedings of the IEEE*, vol.73, no.9, pp. 1349, September 1985.

44. S. Haykin, "*Adaptive Filter Theory*", 3-rd edition, Prentice Hall, New Jersey, 1996.

45. Z. Song, Personal Communication.

46. "Spectrum Map for loop Transmission System", Draft proposal, American National Standard, T1E1.4/2000 – 002R3.

APPENDIX-1

Extension of 2-band wavelet transform to M-band wavelet transform

Let V_j denote the space of signals band-limited from $[0,2^j\pi]$. There exists a set of 'scaling functions' that form an orthonormal basis for V_j. For a fixed value of j, these are defined as:

$$\phi_{j,n}(t) = 2^{j/2}\,\phi(2^j t - n) \qquad \text{(A-1.1)}$$

and are obtained from scaling and translation of the original function $\phi(t)$. Similarly, if W_j be defined as the space of signals band-limited from $[2^j\pi,2^{j+1}\pi]$, there exist a set of functions $\{\psi_{j,n}(t)\}$ that form an orthogonal basis for the space W_j defined by

$$\psi_{j,n}(t) = 2^{j/2}\psi(2^j t - n). \qquad \text{(A-1.2)}$$

The set of functions $\{\psi_{j,n}(t)\}$ are called 'wavelet functions', and are obtained from scaling and translation of the function $\psi(t)$, called the 'mother' wavelet. Any arbitrary function x(t) can be expanded in terms of the basis functions $\phi_{j,n}(t)$ and $\psi_{j,n}(t)$ in the following manner:

$$x(t) = \sum_j x_j(t) = \sum_j \sum_n f_{j,n}\,\Psi_{j,n}(t) \qquad \text{(A-1.3)}$$

and

$$x(t) = \sum_j x_j(t) = \sum_j \sum_n c_{j,n}\,\Phi_{j,n}(t) \qquad \text{(A-1.4)}$$

where the set of coefficients $\{f_{j,n}\}$ and $\{c_{j,n}\}$ are called expansion coefficients, and define the 'wavelet transform' and the 'scaling transform' of x(t) respectively. The spaces spanned by V_j and W_j do not overlap, hence the basis functions $\{\psi_{j,n}(t)\}$ and $\{\phi_{j,n}(t)\}$ are orthogonal to each other. However, both V_j and W_j can be defined as subsets of a larger space V_{j+1}, which spans the space of band-limited functions from $[0,2^{j+1}\pi]$. Thus,

$$V_{j+1} = V_j \oplus W_j, \qquad \text{(A-1.5)}$$

where '$\oplus$' denotes direct sum. W_j can be considered as an orthogonal complement of V_j in V_{j+1}. Each V_j can be further decomposed into V_{j-1} and W_{j-1}. Since both V_j and W_j are subsets of V_{j+1}, their basis functions also are related to those of V_{j+1}. For j=0, we have

$$V_1 = V_0 \oplus W_0. \qquad \text{(A-1.6)}$$

Let $\phi(t)$ and $\psi(t)$ define the basis functions for V_0 and W_0 respectively. Then $\phi(2t)$ defines the basis functions for V_1. Then, there exist sequences $\{h^0(n)\}$ and $\{h^1(n)\}$ such that

$$\Phi(t) = \sum_n h_0(n)\Phi_{1,n}(t) = \sqrt{2}\sum_n h_0(n)\Phi(2t-n) \qquad \text{(A-1.7)}$$

and $$\Psi(t) = \sum_n h_1(n)\Phi_{1,n}(t) = \sqrt{2}\sum_k h_1(n)\Phi(2t-n) \qquad \text{(A-1.8)}$$

These sequences obey certain orthogonality conditions:

$$\sum_n h_0(n) = \sqrt{2}, \text{ so that } \sqrt{2}\sum_n h_0(n) = 2 \quad \text{and} \quad \sum_n h_1(n) = 0 \qquad \text{(A-1.9)}$$

The expansion coefficients $f_{j,n}$ and $c_{j,n}$ of the wavelet and scaling transforms respectively can be obtained as inner product of x(t) with the basis functions:

$$f_{j,n} = \langle x(t), \psi_{j,n}(t)\rangle \text{ and } c_{j,n} = \langle x(t), \phi_{j,n}(t)\rangle \qquad \text{(A-1.10)}$$

From equations (A-1.7) and (A-1.8), the coefficients $c_{j,n}$ can be expressed as

$$c_{j,n} = \sum_p h_0(p-2n)c_{j-1,n} + \sum_p h_1(p-2n)f_{i-1,n}\,, \qquad \text{(A-1.11)}$$

where the first term corresponds to the low pass component and the second term corresponds to high-pass component of the signal. This identity can be explained through a block diagram:

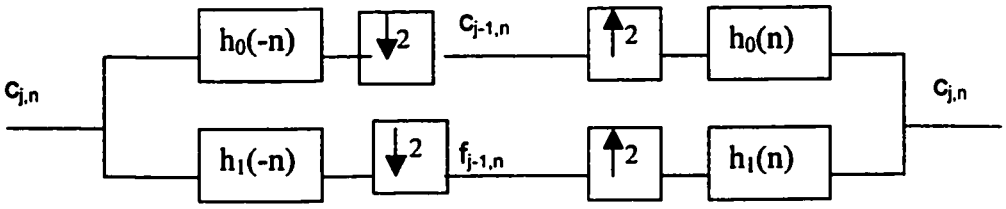

Figure A-1.1: Level –1 2-band wavelet decomposition and reconstruction

The above figure corresponds to level-1 decomposition, where the original signal belonging to the space V_j is decomposed once into two frequency components. The low-pass component belongs to the space V_{j-1} and the high-pass component lies in the space W_{j-1}. According to Mallat's tree algorithm, each low-pass component can be further decomposed further into another pair of signals, giving rise to higher level of decompositions.

This concept can be generalized to M>2 bands. Let W_j^i denote the space of functions band-limited to $[iM^j, (i+1)M^j]$. Then, V_{j+1} spanning the space $[0,M^{j+1}]$ can be expressed as a combination of M spaces Vj and W_j^i, i=1,2...M-1:

$$V_1 = V_0 \oplus W_0^1 \oplus W_0^2 \oplus \ldots\ldots\ldots\ldots \oplus W_0^{M-1} \qquad \text{(A-1.12)}$$

Each of which is orthogonal to each other and span the space starting from $[0,M^j]$, $[M^j,2M^j]$, $[2M^j,3M^j]$,.....$[(M-1)M^j,M^{j+1}]$. As in the 2-band case, V_0 corresponds to low-pass, and all other spaces correspond to band-pass or high-pass components. For such a case, equation (A-1.11) can be generalized into

$$c_{j,n} = \sum_p h_0(p-2n)c_{j-1,n} + \sum_{k=1}^{M-1} \sum_p h_p^k(p-2n)f_{i-1,n} \qquad \text{(A-1.13)}$$

Figure (A-1.2) below explains this identity through a block diagram.

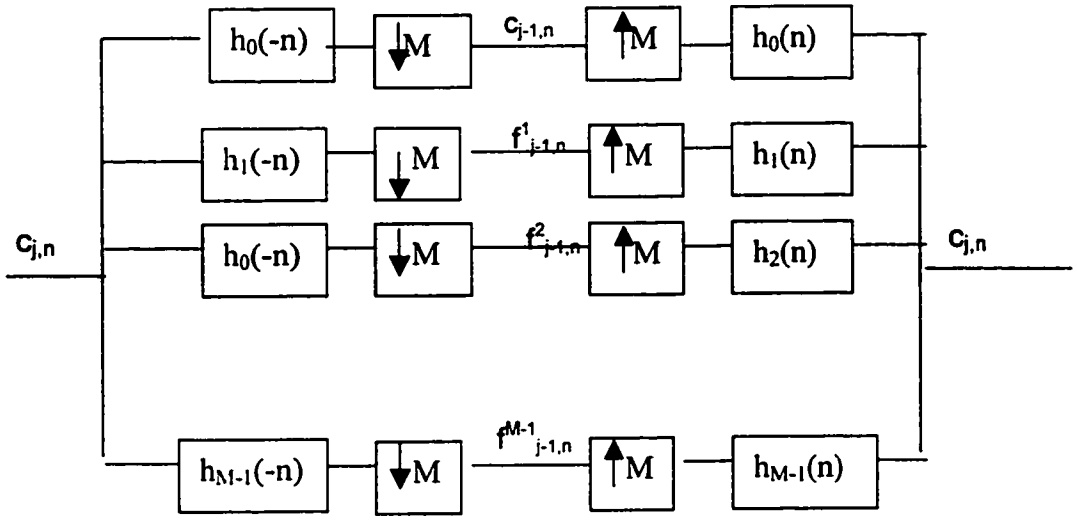

Figure A-1.2: Level-1 M-band wavelet decomposition

The lowest frequency bin in equation (A-1.12) can be further decomposed into M bands, giving a higher-level decomposition, similar to the 2-band case. Such decomposition is called multiplicity-M wavelet decomposition. In most of the applications known so far, only level-1 M-band decomposition is used. The sequences $\{h_k(n)\}$, k=0,1..M-1 correspond to taps of M-band filters, and can be realized through perfect reconstruction M-band wavelet filter banks. The filters on the left form an analysis filter bank, while the filters on the right form a synthesis filter bank.

APPENDIX-2

Symbol Recovery for DWMT system

The received signal, (sampled at rate F_s) is given by:

$$r_l = (c^*x)_l + n_l , \qquad \text{(A-2.1)}$$

where c_l is the composite channel impulse response and n_l is the sequence of noise samples. The operation '*' denotes convolution. At this point, one may choose to use a pre-detection or time-domain equalization filter Q(z). Let

$$y_l = (q^*r)_l \qquad \text{(A-2.2)}$$

denote the sequence at the output of Q(z), and

$$h_l = (q^*c)_l \qquad \text{(A-2.3)}$$

represent the impulse response of the equalized channel. If Q(z) equalizes the channel perfectly, then except for a delay d, we must have

$$h_l = \delta_{l-d} \qquad \text{(A-2.4)}$$

in which case there would be no ISI. In the absence of the time-domain equalizer (TEQ),

$$y_l = r_l \text{ and } h_l = c_l . \qquad \text{(A-2.5)}$$

The detector outputs are appropriate blocks of forward *Fast Wavelet Transform* (FWT) of y_l. The receiver passes y_l through M matched filters, the m-th filter matched to f_l^m, where f_l^m is the impulse response of the band-pass pulse corresponding to the subchannel 'm'. Without any ISI, it is expected that one would obtain one symbol per block-subchannel pair at the

output of the detector. The detector output θ_{i1}^{m1} for subchannel m1 and block i1 can be given as

$$\theta_{i1}^{m1} = \sum_{l} y_l f_{l-i1M-d}^{m1} \tag{A-2.6}$$

where 'd' is some arbitrary delay. From equations (A-2.1) – (A-2.5), it follows that

$$y_l = (h^*x)_l + n_l = \sum_{i=-\infty}^{\infty} h_j x_{l-j} + n_l \tag{A-2.7}$$

Substituting for the value of x_l from equation (2.15), we obtain

$$y_l = \sum_{j} h_j \sum_{i} \sum_{m} s_i^m f_{l-j-iM}^m + n_l \tag{A-2.8}$$

Substituting in equation (5), we have

$$\theta_{i1}^{m1} = \sum_{i}\sum_{m}\sum_{l}\sum_{j} h_j s_i^m f_{l-j-im}^m f_{l-i1M-d}^{m1} + \sum_{l} n_l f_{l-i1M-d}^{m1} \tag{A-2.9}$$

Let us define l' = l-j-iM. Then, making a change of variables, we have

$$\theta_{i1}^{m1} = \sum_{i}\sum_{m}\sum_{l'}\sum_{j} h_j s_i^m f_{l'}^m f_{l'+j+iM-i1M-d}^{m1} + \sum_{i}\sum_{j}\sum_{l'} n_{l'+j+iM} f_{l'+j+iM-i1M-d}^{m1} \tag{A-2.10}$$

Since l' is a dummy variable, we can drop the prime. Substituting j→j+d, we finally obtain

$$\theta_{i1}^{m1} = \sum_{i}\sum_{m} s_i^m \sum_{j} h_{j+d} \sum_{l} f_l^m f_{l-(i1-i)M+j}^{m1} + \sum_{i}\sum_{j}\sum_{l} n_{l+j+d+iM} f_{l-(i1-i)M+j}^{m1} \tag{A-2.11}$$

The right-hand-side corresponds to the total contributions to decision for a symbol in the m1-th subchannel and the i1-th frame.

APPENDIX – 3

Parameters used for Channel modelling

Channel #1:

smplr -- sampling rate, in MHz
fmax --- maximum frequency, in MHz, *nn ----- order of the FIR filter*
km ----- length of the line, in km, *chnn --- the FIR filter's amplitude response*

Attenuation:
attn=5.1+14.3*f^0.59 (dB/km; f in MHz)

Amplitude Response:
amp=10.^(-attn*km/20); (convert dB to linear ratio)

Impulse Response:
chnn=fir2(nn,frq,amp);

Channel #2 and #3:

The attenuation order atten_order and sampling frequency fs is selected by the user. The frequency and impulse response of the channel is calculated systematically as follows:

Phase Shift alpha:
f_Hz = linspace(fs/atten_order,fs/2,atten_order/2)

Primary constant R:
r0c = 286.17578; (Ohms/km),
ac = 0.1476962;
pc_R = (r0c^4 + ac*f_Hz.^2).^0.25;

Primary constant L:
L0 = 675.36888e-6 Hz/km,
L_inf = 488.95186e-6 Hz/km
b = 0.92930728;
fm = 806.33863e3; (in Hz)
temp1 = (f_Hz/fm).^b;
pc_L = (L0 + L_inf*temp1)./(1 + temp1);

Primary constant C:
pc_C = 49e-9; (F/km)

Primary constant G:
g0 = 43e-9; % S/km, ge=0.70;
pc_G = g0 * (f_Hz.^ge);

Characteristic Impedance Z0:

```
omega = 2*pi*f_Hz;
Z = pc_R + j*omega.*pc_L;
Y = pc_G + j*omega.*pc_C;
gamma = sqrt(Z.*Y); % per km
alpha = real(gamma);  % attenuation constant, in nepers/km
beta = imag(gamma);   % phase constant
Z0 = sqrt(Z./Y);
```

The A,B,C,D parameters following two-port network theory are calculated as follows:

```
A = D = cosh(gamma*d);  where d=distance in km
B = Z0.*sinh(gamma*d);
C = sinh(gamma*d)./Z0;
phi_0 = [1 Zsource; 0 1];

phi_out = phi_0 * [A(i) B(i); C(i) A(i)];  % gives transfer function
phi_out = [A(i) B(i); C(i) A(i)];  % gives insertion loss
```